

REPORT DOCUMENTATION PAGE				Form Approved OMB No. 0704-0188	
The public reporting burden for this collection of information is estimated to average 1 hour per response, including the time for reviewing instructions, searching existing data sources, gathering and maintaining the data needed, and completing and reviewing the collection of information. Send comments regarding this burden estimate or any other aspect of this collection of information, including suggestions for reducing the burden, to Department of Defense, Washington Headquarters Services, Directorate for Information Operations and Reports (0704-0188), 1215 Jefferson Davis Highway, Suite 1204, Arlington, VA 22202-4302. Respondents should be aware that notwithstanding any other provision of law, no person shall be subject to any penalty for failing to comply with a collection of information if it does not display a currently valid OMB control number.					
PLEASE DO NOT RETURN YOUR FORM TO THE ABOVE ADDRESS.					
1. REPORT DATE (DD-MM-YYYY) 05/14/2004		2. REPORT TYPE Final		3. DATES COVERED (From - To) 01/01/2002-10/31/2003	
4. TITLE AND SUBTITLE Thermoacoustics with Multiple-Phase Working Fluids				5a. CONTRACT NUMBER	
				5b. GRANT NUMBER N00014-02-1-0227	
				5c. PROGRAM ELEMENT NUMBER	
				5d. PROJECT NUMBER 02PRO5605-00	
6. AUTHOR(S) National Center for Physical Acoustics				5e. TASK NUMBER	
				5f. WORK UNIT NUMBER	
7. PERFORMING ORGANIZATION NAME(S) AND ADDRESS(ES) University of Mississippi National Center for Physical Acoustics 1 Coliseum Drive, University, MS 38677				8. PERFORMING ORGANIZATION REPORT NUMBER	
9. SPONSORING/MONITORING AGENCY NAME(S) AND ADDRESS(ES) Office of Naval Research Regional Office Atlanta 100 Alabama Street SW, Suite 4R15, Atlanta, GA 30303-3104				10. SPONSOR/MONITOR'S ACRONYM(S) ONRRO	
				11. SPONSOR/MONITOR'S REPORT NUMBER(S) RH/HEB0504-F	
12. DISTRIBUTION/AVAILABILITY STATEMENT Approved for Public Release; Distribution is Unlimited.					
13. SUPPLEMENTARY NOTES					
20040521 018					
14. ABSTRACT A one year effort to improve the understanding of thermoacoustic engines and refrigerators using multiple-phase working fluids resulted in a more complete. The specific system considered was an inert gas-condensing vapor mixture in a cylindrical pore with wet walls. It was found that vapor diffusion effects in the mixture are analogous to the heat diffusion effects in the thermoacoustics of inert gases, and that these effects can be expressed in terms of the thermoacoustic viscous function used in the theory of sound propagation of constant cross-section tubes. This theory was reduced to a concept for a practical device. This technical report in contained, for the most part, in two papers published in the Journal of the Acoustical Society of America which are a part of this report and a patent also included here.					
15. SUBJECT TERMS					
16. SECURITY CLASSIFICATION OF:			17. LIMITATION OF ABSTRACT		18. NUMBER OF PAGES
a. REPORT	b. ABSTRACT	c. THIS PAGE	UU		94
U	U	U			19a. NAME OF RESPONSIBLE PERSON Henry E. Bass, Director of NCPA
					19b. TELEPHONE NUMBER (Include area code) 662-915-5840

Thermoacoustics with Multiple-Phase Working Fluids

Abstract

A one year effort to improve the understanding of thermoacoustic engines and refrigerators using multiple-phase working fluids resulted in a more complete. The specific system considered was an inert gas-condensing vapor mixture in a cylindrical pore with wet walls. It was found that vapor diffusion effects in the mixture are analogous to the heat diffusion effects in the thermoacoustics of inert gases, and that these effects can be expressed in terms of the thermoacoustic viscous function used in the theory of sound propagation of constant cross-section tubes. This theory was reduced to a concept for a practical device. This technical report contained, for the most part, in two papers published in the Journal of the Acoustical Society of America which are a part of this report and a patent also included here.

1.0 Introduction

Thermoacoustic prime movers and refrigerators have been developed over several decades.¹ These devices have been promoted for several unique advantages over common refrigeration techniques, particularly in low incremental construction cost and very long maintenance cycles. These advantages are balanced by limitations inherent to acoustic heat engines such as low power density, low efficiency, and complicated heat exchangers. Because of these problems acoustic engines have not made any substantial market penetration outside of orifice pulse-tube cryocoolers on spacecraft.² Thermoacoustic devices use acoustic behavior in a fluid and its interaction with boundary surfaces to pump heat. A refrigerator will move heat at the expense of acoustic power, and a prime mover will generate power from a heat flow. Most machines considered or built have used a noble gas, usually helium, as the working fluid.³ Occasionally other simple fluids have been used, including mixtures of helium and another noble gas or a heavy gas,⁴ air,⁵ and liquid sodium.⁶ Machines have been constructed on scales ranging from a centimeter to tens of meters, and of power ranging from milliwatts⁷ up to tens of kilowatts.⁸ In every case the efficiency, defined as heat pumping power to input power, and power density, defined as heat pumping power to weight or volume, have been disappointing. This has precluded adoption or development of thermoacoustic machines except in highly specialized applications. The theory of thermoacoustic engines, at least in the linear approximation, has been well established^{6,10,11} and is a useful starting point for engine design.

For simple fluids the linear behavior is quite well understood. Non-linear effects, particularly turbulent dissipation and steady-state streaming, can be substantial at the high acoustic amplitudes typical of thermoacoustic engines,^{12,13} and are generally detrimental to engine performance. While these nonlinear effects are commonly seen and discussed in experimental work, they are difficult to predict and prevent. The predictions reported here are based on linear theories, and will likely overestimate actual performance. Work extending thermoacoustics beyond a simple working fluid has developed only recently. Here a simple fluid is defined as one that is homogeneous and has constant composition.

Experiments with heterogeneous fluids include separation of noble gas mixtures in a thermoacoustic device¹⁴ and dehumidification of air in a flow-through thermoacoustic engine.¹⁵ Analysis of these devices has led to development of a linear theory of thermoacoustics in heterogeneous fluids¹⁶ that shows a large change in heat pumping behavior when part of the working fluid is evaporating and condensing during the acoustic cycle. These theories suggest that using a working fluid in multiple phases may substantially increase the power density and efficiency of a thermoacoustic refrigerator over a similar device using a gaseous working fluid. Such an enhancement could bring thermoacoustic devices to the range of power density and cost to economically compete with current technologies, such as vapor-compression cycles.

In order to test these ideas, measurements were made of onset temperature in an extremely simple thermoacoustic prime mover, which operates in atmospheric air.¹⁷ The condensable fluid used is water, which was applied to the stack plates with an atomizer. The engine is a modification of a demonstration device developed by Reh-Lin Chen.¹⁸ Measurements were made with the stack at various positions in the resonator, and with the stack either dry or with a film of water. These experiments showed a dramatic decrease, by about a factor of 3, in the temperature gradient required for the onset of thermoacoustic oscillations when liquid water is present on the surface of the stack.

2.0 Technical Accomplishments

The technical results of this study are contained in two papers and one patent which are attached and a Master Thesis by Dan Brown also attached. PhD candidate Tim Simmons contributed to this project but most of his work was actually supported by a previous ONR contract so his dissertation is not attached. Copies of his dissertation, "Experimental Determination of Thermoacoustic Stack Properties", Aug, 2003 are available upon request.

3.0 References

1. W. A. Marrison, "Heat controlled acoustic wave system," United States Patent 2,836,033, May 27, 1958.
2. Radebaugh, "A review of pulse tube refrigeration," *Adv. Cryogenic Eng.* 35, 191-1205 (1990).
3. Wheatley, T. Hofler, G. W. Swift, and A. Migliori, "Experiments with an intrinsically irreversible acoustic heat engine," *Phys. Rev. Lett.* 50(7), 499-502 (1983).
4. J. R. Belcher, W. V. Slaton, R. Raspet, H. E. Bass, and J. Lightfoot, "Working gases in thermoacoustic engines," *J. Acoust. Soc. Am.* 105 (5), 2677-2684 (1999).
5. R. S. Reid and G. W. Swift, "Cyclic thermodynamics with open flow," *Phys. Rev. Lett.* 80, 4617-4620 (1998).

6. G. W. Swift, "Thermoacoustic engines," J. Acoust. Soc. Am. 84, 1145-1180 (1988).
7. E. Abdel-Rahman, O. G. Symko, A. M. Frates, "Performance of a high-frequency thermoacoustic refrigerator," J. Acoust. Soc. Am. 109, 2404 (2001).
8. D. McKelvey, S. Ballaster, S. Garrett, "Shipboard electronics thermoacoustic cooler," J. Acoust. Soc. Am. 98, 2961 (1995).
9. G. W. Swift, "Thermoacoustic natural gas liquefier," In proceedings of the DOE Natural Gas Conference, Houston, TX, March 1997.
10. Rott, "Damped and thermally driven acoustic oscillations in wide and narrow tubes," Z. Angew. Math. Phys. 20, 203-243 (1969), N. Rott, "Thermally driven acoustic oscillations, part 11: stability limit for helium," Z. Angew. Math. Phys. 24, 54 (1973), N. Rott, "Thermally driven oscillations, part III: second order heat flux," Z. Angew. Math. Phys. 26, 43-49 (1975).
11. W. C. Ward and G. W. Swift, "Design environment for low amplitude thermoacoustic engines (DeltaE)," J. Acoust. Soc. Am. 110, 1808-1821 (2001).
12. H. Baillet, V. Gusev, R. Raspet, R. A. Hiller, "Acoustic streaming in closed thermoacoustic devices," J. Acoust. Soc. Am. 110, 1808-1821 (2001).
13. G. P. Smith, R. A. Hiller, and R. Raspet, "Nonplanar modes and anomalous streaming near a thermoacoustic prime mover stack", Acoustics Research Letters.
14. P. S. Spoor and G. W. Swift, "Thermoacoustic separation of a He-Ar mixture," Phys. Rev. Lett. 85, 1646-1649 (2000).
15. R. A. Hiller and G. W. Swift, "Condensation in a steady-flow thermoacoustic refrigerator," J. Acoust. Soc. Am. 108, 1521-1527 (2000).
16. G. W. Swift and P. S. Spoor, "Thermal diffusion and mixture separation in the acoustic boundary layer," J. Acoust. Soc. Am. 106, 1794-1800 (1999). Errata J. Acoust. Soc. Am. 107, 2299 (2000), J. Acoust. Soc. Am. 109, 1261 (2001).
17. W. V. Slaton, J. W. Rayburn, R. A. Hiller, and R. Raspet, "Reduced onset temperature difference in wet thermoacoustic engines," 142nd meeting of the Acoustical Society of America, Dec. 2001.
18. S. L. Garrett and S. Backhaus, "The power of sound," American Scientist 88 (2000).

Theory of inert gas-condensing vapor thermoacoustics: Propagation equation^{a)}

Richard Raspet,^{b)} William V. Slaton,^{c)} Craig J. Hickey, and Robert A. Hiller
*Department of Physics and Astronomy and National Center for Physical Acoustics,
 University of Mississippi, University, Mississippi 38677*

(Received 20 November 2001; revised 3 July 2002; accepted 11 July 2002)

The theory of acoustic propagation in an inert gas-condensing vapor mixture contained in a cylindrical pore with wet walls and an imposed temperature gradient is developed. It is shown that the vapor diffusion effects in the mixture are analogous to the heat diffusion effects in the thermoacoustics of inert gases, and that these effects occur in parallel with the heat diffusion effects in the wet system. The vapor diffusion effects can be expressed in terms of the thermoviscous function $F(\lambda)$ used in the theory of sound propagation of constant cross-section tubes. As such, these results can be extended to any shape parallel-walled tube. The propagation equations predict that the temperature gradient required for onset of sound amplification in a wet-walled prime mover is much lower than the corresponding temperature gradient for an inert gas prime mover. The results of a measurement of the onset temperature of a simple demonstration prime mover in air with a dry stack and with a stack wetted with water provide a qualitative verification of the theory. © 2002 Acoustical Society of America. [DOI: 10.1121/1.1508113]

PACS numbers: 43.35.Ud [MRS]

LIST OF SYMBOLS

ρ, ρ_1, ρ_2	density of the mixture, gas, and vapor	μ_c	pressure of the mixture
P, P_1, P_2	pressure of the mixture, gas, and vapor	$\gamma, \gamma_1, \gamma_2$	chemical potential of mixture per unit mass
T	temperature of the mixture	l	ratio of specific heats of the mixture, gas, and vapor
$\mathbf{v}, \mathbf{v}_1, \mathbf{v}_2$	hydrodynamic velocity of the mixture, gas, and vapor	c_s	latent heat of vaporization (J/mole)
\mathbf{i}	density-weighted species difference velocity	R_0	speed of sound in the mixture
s	entropy per unit mass of mixture	k	universal gas constant (8.3143 J/mole-K)
C_1	gas concentration	R	Boltzmann's constant
m_1, m_2	molecular mass of the gas, and vapor	N_{Pr}, N_{Sc}	tube radius
n, n_1, n_2	total number density, number density of the gas, and vapor	ω	Prandtl number, Schmitt number
μ	dynamic viscosity of the mixture	$\xi = \omega z / c_s$	angular frequency
β	bulk viscosity of mixture	$\eta = r / R$	nondimensional axial variable
κ	thermal conductivity of the mixture	$\Omega = \omega R / c_s$	nondimensional radial variable
D_{12}	mass diffusion coefficient	$\lambda_\mu = R \sqrt{\rho \omega / \mu}$	reduced frequency
k_T, k_p	thermal diffusion ratio and pressure diffusion ratio	$\lambda_T = R \sqrt{\rho \omega c_p / \kappa}$	shear wave number
c_p	specific heat per unit mass at constant	$\lambda_D = R \sqrt{\omega / D_{12}}$	thermal wave number
		φ	diffusion wave number
			latent heat parameter

^{a)}Portions of this work have been presented in: W. V. Slaton and R. Raspet, "Thermoacoustics of moist air with wet stacks," *J. Acoust. Soc. Am.* **106**, 2265 (1999); "Wet-walled thermoacoustics," *ibid.* **108**, 2569 (2000); R. Raspet, "Thermoacoustics Research at the University of Mississippi," First International Workshop on Thermoacoustics, 's-Hertogenbosch, The Netherlands, 22–25 April (2001); R. Raspet, "Thermoacoustic Refrigeration as an Application of Porous Media Theory," 4th Workshop on Applications of the Physics of Porous Media, Puerto Vallarta, Mexico, 31 Oct.–4 Nov. (2001); W. V. Slaton, J. W. Rayburn, R. A. Hiller, and R. Raspet, "Reduced onset temperature in wet thermoacoustic engines," *J. Acoust. Soc. Am.* **110**, 2677 (2001).

^{b)}Author to whom correspondence should be addressed. Electronic mail: raspet@olemiss.edu

^{c)}Current address: Physics Department, Eindhoven University of Technology, Eindhoven, The Netherlands.

I. INTRODUCTION

Recent work has developed the theory of sound propagation in inert gas-condensing vapor mixtures in narrow pores with wet walls.^{1–3} The assumptions made about the gas, vapor, and pore wall are straightforward, namely: the wavelength and characteristic pore dimension must be much larger than the mean free path of the gas and vapor molecules, steady flow of the gas or vapor is second order in acoustic quantities and may be ignored in the first-order analysis, the amplitude of the acoustic pressure fluctuations is small, and end effects may be ignored. It is assumed that a thin layer of condensed vapor coats the solid surface of the

pore wall. The layer is assumed thin enough to neglect its heat capacity. This layer is the site for evaporation and condensation of vapor. The pores are assumed to be on the order of a few mass diffusion lengths in radius so that condensation will occur preferentially on the walls rather than at any condensation centers in the bulk of the mixture. Considering an evaporation and condensation process implies that the vapor can enter the thin layer but the inert gas cannot. It is also assumed that there are no other sources or sinks of vapor or inert gas within the pore, that the heat capacity and thermal conductivity of the pore walls are high enough to ignore temperature fluctuations in the solid, and finally that the walls can be considered rigid.

The theory demonstrates that the terms describing the diffusion of the vapor are analogous in form to the terms describing thermal diffusion in the mixture, so that heat and mass transfer terms in an inert gas-condensing vapor mixture in a thermoacoustic engine have similar forms. If mixtures could be found with heat and mass transfer terms acting together, then the heat pumping capacity or coefficient of performance of a thermoacoustic refrigerator could be increased.

The thermodynamic cycle an inert gas-vapor mixture undergoes within a standing-wave thermoacoustic refrigerator is similar to that of a pure inert gas, with the addition that during the compressive part of the acoustic cycle the partial pressure of the vapor is raised above the saturation pressure at the temperature of the nearby stack wall so the vapor condenses. Conversely, during the rarefaction part of the acoustic cycle liquid on the stack evaporates. In this way, an inert gas-vapor working fluid will transport both heat and vapor from one end of the stack to the other, towards the pressure antinode. If a temperature gradient is imposed such that the temperature of the wall increases toward the antinode, thermal energy will be transported toward the antinode unless the temperature of the wall is raised to the point that it matches or exceeds the temperature of the mixture. This condition establishes a maximum temperature gradient for heat transfer in that direction. In the system with wet walls, increasing the wall temperature gradient also increases the saturation vapor pressure gradient at the wall. As the vapor pressure gradient at the wall is increased, acoustic vapor transport will occur until the vapor pressure at the wall is equal to the partial pressure of the vapor in the transported parcel. This establishes a different critical temperature gradient for the acoustic vapor transport. The transport of heat from the mixture to the wall depends solely on the transverse temperature gradients in the pore. The transport of vapor to the wall depends solely on the transverse gradient of the partial pressure or concentration in the mixture. The vapor transport also carries heat, since evaporating and condensing vapor transports entropy.

In this paper we develop the acoustic propagation equation in a wet-walled pore with an imposed temperature gradient. This is an extension of the dry inert gas thermoacoustic propagation formulation known as Rott's equation. This equation will be analyzed to display the potential of inert gas-condensing vapor to improve thermoacoustic prime movers and refrigerators. We employ the notation of Arnott

*et al.*⁴ for the thermoviscous functions. In Sec. II the hydrodynamic equations describing the system are introduced and Tijdeman's⁵ "low reduced frequency" approximation is applied to this system of equations. The gradient in ambient quantities associated with the ambient temperature gradient is evaluated. The acoustic boundary conditions are described and the system of equations is then solved for the acoustic wave equation. In Sec. III the derived form of the wave equation is compared to the form found in Raspet *et al.*¹ for wet-walled tubes without an ambient temperature gradient and to the form for dry thermoacoustics.^{4,6} Section IV contains a discussion of our formulation with respect to a thermoacoustic prime mover. Section V contains a summary of results underlying our model of "wet" thermoacoustics and the conclusions.

II. THEORY OF SOUND PROPAGATION

A. Basic equations

The model presented here employs the assumptions used by Raspet *et al.*¹ in the calculation of sound propagation in wet cylinders. A pore consists of a rigid cylindrical tube filled with an inert gas and saturated vapor. A thin layer of liquid coats the interior of the tube. It is assumed that the heat capacity of the tube wall is high enough that the temperature of the tube wall and the layer of liquid do not fluctuate.³ The gas component cannot penetrate the tube wall or the liquid layer, and the gas-vapor mixture does not slip with respect to the liquid layer. The gas and vapor are treated as ideal gases, and properties of the mixture are computed according to the theory of gas mixtures.⁷ It is also assumed that terms containing k_T , the thermal diffusion ratio, and k_p , the pressure diffusion ratio, can be neglected. The effect of k_T on sound propagation in wet pores has been shown to be small for this system.² The effects of streaming on the acoustic propagation are assumed to be negligible.

Equations governing sound propagation in an ideal gas-vapor mixture are presented. The Navier-Stokes equation for the mixture is

$$\rho \frac{D\mathbf{v}}{Dt} = -\nabla P + \mu \nabla^2 \mathbf{v} + \left(\beta + \frac{\mu}{3} \right) \nabla (\nabla \cdot \mathbf{v}). \quad (1)$$

The continuity equation for the gas can be written in terms of the gas concentration as

$$\rho \frac{DC_1}{Dt} + \nabla \cdot \mathbf{i} = 0, \quad (2)$$

where the gas concentration is $C_1 = \rho_1/\rho$ and the density-weighted species difference velocity is given by $\mathbf{i} = (\rho_1 \rho_2 / \rho)(\mathbf{v}_1 - \mathbf{v}_2)$. The continuity equation for the vapor is

$$\frac{\partial \rho_2}{\partial t} + \nabla \cdot (\rho_2 \mathbf{v}_2) = 0, \quad (3)$$

and the continuity equation for the mixture is

$$\frac{\partial \rho}{\partial t} + \nabla \cdot (\rho \mathbf{v}) = 0, \quad (4)$$

where the mixture density is given by $\rho = \rho_1 + \rho_2$ and the

hydrodynamic velocity for the mixture is defined as $\mathbf{v} = (\rho_1 \mathbf{v}_1 + \rho_2 \mathbf{v}_2) / \rho$. Only two independent continuity equations are required to complete the system of equations. The entropy equation for the mixture is

$$\rho T \frac{Ds}{Dt} = \sigma'_{ik} \frac{\partial v_i}{\partial x_k} - \nabla \cdot (\mathbf{q} - \mu_c \mathbf{i}) - \mathbf{i} \cdot \nabla \mu_c, \quad (5a)$$

where the heat flux is given by

$$\mathbf{q} = \left[k_T \left(\frac{\partial \mu_c}{\partial C_1} \right)_{P,T} - T \left(\frac{\partial \mu_c}{\partial T} \right)_{P,C_1} + \mu_c \right] \mathbf{i} - \kappa \nabla T, \quad (5b)$$

the chemical potential for the mixture is

$$\mu_c = \frac{\mu'_1}{m_1} - \frac{\mu'_2}{m_2}, \quad (5c)$$

where μ'_1 and μ'_2 are the chemical potential per molecule of the gas and vapor respectively and σ'_{ik} is the viscous stress tensor.⁸ The ideal gas equation of state is used for both the gas and vapor components, and for the mixture

$$P = nkT, \quad (6a)$$

where the temperature of the components are equal, $T = T_1 = T_2$, the total mixture pressure is the sum of the partial pressures, $P = P_1 + P_2$, and the total number density is given as $n = n_1 + n_2$. In terms of concentration the equation of state is

$$P = nkT = \rho kT \left(\frac{n}{\rho} \right) = \rho kT \left[\left(\frac{m_2 - m_1}{m_1 m_2} \right) C_1 + \frac{1}{m_2} \right]. \quad (6b)$$

The diffusion equation for the mixture is

$$\mathbf{i} = -\rho_0 D_{12} \left[\nabla C_1 + \frac{k_T}{T_0} \nabla T + \frac{k_P}{P_0} \nabla P \right]. \quad (7)$$

For the wet-wall boundary conditions the concentration term dominates the diffusion process and k_T and k_P may be neglected. This differs from the acoustically driven mass diffusion studies,^{9,10} which have dry pore walls and the principal contribution to diffusion is the k_T term.

The ratio of specific heats, γ , for the mixture can be related to the ratios of the two component gases by

$$\frac{n\gamma}{\gamma-1} = \frac{n_1\gamma_1}{\gamma_1-1} + \frac{n_2\gamma_2}{\gamma_2-1}. \quad (8)$$

Please see the list of symbols for a complete guide to variables and symbols used in the equations.

To reduce these equations to a useful form, we follow the analysis of Raspet *et al.*^{1,2} For the sake of brevity we list the required steps and the resulting equations.

- (1) Linearize equations assuming that steady flows are negligible and retaining terms in dT_0/dz and $d\rho_0/dz$.
- (2) Neglect temperature-driven diffusion (Soret effect) and pressure-driven diffusion (Dufour effect); $k_T = 0$, $k_P = 0$.
- (3) Assume that the tubes are small enough that we may use cylindrical coordinates with no azimuthal dependence.
- (4) Introduce normalized variables with $e^{-i\omega t}$ time dependence

$$P = (\rho_0 c_s^2 / \gamma) (1 + P^* e^{-i\omega t}), \quad (9)$$

$$\rho = \rho_0 (1 + \rho^* e^{-i\omega t}), \quad (10)$$

$$C_1 = C_1^0 + C_1^* e^{-i\omega t}, \quad (11)$$

$$T = T_0 (1 + T^* e^{-i\omega t}), \quad (12)$$

$$\mathbf{v} = c_s \mathbf{v}^* e^{-i\omega t}, \quad (13)$$

$$\Delta = \mathbf{v}_1 - \mathbf{v}_2 = c_s \Delta^* e^{-i\omega t}, \quad (14)$$

where c_s denotes the ambient speed of sound in the mixture. Symbols with a superscripted "*" denote small dimensionless quantities, while a subscripted "0" denotes ambient quantities. For convenience, we define

$$\mathbf{v}^* = u^* \hat{e}_z + v^* \hat{e}_r, \quad (15)$$

and

$$\Delta^* = U^* \hat{e}_z + V^* \hat{e}_r. \quad (16)$$

- (5) Define the normalized axial coordinate as

$$\xi = \frac{\omega z}{c_s}, \quad (17)$$

and the normalized radial coordinate as

$$\eta = \frac{r}{R}, \quad (18)$$

where R is the tube radius.

- (6) Another normalized axial variable is given by

$$Z = \frac{z}{L}, \quad (19)$$

where L is the stack length and will be used to describe ambient gradients.

The components of the Navier-Stokes equation are unchanged from the analysis of Raspet *et al.*¹

$$iu^* = \frac{1}{\gamma} \frac{\partial P^*}{\partial \xi} - \frac{\mu}{\rho_0 \omega R^2} \left\{ \frac{\partial^2 u^*}{\partial \eta^2} + \frac{1}{\eta} \frac{\partial u^*}{\partial \eta} + \left(\frac{\omega R}{c_s} \right)^2 \frac{\partial^2 u^*}{\partial \xi^2} \right\} - \frac{\mu}{\rho_0 \omega R^2} \left(\frac{\beta}{\mu} + \frac{1}{3} \right) \frac{\partial}{\partial \xi} \left\{ \left(\frac{\omega R}{c_s} \right) \frac{\partial u^*}{\partial \xi} + \frac{\partial v^*}{\partial \eta} + \frac{v^*}{\eta} \right\}, \quad (20)$$

and

$$iv^* = \frac{1}{\gamma} \left(\frac{c_s}{\omega R} \right) \frac{\partial P^*}{\partial \xi} - \frac{\mu}{\rho_0 \omega R^2} \times \left\{ \frac{\partial^2 v^*}{\partial \eta^2} + \frac{1}{\eta} \frac{\partial v^*}{\partial \eta} - \frac{v^*}{\eta^2} + \left(\frac{\omega R}{c_s} \right)^2 \frac{\partial^2 v^*}{\partial \xi^2} \right\} - \frac{\mu}{\rho_0 \omega R^2} \left(\frac{\beta}{\mu} + \frac{1}{3} \right) \frac{\partial}{\partial \eta} \left\{ \left(\frac{\omega R}{c_s} \right) \frac{\partial u^*}{\partial \xi} + \frac{\partial v^*}{\partial \eta} + \frac{v^*}{\eta} \right\}. \quad (21)$$

The continuity equation for the mixture is

$$i \left(\frac{\omega R}{c_s} \right) \rho^* = \left(\frac{\omega R}{c_s} \right) \frac{\partial u^*}{\partial \xi} + \frac{1}{\eta} \frac{\partial}{\partial \eta} (\eta v^*) + \frac{u^*}{\rho_0} \left[\frac{R}{L} \right] \frac{d\rho_0}{dZ}, \quad (22)$$

and the continuity of gas in terms of concentration is

$$i \left(\frac{\omega R}{c_s} \right) C_1^* = \frac{\rho_1^0 \rho_2^0}{\rho_0^2} \left[\frac{1}{\eta} \frac{\partial}{\partial \eta} (\eta V^*) + \left(\frac{\omega R}{c_s} \right) \frac{\partial U^*}{\partial \xi} \right] + \frac{U^*}{\rho_0} \left[\frac{R}{L} \right] \frac{d}{dZ} \left[\frac{\rho_1^0 \rho_2^0}{\rho_0} \right] + u^* \left[\frac{R}{L} \right] \frac{d}{dZ} \left[\frac{\rho_1^0}{\rho_0} \right]. \quad (23)$$

Following the development of Landau and Lifshitz,⁸ Chap. VI, and using the ideal gas relation for the thermal expansion coefficient, the entropy equation is

$$i \left(\frac{\omega R}{c_s} \right) \left\{ T^* + \frac{\gamma-1}{\gamma} P^* \right\} = - \frac{\kappa}{\rho_0 c_p \omega R^2} \left(\frac{\omega R}{c_s} \right) \left\{ \frac{\partial^2 T^*}{\partial \eta^2} + \frac{1}{\eta} \frac{\partial T^*}{\partial \eta} + \left(\frac{\omega R}{c_s} \right)^2 \frac{\partial^2 T^*}{\partial \xi^2} \right\} + \frac{u^*}{T_0} \left[\frac{R}{L} \right] \frac{dT_0}{dZ} + \frac{\rho_1^0 \rho_2^0}{\rho_0^2} \frac{U^*}{c_p T_0} \left[\frac{R}{L} \right] \frac{d}{dZ}$$

$$\times \left(\frac{\mu_c}{T_0} - T_0 \left(\frac{\partial}{\partial T} \left(\frac{\mu_c}{T_0} \right) \right)_{P, C_1} \right). \quad (24)$$

Use of the continuity equations and the diffusion equation in the equation of state yields

$$\left(\frac{\omega R}{c_s} \right) \{ P^* - T^* - \rho^* \} = i \frac{n_1^0 n_2^0}{n_0 \rho_0} (m_1 - m_2) \left\{ \left(\frac{\omega R}{c_s} \right) \frac{\partial U^*}{\partial \xi} + \frac{1}{\eta} \frac{\partial}{\partial \eta} (\eta V^*) \right\} + i \frac{\rho_0}{n_0} \left(\frac{m_1 - m_2}{m_1 m_2} \right) \left[\frac{R}{L} \right] \left\{ u^* \frac{d}{dZ} \left[\frac{\rho_1^0}{\rho_0} \right] + \frac{U^*}{\rho_0} \frac{d}{dZ} \left[\frac{\rho_1^0 \rho_2^0}{\rho_0} \right] \right\}. \quad (25)$$

The axial component of diffusion is

$$i \frac{\rho_1^0 \rho_2^0}{\rho_0} U^* = - \frac{\rho_0 D_{12}}{\omega R^2} \left(\frac{\rho_1^0 \rho_2^0}{\rho_0^2} \left(\frac{\omega R}{c_s} \right) \frac{\partial}{\partial \xi} \left[\frac{1}{\eta} \frac{\partial}{\partial \eta} (\eta V^*) + \left(\frac{\omega R}{c_s} \right) \frac{\partial U^*}{\partial \xi} \right] - \frac{\rho_0 D_{12}}{\omega R^2} \left(\left[\frac{1}{\eta} \frac{\partial}{\partial \eta} (\eta V^*) + \left(\frac{\omega R}{c_s} \right) \frac{\partial U^*}{\partial \xi} \right] \times \left[\frac{R}{L} \right] \frac{d}{dZ} \left[\frac{\rho_1^0 \rho_2^0}{\rho_0} \right] - \frac{\rho_0 D_{12}}{\omega R^2} \left(\frac{U^*}{\rho_0} \left[\frac{R}{L} \right]^2 \frac{d^2}{dZ^2} \left[\frac{\rho_1^0 \rho_2^0}{\rho_0} \right] + \frac{R^2}{\rho_0} \left(\frac{\omega R}{c_s} \right) \frac{\partial U^*}{\partial \xi} \left[\frac{R}{L} \right] \frac{d}{dZ} \left[\frac{\rho_1^0 \rho_2^0}{\rho_0} \right] \right) - \frac{\rho_0 D_{12}}{\omega R^2} \left(u^* \left[\frac{R}{L} \right]^2 \frac{d^2}{dZ^2} \left[\frac{\rho_1^0}{\rho_0} \right] + R^2 \left(\frac{\omega R}{c_s} \right) \frac{\partial u^*}{\partial \xi} \left[\frac{R}{L} \right] \frac{d}{dZ} \left[\frac{\rho_1^0}{\rho_0} \right] \right), \quad (26)$$

and the radial component of diffusion is

$$i \frac{\rho_1^0 \rho_2^0}{\rho_0^2} V^* = - \frac{D_{12}}{\omega R^2} \left(\frac{\rho_1^0 \rho_2^0}{\rho_0^2} \frac{\partial}{\partial \eta} \left[\frac{1}{\eta} \frac{\partial}{\partial \eta} (\eta V^*) + \left(\frac{\omega R}{c_s} \right) \frac{\partial U^*}{\partial \xi} \right] - \frac{D_{12}}{\omega R^2} \left(\frac{1}{\rho_0} \frac{\partial U^*}{\partial \eta} \left[\frac{R}{L} \right] \frac{d}{dZ} \left[\frac{\rho_1^0 \rho_2^0}{\rho_0} \right] \right) - \frac{D_{12}}{\omega R^2} \left(\frac{\partial u^*}{\partial \eta} \left[\frac{R}{L} \right] \frac{d}{dZ} \left[\frac{\rho_1^0}{\rho_0} \right] \right). \quad (27)$$

The eight equations above form a complete set for the variables, u^* , v^* , P^* , ρ^* , U^* , V^* , T^* , C_1^* . We note that the system of equations can be solved for u^* , v^* , P^* , ρ^* , U^* , V^* , T^* without using Eq. (23). This equation is retained here for convenience in future calculations.

B. Evaluation of ambient gradients

Derivatives with respect to the ambient density, ρ_0 , and ambient concentration, ρ_1^0/ρ_0 , must be evaluated. In dry thermoacoustics the ambient density is inversely proportional to the ambient temperature. In a wet-walled stack with a temperature gradient, the temperature dependence of the vapor pressure of the liquid coating the stack must be taken into account. This will affect the ambient ratio of gas to

vapor in the mixture. Since the total pressure in the resonator is a constant, then at high ambient temperature there is a higher ratio of vapor to gas in the mixture; likewise, at lower ambient temperature there is a lower ratio of vapor to gas in the mixture.

We assume that the pore is small enough so that the ambient partial pressure is a function only of the axial position. This is equivalent to the assumption that the ambient gas temperature is a function only of the axial position assumed in inert gas thermoacoustics.

Using the expressions $\rho_0 = \rho_1 + \rho_2$, $\rho_1 = n_1 m_1$, and $\rho_2 = n_2 m_2$, derivatives with respect to the ambient density can be written as

$$\begin{aligned} \frac{d\rho_0}{dZ} &= m_1 \frac{dn_1^0}{dZ} + m_2 \frac{dn_2^0}{dZ} \\ &= m_1 \frac{dn_0}{dZ} + (m_2 - m_1) \frac{dn_2^0}{dZ} \\ &= m_1 \frac{dn_0}{dT_0} \frac{dT_0}{dZ} + (m_2 - m_1) \frac{dn_2^0}{dT_0} \frac{dT_0}{dZ}. \end{aligned} \quad (28)$$

The term, dn_0/dT_0 , can be calculated using the ideal gas law, yielding $dn_0/dT_0 = -n_0/T_0$ after simplification. The Clausius-Clapeyron¹¹ equation for the vapor pressure is

$$P_2 = P_{\text{ref}} \exp \left[-\frac{l}{R_0} \left(\frac{1}{T_0} - \frac{1}{T_{\text{ref}}} \right) \right] = n_2 k T_0, \quad (29)$$

where T_{ref} is the boiling point at pressure P_{ref} . Evaluating for dn_2^0/dT_0 yields

$$\frac{dn_2^0}{dT_0} = \frac{n_2^0}{T_0} \left(\frac{l}{R_0 T_0} - 1 \right). \quad (30)$$

We now introduce the "latent heat parameter," $\varphi = [(\gamma - 1)/\gamma](l/R_0 T_0)$, as defined by Marble.¹² Substituting into Eq. (28), the derivative of the ambient density, after some manipulation, can be expressed as

$$\frac{d\rho_0}{dZ} = -\frac{\rho_0}{T_0} \frac{dT_0}{dZ} \left[1 - \varphi \frac{\gamma}{\gamma - 1} \left(1 - \frac{m_1}{m_2} \right) \frac{\rho_2^0}{\rho_0} \right]. \quad (31)$$

Derivatives of the ambient gas concentration, ρ_1^0/ρ_0 , can be evaluated in a similar fashion

$$\begin{aligned} \frac{d}{dZ} \left[\frac{\rho_1^0}{\rho_0} \right] &= \frac{1}{\rho_0} \frac{d\rho_1^0}{dZ} + \rho_1^0 \frac{d}{dZ} \left[\frac{1}{\rho_0} \right] \\ &= \frac{1}{\rho_0^2} \left\{ (\rho_1^0 + \rho_2^0) \frac{d\rho_1^0}{dZ} - \rho_1^0 \frac{d\rho_1^0}{dZ} - \rho_1^0 \frac{d\rho_2^0}{dZ} \right\} \\ &= \frac{m_1 m_2}{\rho_0^2} \left\{ n_2^0 \frac{dn_0}{dT_0} \frac{dT_0}{dZ} - n_0^0 \frac{dn_2^0}{dT_0} \frac{dT_0}{dZ} \right\}. \end{aligned} \quad (32)$$

Making use of the derivatives found earlier for dn_0/dT_0 and dn_2^0/dT_0 , our expression simplifies to

$$\frac{dC_1^0}{dZ} = \frac{d}{dZ} \left[\frac{\rho_1^0}{\rho_0} \right] = -\varphi \frac{\gamma}{\gamma - 1} \frac{\rho_1^0 \rho_2^0}{\rho_0^2} \frac{n_0}{n_1^0} \frac{1}{T_0} \frac{dT_0}{dZ}. \quad (33)$$

If there is no vapor present, then there is no ambient gradient in the gas concentration. Note also that this term, like the one above for the derivative of the ambient density, is scaled by the latent heat parameter.

C. Boundary conditions

The boundary conditions at the wall of the tube, $\eta = 1$, and at the center, $\eta = 0$, are the same as used by Raspet *et al.*¹ These boundary conditions must be cast into the present variables. The boundary conditions at the tube wall, $\eta = 1$, are as follows.

- (1) It is assumed that the heat capacity of the tube wall is high enough that the temperature of the tube wall and the layer of condensate do not fluctuate

$$T^* = 0. \quad (34)$$

- (2) No axial slip for the mixture hydrodynamic velocity

$$u^* = 0. \quad (35)$$

- (3) The gas cannot penetrate the tube wall or condensate layer, $v_1^* = 0$, which can be written as

$$v^* + \frac{\rho_2^0}{\rho_0} V^* = 0. \quad (36)$$

- (4) The vapor pressure is constant at the wall since the vapor pressure is only a function of temperature, and by the first boundary condition we have assumed that there are no temperature fluctuations at the wall. This implies that

$p_2^* = 0$ at the wall. Use of the continuity conditions, the definition of Δ , and the equation of state gives

$$i\Omega P^* = \frac{n_1^0}{n_0} \frac{1}{\eta} \frac{\partial}{\partial \eta} (\eta V^*). \quad (37)$$

The boundary conditions on the axis of the tube, $\eta = 0$, are that P^* , T^* , u^* , U^* , ρ_1^* , and ρ_2^* be finite. The latter two conditions on ρ_1^* and ρ_2^* can be related to v^* and V^* by the continuity equations, which are singular unless v and V are zero at $\eta = 0$. Thus, our final boundary conditions are

- (5) Axis of tube is not a source or sink of vapor

$$V^* = 0. \quad (38)$$

- (6) Axis of tube is not a source or sink of mixture

$$v^* = 0. \quad (39)$$

D. Solution

A formal approach to the approximation and interpretation of the complicated equations of wet thermoacoustics is the "low reduced frequency" analysis of Tijdeman.⁵ This technique has been applied to the mass transfer problem by Raspet *et al.*¹

The principal approximation is to require that the reduced frequency, Ω , be small

$$\Omega = \frac{\omega R}{c_s} = \frac{2\pi R}{\lambda} \ll 1. \quad (40)$$

This spans a wide range of frequencies for small tubes and in fact includes regions where the Kirchhoff wide-tube approximation holds, as well as the Rayleigh narrow-tube/low-frequency region. The physical meaning of this approximation is to assume that the tube radius is much smaller than the wavelength. This assures that there will be no cross modes within the tube and that radial derivatives are much larger than axial derivatives. A second set of criteria is also used to retain some terms that would otherwise be neglected

$$u^* \gg v^*, \quad (41)$$

and

$$v^* \approx V^*. \quad (42)$$

We expect the first condition to be met since the radial velocity must be zero at the center and the displacement per cycle is at most on the order of one radius. The second condition arises since v^* and V^* are the same order of magnitude at the wall and both are zero at the center, since the tube axis is not a source or sink. The above criteria are the same as those of Raspet *et al.*¹ Generalization to include an ambient temperature gradient naturally implies a length scale, which has been chosen to be the stack length L . It is usually justifiable to assume that the characteristic pore dimension, i.e., pore radius, is much smaller than the stack length

$$\frac{R}{L} \ll 1. \quad (43)$$

The system is solvable without this assumption, but this added complexity is not justified in this study.

Certain nondimensional groupings of parameters may be identified:

the dimensionless shear wave number

$$\lambda_\mu = R \sqrt{\frac{\rho\omega}{\mu}} = \frac{\sqrt{2}R}{\delta_\mu}, \quad (44)$$

the dimensionless thermal wave number

$$\lambda_T = R \sqrt{\frac{nk\gamma}{\gamma-1} \frac{\omega}{\kappa}} = R \sqrt{\frac{\rho\omega c_p}{\kappa}} = \frac{\sqrt{2}R}{\delta_T}, \quad (45)$$

and the dimensionless diffusion wave number,

$$\lambda_D = R \sqrt{\frac{\omega}{D_{12}}} = \frac{\sqrt{2}R}{\delta_D}. \quad (46)$$

These wave numbers are inversely proportional to the associated penetration depths.

We rewrite Eqs. (20)–(27) using Eqs. (31) and (33) for ambient gradients and retain the lowest-order terms in Ω and R/L . We treat terms in v^* and V^* as first-order terms in Ω , which is consistent with Eq. (40) and Eq. (43). With the definitions above and the application of the low reduced frequency approximation, the axial component of Navier–Stokes is

$$iu^* = \frac{1}{\gamma} \frac{\partial P^*}{\partial \xi} - \frac{1}{\lambda_\mu^2} \left[\frac{\partial^2 u^*}{\partial \eta^2} + \frac{1}{\eta} \frac{\partial u^*}{\partial \eta} \right], \quad (47)$$

and the radial component of Navier–Stokes is

$$\frac{1}{\gamma} \frac{\partial P^*}{\partial \eta} = 0. \quad (48)$$

The axial diffusion equation simplifies to

$$iU^* = 0, \quad (49)$$

which will be used to eliminate U^* and $\partial U^*/\partial \xi$ in the following equations. The radial diffusion equation is

$$iV^* = -\frac{1}{\lambda_D^2} \left\{ \frac{\partial}{\partial \eta} \left(\frac{1}{\eta} \frac{\partial}{\partial \eta} (\eta V^*) \right) - \varphi \frac{\gamma}{\gamma-1} \frac{n_0}{n_1^0} \left[\frac{R}{L} \right] \frac{1}{T_0} \frac{dT_0}{dZ} \frac{\partial u^*}{\partial \eta} \right\}. \quad (50)$$

The continuity of the gas in terms of concentration is

$$i\Omega C_1^* = \frac{\rho_1^0 \rho_2^0}{\rho_0^2} \frac{1}{\eta} \frac{\partial}{\partial \eta} (\eta V^*) - u^* \varphi \frac{\gamma}{\gamma-1} \frac{\rho_1^0 \rho_2^0}{\rho_0^2} \frac{n_0}{n_1^0} \left[\frac{R}{L} \right] \frac{1}{T_0} \frac{dT_0}{dZ}, \quad (51)$$

the continuity equation for the mixture is

$$i\Omega \rho^* = \Omega \frac{\partial u^*}{\partial \xi} + \frac{1}{\eta} \frac{\partial}{\partial \eta} (\eta v^*) - \left[\frac{R}{L} \right] \frac{u^*}{T_0} \frac{dT_0}{dZ} \left(1 - \varphi \frac{\gamma}{\gamma-1} \left(1 - \frac{m_1}{m_2} \right) \frac{\rho_2^0}{\rho_0} \right), \quad (52)$$

the entropy equation is

$$i\Omega T^* - i\Omega \frac{\gamma-1}{\gamma} P^* + \frac{\Omega}{\lambda_T^2} \left[\frac{\partial^2 T^*}{\partial \eta^2} + \frac{1}{\eta} \frac{\partial T^*}{\partial \eta} \right] = \left[\frac{R}{L} \right] \frac{u^*}{T_0} \frac{dT_0}{dZ}, \quad (53)$$

and the equation of state is

$$\Omega(P^* - T^* - \rho^*) = i \frac{n_1^0 n_2^0}{n_0 \rho_0} (m_1 - m_2) \left[\frac{1}{\eta} \frac{\partial}{\partial \eta} (\eta V^*) - u^* \varphi \frac{\gamma}{\gamma-1} \frac{n_0}{n_1^0} \left[\frac{R}{L} \right] \frac{1}{T_0} \frac{dT_0}{dZ} \right]. \quad (54)$$

The axial and radial components of the Navier–Stokes equation are unchanged and demonstrate that the pressure is not a function of radial position. The axial component (47) shows that acoustic velocity is generated by axial gradients in pressure, with some modifications to account for shearing due to the pore walls. The terms on the right-hand side of the continuity equation (52) represent mass entering or leaving a region due to acoustic density fluctuations or by acoustic convection of a density gradient. The entropy equation (53) describes how temperature fluctuations are generated by pressure oscillations and by fluid oscillating between regions with varying ambient temperature. The equation of state (54) describes how the density fluctuations are generated by pressure and temperature oscillations as well as diffusion of vapor into or out of a region. Density fluctuations are also generated by fluid oscillating back and forth between regions with different ambient temperatures. However, if the two components have the same mass, diffusion does not contribute to density fluctuations since the additional term describes density changes due to the species velocity differing from the hydrodynamic velocity. Last, the radial diffusion equation (50) describes how interspecies diffusion is driven by gradients in the radial diffusion velocity and by fluid oscillating between regions of different ambient temperatures.

Note that the Navier–Stokes, entropy, and diffusion equations are decoupled. The solutions will be in terms of separate diffusion, thermal, and viscous wave numbers. This is the principal result of the low reduced frequency approximation. This shows that these processes are independent, to first order, and only coupled in the equation of continuity and equation of state for the mixture.

The axial Navier–Stokes equation is solved by noting that the pressure is only a function of the axial coordinate and by applying the no-slip boundary condition at the wall to obtain the axial hydrodynamic velocity

$$u^* = -\frac{i}{\gamma} \frac{dP^*}{d\xi} \left[1 - \frac{J_0(\sqrt{i}\lambda_\mu \eta)}{J_0(\sqrt{i}\lambda_\mu)} \right] = -\frac{i}{\gamma} \frac{dP^*}{d\xi} F_\mu(\eta). \quad (55)$$

We have introduced here the definitions

$$F_j(\eta) = 1 - \frac{J_0(\sqrt{i}\lambda_j \eta)}{J_0(\sqrt{i}\lambda_j)}, \quad (56a)$$

where

$$\int_0^1 F_j(\eta) \eta d\eta = \frac{1}{2} \left(1 - \frac{2J_1(\sqrt{i}\lambda_j)}{\sqrt{i}\lambda_j J_0(\sqrt{i}\lambda_j)} \right) = \frac{1}{2} F(\lambda_j). \quad (56b)$$

$F(\lambda_j)$ is the porous media dissipation function for cylindrical tubes and $j=T, D, \mu$. The recursion relation for the Bessel functions has been used to evaluate the integral. The evaluation in terms of generalized dissipation functions is given in Ref. 4.

Making use of this solution and the boundary condition on vapor pressure at the wall, the radial diffusion equation is solved using separation of variables to obtain the radial diffusion velocity

$$V^* = i\Omega \frac{n_0}{n_1} \left\{ P^* - \frac{1}{\Omega} \frac{1}{1-N_{Sc}} \frac{\varphi}{\gamma-1} \frac{1}{T_0} \frac{dT_0}{dZ} \left[\frac{R}{L} \right] \frac{dP^*}{d\xi} \right. \\ \times \frac{J_1(\sqrt{i}\lambda_D \eta)}{\sqrt{i}\lambda_D J_0(\sqrt{i}\lambda_D)} + \frac{1}{\Omega} \frac{1}{1-N_{Sc}} \frac{\varphi}{\gamma-1} \frac{1}{T_0} \frac{dT_0}{dZ} \\ \times \left[\frac{R}{L} \right] \frac{dP^*}{d\xi} \frac{J_1(\sqrt{i}\lambda_\mu \eta)}{\sqrt{i}\lambda_\mu J_0(\sqrt{i}\lambda_\mu)} \left. \right\}, \quad (57)$$

where the Schmidt number is $N_{Sc} = \lambda_D^2 / \lambda_\mu^2 = \mu / \rho_0 D_{12}$.

In anticipation of later results it is convenient to calculate the fluctuating component of the gas concentration, C_1^* by making use of the solutions for u^* and V^* above to obtain

$$C_1^* = \frac{\rho_1^0 \rho_2^0}{\rho_0^2} \frac{n_0}{n_1} \left\{ P^* (1 - F_D(\eta)) \right. \\ + \frac{1}{\Omega} \frac{\varphi}{\gamma-1} \frac{1}{T_0} \frac{dT_0}{dZ} \left[\frac{R}{L} \right] \frac{dP^*}{d\xi} F_\mu(\eta) \\ + \frac{1}{\Omega} \frac{\varphi}{\gamma-1} \frac{1}{T_0} \frac{dT_0}{dZ} \left[\frac{R}{L} \right] \frac{dP^*}{d\xi} \frac{F_D(\eta) - F_\mu(\eta)}{1 - N_{Sc}} \left. \right\}. \quad (58)$$

Substituting the solution for u^* into the entropy equation and using the boundary condition, $T^* = 0$ at $\eta = 1$ yields the dimensionless temperature fluctuations

$$T^* = \frac{\gamma-1}{\gamma} P^* F_T(\eta) \\ - \frac{1}{\Omega} \frac{1}{\gamma} \frac{dP^*}{d\xi} \left[\frac{R}{L} \right] \frac{1}{T_0} \frac{dT_0}{dZ} \left[\frac{F_T(\eta) - N_{Pr} F_\mu(\eta)}{1 - N_{Pr}} \right], \quad (59)$$

where the Prandtl number $N_{Pr} = \lambda_T^2 / \lambda_\mu^2 = \mu c_p / \kappa$.

We eliminate ρ^* from the equation of state using Eq. (52) and substitute the solutions for T^* , V^* , and u^* to find

$$\frac{1}{\eta} \frac{\partial}{\partial \eta} (\eta v^*) = \frac{i\Omega}{\gamma} \frac{d^2 P^*}{d\xi^2} F_\mu(\eta) + i\Omega P^* \left(1 - \frac{\gamma-1}{\gamma} F_T(\eta) \right) \\ + \frac{n_1^0 n_2^0}{n_0 \rho_0} (m_1 - m_2) \frac{\partial}{\partial \eta} (\eta V^*) \\ + \frac{i}{\gamma} \left[\frac{R}{L} \right] \frac{1}{T_0} \frac{dT_0}{dZ} \frac{dP^*}{d\xi} \\ \times \left\{ \frac{F_T(\eta) - N_{Pr} F_\mu(\eta)}{1 - N_{Pr}} - F_\mu(\eta) \right\}. \quad (60)$$

Multiply through by $\eta d\eta$ and integrate from 0 to 1 using the boundary condition on v^* and V^* at $\eta = 0$ to eliminate the constants of integration

$$v^*|_{\eta=1} = \frac{i\Omega}{\gamma} \frac{d^2 P^*}{d\xi^2} \frac{F(\lambda_\mu)}{2} + \frac{i\Omega P^*}{2} \left(1 - \frac{\gamma-1}{\gamma} F(\lambda_T) \right) \\ + \frac{n_1^0 n_2^0}{n_0 \rho_0} (m_1 - m_2) V^*|_{\eta=1} \\ + \frac{i}{2\gamma} \left[\frac{R}{L} \right] \frac{1}{T_0} \frac{dT_0}{dZ} \frac{dP^*}{d\xi} \\ \times \left\{ \frac{F(\lambda_T) - N_{Pr} F(\lambda_\mu)}{1 - N_{Pr}} - F(\lambda_\mu) \right\}. \quad (61)$$

Now, employ the final boundary condition, $v^* + (\rho_2^0 / \rho_0) V^* = 0$ at $\eta = 1$, using the above expression for the dimensionless radial diffusion velocity evaluated at $\eta = 1$, to obtain the following form:

$$\frac{d^2 P^*}{d\xi^2} F(\lambda_\mu) + \gamma P^* \left(1 - \frac{\gamma-1}{\gamma} F(\lambda_T) + \frac{n_2^0}{n_1^0} (1 - F(\lambda_D)) \right) \\ + \frac{1}{\Omega} \left[\frac{R}{L} \right] \frac{1}{T_0} \frac{dT_0}{dZ} \frac{dP^*}{d\xi} \left\{ \frac{F(\lambda_T) - F(\lambda_\mu)}{1 - N_{Pr}} \right. \\ + \left. \frac{n_2^0}{n_1^0} \frac{\gamma}{\gamma-1} \left(\frac{F(\lambda_D) - F(\lambda_\mu)}{1 - N_{Sc}} \right) \right\} = 0. \quad (62)$$

Converting to dimensional form in terms of the complex pressure amplitude, $P_{AC} = P_0 P^*$, we have

$$\frac{d^2 P_{AC}}{dz^2} + 2\alpha \frac{dP_{AC}}{dz} + k^2 P_{AC} = 0, \quad (63)$$

where

$$\alpha = \frac{1}{2} \frac{1}{T_0} \frac{dT_0}{dz} \left\{ \frac{F(\lambda_T)/F(\lambda_\mu) - 1}{1 - N_{Pr}} \right. \\ + \left. \frac{\gamma}{\gamma-1} \frac{n_2^0}{n_1^0} \frac{F(\lambda_D)/F(\lambda_\mu) - 1}{1 - N_{Sc}} \right\}, \quad (64)$$

and

$$k^2 = \frac{\omega^2}{c^2} \frac{\gamma}{F(\lambda_\mu)} \left\{ 1 - \frac{\gamma-1}{\gamma} F(\lambda_T) + \frac{n_2^0}{n_1^0} (1 - F(\lambda_D)) \right\}. \quad (65)$$

Equation (63) describes the acoustic pressure fluctuations in a wet-walled tube with a temperature gradient. We note that although we have solved this for cylindrical pores, parallel walled pores of other shapes can be described by substitution of the appropriate thermoviscous dissipation function, $F(\lambda_j)$.⁴

For purposes of discussion and numerical integration, it is useful to rewrite Eq. (63) as two first-order differential equations in the acoustic pressure and volume velocity. Averaging Eq. (55), the axial hydrodynamic velocity, over the cross-sectional area of the pore in terms of the dimensionless radial coordinate $\eta = r/R$ and ignoring the thin condensate layer gives

$$\begin{aligned}
u_{Ave}^* &= \frac{1}{A_{pore}} \int_{A_{pore}} u^* dA_{pore} \\
&= -\frac{2i}{\gamma} \frac{dP^*}{d\xi} \int_0^1 \left(1 - \frac{J_0(\sqrt{i}\lambda_\mu \eta)}{J_0(\sqrt{i}\lambda_\mu)} \right) \eta d\eta \\
&= -\frac{2i}{\gamma} \frac{dP^*}{d\xi} \frac{F(\lambda_\mu)}{2}, \tag{66}
\end{aligned}$$

where recursion relations for the Bessel functions have been used to evaluate the integral. Rearranging to solve for the acoustic pressure gradient while making use of the following expressions, $P^* = P_{AC}/P_0$, $P_0 = \rho_0 c_s^2/\gamma$, and $\xi = \omega z/c_s$, and realizing that the acoustic volumetric velocity $U_{vol} = A_{mix} c_s u_{Ave}^*$ yields

$$\frac{dP_{AC}}{dz} = \frac{i\omega\rho_0}{A_{mix}} \frac{U_{vol}}{F(\lambda_\mu)}, \tag{67}$$

where A_{mix} is the total stack cross-sectional area available to the gas/vapor mixture. Using this expression in Eq. (63) and using the expressions above for P^* , P_0 , and ξ gives, after rearrangement

$$\frac{dU_{vol}}{dz} = -\frac{A_{mix}}{i\omega\rho_0} F(\lambda_\mu) k^2 P_{AC} - 2\alpha U_{vol}, \tag{68}$$

where α and k^2 are defined in Eq. (64) and Eq. (65). Equations (67) and (68) are coupled first-order equations for acoustic pressure fluctuations and acoustic volumetric velocity fluctuations.

III. LIMITING CASES

A. Acoustics of wet porous media

To compare to recent work in porous media theory, we let the ambient temperature gradient, dT_0/dz , go to zero in Eqs. (63)–(65). This makes the term $\alpha=0$, and our acoustic wave equation becomes

$$\frac{d^2 P_{AC}}{dz^2} + k^2 P_{AC} = 0, \tag{69}$$

with

$$k^2 = \frac{\omega^2}{c^2} \frac{\gamma}{F(\lambda_\mu)} \left\{ 1 - \frac{\gamma-1}{\gamma} F(\lambda_T) + \frac{n_2^0}{n_1^0} (1 - F(\lambda_D)) \right\}. \tag{70}$$

This agrees with Raspet *et al.*¹ subject to the assumption that the thermal diffusion ratio, k_T , is zero.

B. Dry thermoacoustics

To compare to dry thermoacoustics, we let the number density of the vapor, n_2^0 , go to zero in Eqs. (63)–(65). The solution for the wave equation then becomes

$$\frac{d^2 P_{AC}}{dz^2} + 2\alpha \frac{dP_{AC}}{dz} + k^2 P_{AC} = 0, \tag{71}$$

with

$$\alpha = \frac{1}{2} \frac{1}{T_0} \frac{dT_0}{dz} \left\{ \frac{F(\lambda_T)/F(\lambda_\mu) - 1}{1 - N_{Pr}} \right\}, \tag{72}$$

and

$$k^2 = \frac{\omega^2}{c^2} \frac{\gamma}{F(\lambda_\mu)} \left\{ 1 - \frac{\gamma-1}{\gamma} F(\lambda_T) \right\}. \tag{73}$$

Note that this compares with the solution obtained by Arnott *et al.*⁴ To compare with the Rott formulation,⁶ note that the relation between shear wave number, λ_μ , and viscous penetration depth, δ_μ , is given by $\lambda_\mu = \sqrt{2R}/\delta_\mu$, and the relation between thermal wave number, λ_T , and thermal penetration depth, δ_T , is given by $\lambda_T = \sqrt{2R}/\delta_T$, where R is the effective radius defined as twice the pore area divided by the pore perimeter. The relations between $F(\lambda_\mu)$ and $F(\lambda_T)$ and the Rott functions, f_ν and f_κ , are given by, $\bar{F}(\lambda_\mu) = 1 - f_\nu$ and $\bar{F}(\lambda_T) = 1 - f_\kappa$. The complex conjugate arises due to our use of $e^{-i\omega t}$ notation, rather than Rott's $e^{i\omega t}$ notation.

IV. DISCUSSION

Equations (63)–(68) clearly demonstrate that the thermal diffusion terms for inert gas thermoacoustics are augmented by additional analogous terms in mass diffusion in the inert gas-condensing vapor mixture in pores with wet walls. Swift¹³ discusses the contribution of each term in the equations of inert gas thermoacoustics corresponding to Eqs. (67) and (68). The term corresponding to $-2\alpha U_{vol}$ is identified as the temperature-gradient-dependent complex acoustic gain/attenuation. For standing-wave devices, the imaginary part of this term is the dominant contribution to the gain; in a pure traveling wave device it is the real part that is the dominant contribution. Losses are primarily determined by the imaginary part of k , the complex square root of Eq. (65). For the inert gas-vapor mixtures we have examined, λ_D and λ_T are of the same order of magnitude, while φ can be quite large. The additional gain terms are larger than the additional loss terms so that lower onset temperatures and higher work can be expected from a wet prime mover.

In order to test these ideas, measurements were made of onset temperature in an extremely simple thermoacoustic prime mover, which operates in atmospheric air. The gas properties needed to compare the dry and wet gain and loss terms have been estimated using the methods of Ref. 1. The condensable fluid used is water, which was applied to the stack plates with an atomizer. The engine is a modification of a demonstration device developed by Reh-Lin Chen.¹⁴ The resonator section is a 100-ml Pyrex graduated cylinder (diameter 26 mm, length 240 mm) which forms a closed-open resonator exposed to the atmosphere. The stack is a 1-in.-long cylindrical section of Celcor square-celled ceramic honeycomb with 200 cells per square inch. The lower end is woven with about 250 mm of 30-AWG nichrome wire which can be electrically heated. The upper, cold, end of the stack has no heat exchanger at all, and dissipates heat into the nearby glass wall, convection of the air above it, and its own heat capacity.

Beginning with the entire system at ambient temperature, electrical power is applied to the heating wire over

20–30 s to produce an increasing temperature gradient across the stack, measured with thermocouples cemented to the stack at each end. The temperatures are recorded when sound is detected radiating from the open end of the resonator. Measurements were made with the stack at various positions in the resonator, and with the stack either dry or with a film of water. The stack was located near its optimum location for low onset temperature. Since there is no cold heat exchanger, these experiments were performed with rapid heating. With only two thermocouples, we could not measure the actual temperature distribution in the stack. For this reason careful comparison of data and theory is not justified. These experiments showed a dramatic decrease in the temperature difference required for the onset of thermoacoustic oscillations when liquid water was present on the surface of the stack. With a wet stack, the onset temperature difference was about 80 K, with a dry stack about 280 K. At the average temperature of the wet stack (330 K), $n_2/n_1 = 0.22$, $\phi = 4.2$, $\gamma = 1.388$. This gives a coefficient of about 3.2 for the diffusion-related gain term in Eq. (64). The coefficient of the diffusion loss term is 0.22 in Eq. (65), while the coefficient of the thermal loss term is about 0.29. The viscous losses are usually larger than the thermal losses, and the viscosity of dry air at 430 K is larger than the viscosity of saturated air at 330 K (2.4×10^{-5} vs 1.8×10^{-5} kg/m s). If the viscous, thermal, and diffusion lengths are approximated as equal, then the ratio of the critical temperature gradient with and without diffusion should be on the order of 4. This agrees reasonably well with the measured ratio of 3.5. The measurements provide qualitative confirmation that the gains predicted by the theory can be realized in a real system. Measurements with better instrumentation may provide quantitative confirmation in the future.

These results are promising for improving the heat flow and efficiency of thermoacoustic refrigeration, since the mass diffusion effects act in parallel with the heat diffusion effects and can augment the heat transport. To analyze such a system requires expressions for the enthalpy, heat, and work flows within the stack. The derivation of these expressions and the analysis of “wet” thermoacoustic refrigeration are presented in the following paper.

V. CONCLUSIONS

The basic propagation equations and equations for first-order acoustic variables have been derived for an inert gas-condensing vapor mixture in wet-walled tubes with imposed

temperature gradients. These equations demonstrate that the addition of wet walls and condensing and evaporating vapor increases the acoustic gain produced for a given temperature difference across the stack. A simple measurement demonstrates that the predicted gains can be realized in physical systems. The derived equations also form the basis for the development of work and heat flow equations and therefore the analysis of “wet” thermoacoustic refrigeration.

ACKNOWLEDGMENTS

This research was supported by the Office of Naval Research. We wish to thank Henry E. Bass for valuable discussions and encouragement, and Dr. F. Eisinger for sharing his observations about thermoacoustic oscillations in burner/furnace systems.

- ¹R. Raspet, C. Hickey, and J. Sabatier, “The effect of evaporation–condensation on sound propagation in cylindrical tubes using the low reduced frequency approximation,” *J. Acoust. Soc. Am.* **105**, 65–73 (1999).
- ²C. Hickey, R. Raspet, and W. Slaton, “Effects of thermal diffusion on sound attenuation in evaporating and condensing gas–vapor mixtures in tubes,” *J. Acoust. Soc. Am.* **107**, 1126–1130 (2000).
- ³W. Slaton, R. Raspet, and C. Hickey, “The effect of the physical properties of the tube wall on the attenuation of sound in evaporating and condensing gas–vapor mixtures,” *J. Acoust. Soc. Am.* **108**, 2120–2124 (2000).
- ⁴W. P. Arnott, H. E. Bass, and R. Raspet, “General formulation of thermoacoustics for stacks having arbitrarily shaped pore cross sections,” *J. Acoust. Soc. Am.* **90**, 3228–3237 (1991).
- ⁵H. Tijdeman, “On the propagation of sound waves in cylindrical tubes,” *J. Sound Vib.* **39**, 1–33 (1975).
- ⁶G. Swift, *Thermoacoustics: A Unifying Perspective for some Engines and Refrigerators*, LA-UR-99-895 (Los Alamos National Laboratory, Los Alamos, NM, 1999).
- ⁷J. V. Hirschfelder, C. Curtiss, and R. B. Bird, *Molecular Theory of Gases and Liquids* (Wiley, New York, 1954).
- ⁸L. D. Landau and E. M. Lifshitz, *Fluid Mechanics*, 2nd ed. (Butterworth-Heinemann, Oxford, 1997).
- ⁹G. W. Swift and P. S. Spoor, “Thermal diffusion and mixture separation in the acoustic boundary layer,” *J. Acoust. Soc. Am.* **106**, 1794–1800 (1999).
- ¹⁰D. A. Geller and G. W. Swift, “Saturation of thermoacoustic mixture separation,” *J. Acoust. Soc. Am.* **111**, 1675–1684 (2002).
- ¹¹F. Reif, *Fundamentals of Statistical and Thermal Physics* (McGraw-Hill, New York, 1965).
- ¹²F. Marble, “Some gas dynamic problems in the flow of condensing vapors,” *Astronaut. Acta.* **14**, 585–614 (1969).
- ¹³G. Swift, *Thermoacoustics: A Unifying Perspective for some Engines and Refrigerators*, LA-UR-99-895 (Los Alamos National Laboratory, Los Alamos, NM, 1999), see pp. 59–62.
- ¹⁴S. L. Garrett and S. Backhaus, “The power of sound,” *Am. Sci.* **88**, 516–525 (2000).

Theory of inert gas-condensing vapor thermoacoustics: Transport equations^{a)}

William V. Slaton,^{b)} Richard Raspet,^{c)} Craig J. Hickey, and Robert A. Hiller
*Department of Physics and Astronomy and National Center for Physical Acoustics,
University of Mississippi, University, Mississippi 38677*

(Received 20 November 2001; revised 3 July 2002; accepted 11 July 2002)

The preceding paper [J. Acoust. Soc. Am. **112**, 1414–1422 (2002)] derives the propagation equation for sound in an inert gas-condensing vapor mixture in a wet-walled pore with an imposed temperature gradient. In this paper the mass, enthalpy, heat, and work transport equations necessary to describe the steady-state operation of a wet-walled thermoacoustic refrigerator are derived and presented in a form suitable for numerical evaluation. The requirement that the refrigerator operate in the steady state imposes zero mass flux for each species through a cross section. This in turn leads to the evaluation of the mass flux of vapor in the system. The vapor transport and heat transport are shown to work in parallel to produce additional cooling power in the wet refrigerator. An idealized calculation of the coefficient of performance (COP) of a wet-walled thermoacoustic refrigerator is derived and evaluated for a refrigeration system. The results of this calculation indicate that the wet-walled system can improve the performance of thermoacoustic refrigerators. Several experimental and practical questions and problems that must be addressed before a practical device can be designed and tested are described. © 2002 Acoustical Society of America.

[DOI: 10.1121/1.1508114]

PACS numbers: 43.35.Ud [MRS]

I. INTRODUCTION

In a companion paper [J. Acoust. Soc. Am. **112**, 1414–1422 (2002)], hereafter referred to as Paper I, the acoustic propagation equation was derived for the pressure wave in an inert gas-condensing vapor mixture in a wet-walled pore with an applied temperature gradient.¹ The expressions for other first-order acoustic variables were also derived, such as the acoustic temperature fluctuations, acoustic velocity fluctuations, and acoustic concentration fluctuations. A complete analysis of the potential of the inert gas-condensing vapor system to thermoacoustic refrigeration requires expressions for the total axial enthalpy flux, heat, and work fluxes, as well as the total mass flux. With these expressions the coefficient of performance can be evaluated and compared to the analogous expressions for inert gas thermoacoustics. In addition, the system of equations for numerical integration of realistic stacks can be developed. In the derivations we use Swift's review article² as a guide, but employ the notation of Arnott *et al.*³ Cylindrical geometry is chosen for the pores within the stack for simplicity. The resulting equations may be adapted to other pore shapes by substituting different functional forms of the porous media dissipation functions. The work of Arnott *et al.*³ contains expressions for the porous media dissipation functions for various pore geometries. Also, Swift's thermoacoustics textbook contains these dissipa-

tion functions in Rott's notation.⁴ The use of Arnott's notation is consistent with our earlier papers on sound propagation in wet pores.^{5–7}

In a "wet" thermoacoustic refrigerator, energy is transported along the temperature gradient in the stack both in the form of heat and as energy carried by the condensable species. The vapor condenses and evaporates on a thin layer of liquid on the wall of the pore. Proper phasing between the evaporation/condensation of vapor from this film and the axial acoustic velocity will result in net pumping of vapor from one end of the stack to the other. In its simplest form, we suppose that the condensable fluid returns by flow in the thin liquid layer. This represents a loss mechanism analogous to heat conduction in the stack and its contribution must be evaluated.

DeltaE is a well-established numerical code for modeling the performance of thermoacoustic devices.⁸ The transport equations will be evaluated in forms suitable for use in DeltaE. DeltaE uses the conservation of the total time-averaged, second-order steady-state enthalpy flow within the stack to calculate the temperature gradient and temperature profile through the stack. The enthalpy is conserved because the stack and refrigerator are assumed to be insulated and that heat exchange with the environment only occurs at the heat exchangers at each end of the stack. This assumption is also valid for the wet system.

In Sec. II, the first-order differential equations for the volumetric velocity and acoustic pressure are presented and their use in numerical calculations discussed. Section III develops the expression for the mass flux in the stack in steady-state operation. Section IV develops the equations for the time-averaged enthalpy flux, and the heat and work fluxes in the stack. From the expression for the total enthalpy flow, the

^{a)}Portions of this work have been presented in William V. Slaton and Richard Raspet, "Wet-walled Thermoacoustics," First International Workshop on Thermoacoustics, 's-Hertogenbosch, The Netherlands, 22–25 April (2001); William V. Slaton and Richard Raspet, "Wet-walled thermoacoustics," J. Acoust. Soc. Am. **110**, 2677 (2001).

^{b)}Current address: Physics Department, Eindhoven University of Technology, Eindhoven, The Netherlands.

^{c)}Author to whom correspondence should be addressed. Electronic mail: raspet@olemiss.edu

heat and mass pumping by acoustic processes and loss mechanisms may be identified. Section V describes the process occurring in a wet thermoacoustic refrigerator stack and identifies a useful regime of operation. The coefficient of performance of an idealized inert gas-vapor thermoacoustic refrigerator is developed in Sec. VI. This expression for the coefficient of performance is then analyzed to determine the potential of wet-walled system to improve the practicality of thermoacoustic refrigeration. Section VII contains the conclusions of this research.

II. PROPAGATION EQUATIONS

DeltaE numerically integrates the two coupled first-order differential equations in acoustic pressure and volumetric velocity to determine the acoustic propagation through the stack. From Ref. 1 we have

$$\frac{dP_{AC}}{dz} = \frac{i\omega\rho_0}{A_{mix}} \frac{U_{vol}}{F(\lambda_\mu)}, \quad (1)$$

where A_{mix} is the total stack cross-sectional area available to the gas-vapor mixture, U_{vol} is the volume velocity in the stack governed by

$$\frac{dU_{vol}}{dz} = -\frac{A_{mix}}{i\omega\rho_0} F(\lambda_\mu) k^2 P_{AC} - 2\alpha U_{vol}, \quad (2)$$

where α and k^2 are defined as

$$\alpha = \frac{1}{2} \frac{1}{T_0} \frac{dT_0}{dz} \left\{ \frac{F(\lambda_T)/F(\lambda_\mu) - 1}{1 - N_{Pr}} + \varphi \frac{\gamma}{\gamma - 1} \frac{n_2^0}{n_1^0} \frac{F(\lambda_D)/F(\lambda_\mu) - 1}{1 - N_{Sc}} \right\}, \quad (3)$$

and

$$k^2 = \frac{\omega^2}{c^2} \frac{\gamma}{F(\lambda_\mu)} \left\{ 1 - \frac{\gamma - 1}{\gamma} F(\lambda_T) + \frac{n_2^0}{n_1^0} (1 - F(\lambda_D)) \right\}. \quad (4)$$

Equations (1) and (2) are coupled first-order equations for acoustic pressure fluctuations and acoustic volumetric velocity fluctuations. In steady state, knowledge of the value of the fluctuating variables and the total enthalpy within the stack at one location allows calculation of the fluctuating variables at another location within the stack. It can be seen that thermal and mass transfer processes have similar functional forms in Eqs. (3) and (4). The behavior of the ambient temperature gradient is evaluated from the enthalpy equation to be derived in Sec. IV.

III. MASS FLUX

Within a closed resonator in steady state, the second-order time-averaged mass flux of the inert gas must be zero. Acoustic pumping of inert gas in the axial direction must be balanced by an axial return mean flow of gas to equalize the mean pressure within the resonator. Thus, we may write

$$\int (\overline{\rho_1 v} + \rho_1^0 v_{s,1})_z dA_{mix} = 0, \quad (5)$$

where $v_{s,1}$ is the steady-state flow velocity of inert gas. v is the first-order acoustic fluctuation velocity. In Ref. 1 it is shown that there is no axial acoustic difference velocity term in the low reduced frequency solution. Therefore, the acoustic velocity of each species is the same as the mixture acoustic velocity. We have proposed an acoustic propagation model in which there is a net mass flux of vapor due to acoustic processes. An analogous expression may be written for the vapor

$$\int (\overline{\rho_2 v} + \rho_2^0 v_{s,2})_z dA_{mix} = \dot{m}_{vapor} = -\dot{m}_{liquid}, \quad (6)$$

where \dot{m}_{liquid} is the mass flow rate in the condensed liquid layer and $v_{s,2}$ is the steady-state flow velocity of the vapor. For steady-state operation the vapor transported in one direction in the mixture must return as liquid flow in the other direction. The ambient steady flow of inert gas and vapor is also related to the ambient concentration of the inert gas within the stack. This is illustrated by recalling the expression for the ambient-density-weighted species difference velocity

$$i_0 = -\rho_0 D_{12} \nabla C_1^0 = \frac{\rho_1^0 \rho_2^0}{\rho_0} (v_{s,1} - v_{s,2}), \quad (7)$$

and that the acoustic concentration fluctuation can be expressed by

$$C_1^* = \frac{\rho_1^0 \rho_2^0 (\rho_1^* - \rho_2^*)}{\rho_0^2}. \quad (8)$$

Equations (5)–(8) may be combined and rearranged to form two useful expressions. The first is

$$\int (\overline{v C_1^*} - D_{12} \nabla C_1^0)_z dA_{mix} = -\frac{\rho_1^0}{\rho_0^2} \dot{m}_{vapor} = \frac{\rho_1^0}{\rho_0^2} \dot{m}_{liquid}, \quad (9)$$

and the second is

$$\int (\overline{\rho v} + \rho_0 v_s)_z dA_{mix} = \dot{m}_{vapor} = -\dot{m}_{liquid}, \quad (10)$$

where $v_s = (\rho_1^0 v_{s,1} + \rho_2^0 v_{s,2})/\rho_0$ is the ambient hydrodynamic steady flow of the mixture.

Using expressions for C_1^0 , C_1^* , and u^* from Ref. 1 and expressing the time average of the product of the acoustic quantities as $\frac{1}{2} \text{Re}[u^* \tilde{C}_1^*]$, we find

$$\begin{aligned} \dot{m}_{vapor} = & -\frac{1}{2} A_{mix} \frac{\rho_0^2}{\rho_1^0} \left\{ c_s \text{Re} \left[\frac{1}{\pi} \int_0^1 u^* \tilde{C}_1^* 2\pi \eta d\eta \right] \right. \\ & \left. - \varphi \frac{n_0}{n_1} \frac{\gamma}{\gamma - 1} \frac{A_{mix} D_{12} \rho_2^0}{T_0} \frac{dT_0}{dz} \right\}, \end{aligned} \quad (11)$$

where $\varphi = [(\gamma - 1)/\gamma](l/R_0 T_0)$.

Substitution of u^* and \tilde{C}_1^* yield integrals of $F_i(\eta)$ or of products $F_i(\eta) \tilde{F}_j(\eta)$. Reference 4 shows that these integrals are given as

$$\int_0^1 \tilde{F}_i(\eta) F_i(\eta) \eta d\eta = \frac{1}{2} \text{Re}[F(\lambda_i)], \quad (12a)$$

$$\int_0^1 \tilde{F}_i(\eta) F_j(\eta) \eta d\eta = \frac{1}{2} \frac{F(\lambda_j) N_{ij} + \tilde{F}(\lambda_i)}{N_{ij} + 1}, \quad (12b)$$

and

$$\int_0^1 F_i(\eta) \eta d\eta = \frac{1}{2} F(\lambda_i), \quad (12c)$$

where $N_{ij} = \lambda_i^2 / \lambda_j^2$.

Using these integrals, we find

$$\begin{aligned} \dot{m}_{\text{vapor}} = & \frac{1}{2} \frac{\rho_2^0 n_0}{\rho_0 n_1^0} \frac{\gamma}{\gamma - 1} \frac{1}{T_0 c_p} \left[\text{Re}[\tilde{P}_{AC} U_{\text{vol}} \Xi_1(\lambda_D)] \right. \\ & - \varphi \frac{c_p \rho_0}{\omega A_{\text{mix}}} \frac{dT_0}{dz} \left| \frac{U_{\text{vol}}}{F(\lambda_\mu)} \right|^2 \text{Im}[\Xi_2(\lambda_D)] \\ & \left. - \varphi \frac{n_0}{n_1^0} \frac{\gamma}{\gamma - 1} \frac{A_{\text{mix}} \dot{D}_{12} \rho_2^0}{T_0} \frac{dT_0}{dz} \right], \end{aligned} \quad (13)$$

where we introduce the notation

$$\Xi_1(\lambda_j) = \frac{\tilde{F}(\lambda_j)/F(\lambda_\mu) - 1}{1 + N_j}, \quad (14)$$

and

$$\Xi_2(\lambda_j) = \frac{F(\lambda_\mu) N_j + \tilde{F}(\lambda_j)}{1 - N_j^2}, \quad (15)$$

with j taken as T referring to thermal effects or D referring to mass diffusion effects and N_j referring either to the Prandtl number for thermal effects or the Schmidt number for mass diffusion effects.

The acoustically driven terms can be recognized as very similar in form to the heat transport equations for inert gas thermoacoustics: there is an acoustically driven term independent of temperature gradient and another acoustically driven term proportional to temperature gradient. Determination of the direction of these terms is most easily accomplished by comparison with the well-understood enthalpy flux terms of inert gas thermoacoustics, so we defer the discussion of the direction of mass flux until the enthalpy and heat flux terms have been derived and discussed.

IV. ENTHALPY BALANCE

The enthalpy flow expression is derived from the energy density equation given by Landau and Lifshitz⁹

$$\frac{\partial}{\partial t} \left(\frac{1}{2} \rho v^2 + \rho \varepsilon \right) = -\nabla \cdot \left[\rho v \left(\frac{1}{2} v^2 + w \right) - \mathbf{v} \cdot \boldsymbol{\sigma}' + \mathbf{q}_0 \right]. \quad (16)$$

ε is the internal energy per unit mass, w is the enthalpy per unit mass, $\mathbf{v} \cdot \boldsymbol{\sigma}'$ is the energy flux due to internal friction, and \mathbf{q}_0 is the heat flux. Use of this basic expression insures that we have included all relevant terms in our derivation at the cost of initial complexity. The terms in the divergence represent the energy flux within the stack. The axial component of the enthalpy flux within the stack is of interest because it is a conserved quantity in steady-state operation. The time-averaged axial enthalpy flow is found by averaging Eq. (16) over the whole stack and taking the time average. The

integral over the whole stack can be broken up into integrals over the solid, liquid, and open areas of the stack. We retain second-order terms in acoustically fluctuating variables and steady-state terms in the time average, and ignore acoustic terms in the solid and liquid layer and all viscous heating terms, $\mathbf{v} \cdot \boldsymbol{\sigma}'$. Streaming velocities are assumed to be at least first order in acoustic quantities. Thus, the axial component of the total enthalpy flux is

$$\begin{aligned} \bar{H} = & \int (w_{\text{mix}}^0 (\overline{\mathbf{v}\rho} + \rho_0 \mathbf{v}_s) + \rho_0 \overline{\mathbf{v}w} + \mathbf{q}_0)_z dA_{\text{mix}} \\ & + \int \left(\rho_{\text{liquid}}^0 U_{\text{liquid}}^0 w_{\text{liquid}}^0 - \kappa_{\text{liquid}} \frac{dT_0}{dz} \right) dA_{\text{liquid}} \\ & - \int \kappa_{\text{solid}} \frac{dT_0}{dz} dA_{\text{solid}}, \end{aligned} \quad (17)$$

where the overbars denote time averaging, and the ambient loss mechanisms within the gas mixture are contained within

$$\mathbf{q}_0 = \left[\mu_c - T_0 \left(\frac{\partial \mu_c}{\partial T} \right)_{P, C_1} \right] \mathbf{i}_0 - \kappa \nabla T_0. \quad (18)$$

The Soret effect coefficient, k_T , and the Dufour effect coefficient, k_P , have been ignored to conform with earlier derivations. μ_c is the chemical potential of the mixture and is defined as $\mu_c = (\mu'_1/m_1) - (\mu'_2/m_2)$, where μ'_1 and μ'_2 are the chemical potentials per molecule. Using Eq. (7) for the ambient-density-weighted species difference velocity, Eq. (18) may be rewritten as

$$\mathbf{q}_0 = - (w_1^0 - w_2^0) \rho_0 D_{12} \nabla C_1^0 - \kappa \nabla T_0, \quad (19)$$

where w_j^0 is the ambient enthalpy per unit mass of species j .

Equation (10) can be used to express the enthalpy flux for the mixture in terms of \dot{m}_{liquid} or \dot{m}_{vapor}

$$\begin{aligned} \bar{H} = & (w_{\text{mix}}^0 - w_{\text{liquid}}^0) \dot{m}_{\text{vapor}} + \int \left(\overline{\rho_0 u w_{\text{mix}}} \right. \\ & - (w_1^0 - w_2^0) \rho_0 D_{12} \frac{dC_1^0}{dz} - \kappa_{\text{mix}} \frac{dT_0}{dz} \Big) dA_{\text{mix}} \\ & - \int \kappa_{\text{solid}} \frac{dT_0}{dz} dA_{\text{solid}} - \int \kappa_{\text{liquid}} \frac{dT_0}{dz} dA_{\text{liquid}}. \end{aligned} \quad (20)$$

Terms in Eq. (20) may be identified: $\overline{\rho_0 u w}$ represents the enthalpy flow down the stack due to acoustics. The term containing $w_1^0 - w_2^0$ represents the enthalpy flow due to the ambient diffusion of the inert gas and vapor. The term $(w_{\text{mix}}^0 - w_{\text{liquid}}^0) \dot{m}_{\text{vapor}}$ represents the enthalpy flow due to the net transport of the gas mixture and the return flow in the liquid layer. The diffusion loss and the ambient steady flow loss terms will be combined to form a simpler expression below. The loss mechanism of ambient thermal conduction through the gas mixture and solid stack material are given by $\kappa_{\text{mix}}(dT_0/dz)$ and $\kappa_{\text{solid}}(dT_0/dz)$, respectively, while $\kappa_{\text{liquid}}(dT_0/dz)$ represents an additional loss by thermal conduction through the liquid layer. Use of Eqs. (9) and (10) leads to considerable simplifications as various terms combine.

The acoustically fluctuating enthalpy for an ideal mixture is written in terms of temperature and concentration fluctuations, and is given by $w_{\text{mix}} = c_p T_0 \tilde{T}^* + \mu_c C_1^*$, where c_p is the mixture isobaric specific heat and μ_c is the mixture chemical potential. The integration over the solid, liquid, and gaseous parts of the stack is performed and the expressions for the normalized temperature, axial acoustic velocity, and concentration fluctuations are substituted and time averaged. With these modifications, Eq. (20) becomes

$$\begin{aligned} \bar{H} = & \frac{1}{2} A_{\text{mix}} \text{Re} \left[\rho_0 c_s \int_0^1 u^* c_p T_0 \tilde{T}^* 2 \eta d\eta \right] \\ & + \frac{1}{2} A_{\text{mix}} \text{Re} \left[\rho_0 c_s \left(\mu_c - \frac{\rho_0}{\rho_1} w_{\text{mix}}^0 + \frac{\rho_0}{\rho_1} w_{\text{liquid}}^0 \right) \right. \\ & \times \int_0^1 u^* \tilde{C}_1^* 2 \eta d\eta \left. + A_{\text{mix}} \left[\frac{\rho_0}{\rho_1} (w_{\text{mix}}^0 - w_{\text{liquid}}^0) \right. \right. \\ & \left. \left. - (w_1^0 - w_2^0) \right] \rho_0 D_{12} \frac{dC_1^0}{dz} - [\kappa_{\text{mix}} A_{\text{mix}} \right. \right. \\ & \left. \left. + \kappa_{\text{liquid}} A_{\text{liquid}} + \kappa_{\text{solid}} A_{\text{solid}}] \frac{dT_0}{dz} \right], \quad (21) \end{aligned}$$

where the integral over the mixture has been converted to an integral over a single pore in terms of the dimensionless radial coordinate η . Use of standard thermodynamic identities yields further simplifications

$$\mu_c - \frac{\rho_0}{\rho_1} w_{\text{mix}}^0 + \frac{\rho_0}{\rho_1} w_{\text{liquid}}^0 = - \frac{\rho_0}{\rho_1} T_0 (s_{\text{mix}}^0 - s_{\text{liquid}}^0), \quad (22a)$$

and

$$(w_{\text{mix}}^0 - w_{\text{liquid}}^0) \frac{\rho_0}{\rho_1} - (w_1^0 - w_2^0) = \frac{\rho_0}{\rho_1} T_0 (s_2^0 - s_{\text{liquid}}^0), \quad (22b)$$

where s_{mix}^0 , s_2^0 , and s_{liquid}^0 are the ambient entropies per unit mass of the mixture, vapor, and liquid at the temperature T_0 , respectively. With the identity for dC_1^0/dz from Ref. 1, Eq. (21) becomes

$$\begin{aligned} \bar{H} = & \frac{1}{2} A_{\text{mix}} \text{Re} \left[\rho_0 c_s \int_0^1 u^* c_p T_0 \tilde{T}^* 2 \eta d\eta \right] \\ & - \frac{1}{2} A_{\text{mix}} \text{Re} \left[\frac{\rho_0^2}{\rho_1} c_s T_0 (s_{\text{mix}}^0 - s_{\text{liquid}}^0) \int_0^1 u^* \tilde{C}_1^* 2 \eta d\eta \right] \\ & - A_{\text{mix}} \left[\varphi \frac{\gamma}{\gamma-1} \rho_2^0 \frac{n_0}{n_1} (s_2^0 - s_{\text{liquid}}^0) D_{12} \right] \frac{dT_0}{dz} \\ & - [\kappa_{\text{mix}} A_{\text{mix}} + \kappa_{\text{liquid}} A_{\text{liquid}} + \kappa_{\text{solid}} A_{\text{solid}}] \frac{dT_0}{dz}. \quad (23) \end{aligned}$$

The first two terms represent the acoustically transported enthalpy $\dot{Q}_{\text{AC}} + \dot{W}_{\text{AC}}$. The first term can be evaluated much like Eq. (11) or can be recognized as the acoustic heat flux term of inert gas thermoacoustics.^{2,3} The second term is $T_0 (s_{\text{mix}}^0 - s_{\text{liquid}}^0)$ times the acoustic mass transport of vapor. The integrals for acoustic mass transport are evaluated in Eq. (12). The third term is the enthalpy loss term due to the

steady flow of vapor and its subsequent return flow as a liquid.

Equation (23) is the most convenient form for evaluation from first-order acoustic quantities, but is not the best form for understanding the physical properties of the system. If the $\rho_0 u w$ term in Eq. (20) is expressed in terms of \dot{m}_{vapor} , we find

$$\begin{aligned} \bar{H} = & \frac{1}{2} A_{\text{mix}} \text{Re} \left[\rho_0 c_s \int_0^1 u^* c_p T_0 \tilde{T}^* 2 \eta d\eta \right] \\ & + T_0 (s_{\text{mix}}^0 - s_{\text{liquid}}^0) \dot{m}_{\text{vapor}} - A_{\text{mix}} T_0 (s_1^0 - s_2^0) \rho_0 D_{12} \frac{dC_1^0}{dz} \\ & - (\kappa_{\text{mix}} A_{\text{mix}} + \kappa_{\text{liquid}} A_{\text{liquid}} + \kappa_{\text{solid}} A_{\text{solid}}) \frac{dT_0}{dz}. \quad (24) \end{aligned}$$

This form resolves the additional transport terms into entropy transport due to the mass transport of the mixture and the return flow of the liquid and entropy transport due to the ambient diffusion of the inert gas and vapor components.

Evaluation in terms of the volume velocity yields

$$\begin{aligned} \bar{H} = & \frac{1}{2} \text{Re} [\tilde{P}_{\text{AC}} U_{\text{vol}}] + \frac{1}{2} \text{Re} [\tilde{P}_{\text{AC}} U_{\text{vol}} (\Xi_1(\lambda_T) \\ & + \varepsilon_D \Xi_1(\lambda_D))] - \frac{c_p \rho_0}{2 \omega A_{\text{mix}}} \frac{dT_0}{dz} \left| \frac{U_{\text{vol}}}{F(\lambda_\mu)} \right|^2 \\ & \times \text{Im} [\Xi_2(\lambda_T) + \varepsilon_D \varphi \Xi_2(\lambda_D)] - \bar{Q}_{\text{loss}}, \quad (25) \end{aligned}$$

where

$$\varepsilon_D = \frac{1}{c_p} \frac{\rho_2^0}{\rho_0} \frac{n_0}{n_1} \frac{\gamma}{\gamma-1} (s_{\text{mix}}^0 - s_{\text{liquid}}^0), \quad (26)$$

$$\begin{aligned} \bar{Q}_{\text{loss}} = & (A_{\text{mix}} \kappa_{\text{mix}} + A_{\text{solid}} \kappa_{\text{solid}} + A_{\text{liquid}} \kappa_{\text{liquid}}) \frac{dT_0}{dz} \\ & + A_{\text{mix}} \left[\varphi \frac{\gamma}{\gamma-1} \rho_2^0 \frac{n_0}{n_1} (s_2^0 - s_{\text{liquid}}^0) D_{12} \right] \frac{dT_0}{dz}, \quad (27) \end{aligned}$$

and the functions $\Xi_1(\lambda_j)$ and $\Xi_2(\lambda_j)$ are defined in Eq. (14) and Eq. (15).

We assume that the liquid layer coating all surface area of the stack represents a small fraction of the total cross-sectional area of the stack and that the heat conduction through the liquid film may be neglected. This assumption must be investigated experimentally. Since the axial acoustic density weighted species difference velocity is shown to be zero in Ref. 1, the time-averaged acoustic power is

$$\bar{W}_{\text{AC}} = \frac{1}{2} \text{Re} [\tilde{P}_{\text{AC}} U_{\text{vol}}]. \quad (28)$$

This is the first term in Eq. (25). The remainder of Eq. (25) is the total heat flux \bar{Q} .

Equations (25) and (28) provide a complete description of energy fluxes in a thermoacoustic stack with an inert gas-condensing vapor working fluid in a pore with wet walls under the approximations described above.

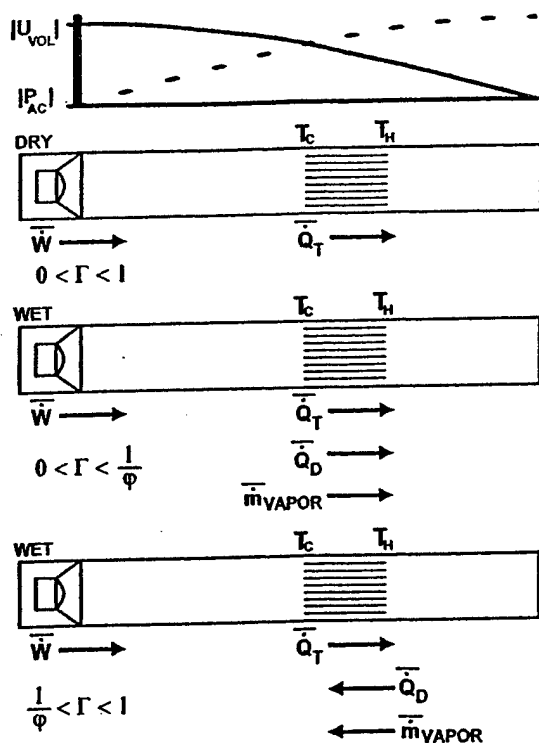


FIG. 1. Mass transport directions in an inert gas-condensing vapor refrigerator for different values of the temperature gradient compared to the heat transport in an inert gas refrigerator. \bar{Q}_T is the thermal heat transport flux, \bar{Q}_D is the heat transport by evaporation-condensation, and \bar{m}_{vapor} is the mass flux of vapor.

V. DISCUSSION

Although Eq. (25) is quite complex, the behavior of the different terms can be explained in terms of the well-understood inert gas thermoacoustic refrigerator. The terms in Eq. (25) containing λ_T are identical to those in Ref. 3 for inert gas refrigeration, as are the gas and solid material heat conduction terms. The new terms, those containing λ_D and the additional term due to steady flow and diffusion, contain the same functions evaluated for slightly different variables. N_{Pr} and N_{Sc} are both on the order of 1, so the behavior of the heat diffusion and mass diffusion terms are similar.

Figure 1 shows that in an inert gas refrigerator with the stack properly positioned, the acoustic power difference across the stack is converted into heat flow toward the hot end of the stack (maintained near room temperature by a heat exchanger). This removes heat from the cold end of the stack leading to cooling below room temperature. The acoustic heat flow is opposed by heat conduction in the gas and stack material and by the second acoustically driven heat term. If losses are ignored, cooling is possible until the temperature gradient is large enough so that the second acoustic heat flux term is equal to and opposite in direction to the first term. This establishes a critical gradient for refrigeration and that the term $\frac{1}{2} \text{Re}[P_{AC} U_{vol} \Xi_1(\lambda_T)]$ produces a heat flux away from the cold end of the stack and the term containing $\text{Im}[\Xi_2(\lambda_T)]$ produces a heat flux toward the cold end.

Equation (13) for the mass flux contains the same functions as the heat flux but evaluated for mass diffusion rather than heat diffusion. The vapor flux terms are in the same

direction as the heat flux terms. When the temperature gradient is small, the total vapor mass flux resulting from the two diffusion terms is in the same direction as the acoustic heat transfer. The ideal critical gradient for the vapor transfer to stop and reverse directions is equal to the critical gradient for heat diffusion multiplied by the factor $1/\phi$. ϕ is usually greater than 1. Here, "ideal" means that the third term in Eq. (13) describing ambient diffusion can be neglected.

The vapor transport heat flux terms in Eq. (25) display the same behavior as the mass flux. We expect ε_D to be positive, since the entropy of the mixture should be greater than the liquid entropy, so that the vapor transport terms add to the acoustic heat transfer terms when the normalized temperature gradient is less than $1/\phi$. When the temperature gradient exceeds the critical gradient for vapor transport, the flow of vapor reverses and the heat transport by acoustic heat diffusion and vapor diffusion oppose each other.

VI. IDEAL COEFFICIENT OF PERFORMANCE AND HEAT TRANSFER

A. Theoretical expressions

The coefficient of performance (COP) is a measure of the efficiency of a refrigerator and is equal to the amount of heat pumped from a cold reservoir divided by the net work input. Thus, the coefficient of performance is

$$\text{COP} = \frac{\bar{Q}_{\text{Net},C}}{\Delta \bar{W}}. \quad (29)$$

The COP can be evaluated numerically by integrating through the stack using Eqs. (1) and (2) and the constancy of Eq. (25). Then, the net work can be evaluated from Eq. (28) evaluated at each end of the stack and by $\bar{Q}_{\text{Net},C}$ evaluated at the cold end of the stack using Eqs. (25) and (28). For this preliminary paper, the inert gas-condensing vapor COP is compared to the inert gas COP in an idealized form to provide an estimate of the potential improvements provided by the wet-walled system. We shall consider the coefficient of performance of an inert gas-vapor thermoacoustic refrigerator in the inviscid, boundary layer, and standing wave limit. The amount of acoustic work used to pump \bar{Q}_C is the difference in acoustic intensity on the hot and cold sides of the stack. Thus,

$$\begin{aligned} \Delta \bar{W} &= -A_{\text{mix}}[(\bar{P}_{AC} \bar{u})_{\text{right}} - (\bar{P}_{AC} \bar{u})_{\text{left}}] \\ &= -L \frac{d}{dz} (\bar{P}_{AC} \bar{U}_{vol}) \\ &= -\frac{L}{2} \frac{d}{dz} (\text{Re}[P_{AC} \bar{U}_{vol}]) \\ &= -\frac{L}{2} \text{Re} \left[P_{AC} \frac{d\bar{U}_{vol}}{dz} + \frac{dP_{AC}}{dz} \bar{U}_{vol} \right], \end{aligned} \quad (30)$$

where we have used the fact that $A_{\text{mix}} u = U_{vol}$ and L is the stack length. The coordinates are indicated in Fig. 1. This approximation puts an upper bound on COP since it assumes losses in other parts of the refrigerator are negligible.

In the standing wave limit, $U_{\text{vol}} = U_{\text{vol},S}$ and $P_{AC} = iP_{AC,S}$. The boundary layer limit of the $F(\lambda_j)$ functions is

$$F(\lambda_j) = 1 - 2\sqrt{i/\lambda_j} = 1 - (1-i)\delta_j/R, \quad (31)$$

with j taken as T referring to thermal effects or D referring to mass diffusion effects.

Applying these limits to the change in acoustic work yields

$$\Delta \bar{W} = -\frac{L}{2} \left[P_{AC,S}^2 \frac{\omega A_{\text{mix}}}{\rho_0 c_p T_0} \left\{ \frac{\delta_T}{R} + \frac{n_2^0}{n_1^0} \frac{\gamma}{\gamma-1} \frac{\delta_D}{R} \right\} - \frac{P_{AC,S} U_{\text{vol},S}}{T_0} \frac{dT_0}{dz} \left\{ \frac{\delta_T}{R} + \frac{n_2^0}{n_1^0} \frac{\gamma}{\gamma-1} \frac{\delta_D}{R} \right\} \right]. \quad (32)$$

The acoustic heat pumped from the cold reservoir can be written with these limits as

$$\bar{Q}_C = \frac{-P_{AC,S} U_{\text{vol},S}}{2} \left\{ \frac{\delta_T}{R} + \varepsilon_D \frac{\delta_D}{R} \right\} + \frac{c_p \rho_0}{2 \omega A_{\text{mix}}} U_{\text{vol},S}^2 \frac{dT_0}{dz} \left\{ \frac{\delta_T}{R} + \varepsilon_D \frac{\delta_D}{R} \right\}. \quad (33)$$

Taking the ratio of Eq. (33) and Eq. (32) and factoring out $-P_{AC,S} U_{\text{vol},S}/2$ from the numerator and $-L \omega A_{\text{mix}} \times P_{AC,S}^2 / \rho_0 c_p T_0$ from the denominator yields

$$\text{COP} = \frac{\rho_0 c_p U_{\text{vol}}}{\omega A_{\text{mix}} P_{AC}} \frac{T_0}{L} \left[\frac{\left\{ \delta_T + \varepsilon_D \delta_D \right\} - \frac{c_p \rho_0 U_{\text{vol},S}}{\omega A_{\text{mix}} P_{AC,S}} \frac{dT_0}{dz} \left\{ \delta_T + \varepsilon_D \frac{\delta_D}{\varphi} \right\}}{\left\{ \delta_T + \frac{n_2^0}{n_1^0} \frac{\gamma}{\gamma-1} \delta_D \right\} - \frac{c_p \rho_0 U_{\text{vol},S}}{\omega A_{\text{mix}} P_{AC,S}} \frac{dT_0}{dz} \left\{ \delta_T + \frac{n_2^0}{n_1^0} \frac{\gamma}{\gamma-1} \delta_D \right\}} \right]. \quad (34)$$

Two factors used in the literature² of inert gas thermoacoustics can be identified:

the dry critical temperature gradient

$$\nabla T_{\text{crit}} = \frac{\omega A_{\text{mix}} P_{AC,S}}{c_p \rho_0 U_{\text{vol},S}}, \quad (35)$$

and the normalized temperature gradient

$$\Gamma = \frac{\nabla T_{\text{mean}}}{\nabla T_{\text{crit}}} = \frac{dT_0/dz}{\nabla T_{\text{crit}}}. \quad (36)$$

The critical temperature gradient is the ambient temperature gradient at which the temperature oscillations in the mixture due to acoustic pressure changes are the same as the local stack temperature when the acoustic wave displaces the mixture along the stack. In other words, at the critical gradient a parcel of gas in the mixture will always be in thermal equilibrium with the local stack temperature and thus will not exchange thermal energy with the stack. However, in a wet system heat is transported by the vapor, as long as the changes in the partial pressure of vapor due to acoustic pressure changes are different from the vapor pressure at the stack wall. The partial pressure at the wall depends only on the temperature and the latent heat through the parameter φ .

We further identify and approximate the Carnot coefficient of performance as

$$\text{COP}_{\text{Carnot}} = \frac{T_C}{T_H - T_C} \approx \frac{T_0}{L} \frac{dz}{dT_0}. \quad (37)$$

This approximation assumes that the temperature gradient is linear and that the cold temperature and the stack average temperature are comparable. Equation (34) can then be expressed as

$$\text{COP} = \Gamma \text{COP}_{\text{Carnot}} \frac{\delta_T(1-\Gamma) + \varepsilon_D \delta_D(1-\varphi\Gamma)}{\delta_T(1-\Gamma) + \frac{\gamma}{\gamma-1} \frac{n_2^0}{n_1^0} \delta_D(1-\varphi\Gamma)}. \quad (38)$$

If there is no vapor in the system, $n_2 = \varepsilon_D = 0$ and the coefficient of performance reduces to the expression $\text{COP} = \Gamma \text{COP}_{\text{Carnot}}$, which agrees with Swift's expression for inert gas thermoacoustics.²

This idealized expression is a valuable aid to understanding the transport properties. The relationship of the change in sign of the mass diffusion acoustic transport as Γ exceeds $1/\varphi$ is clear. The ideal COP will be increased for systems in which the normalized temperature gradient is between zero and $1/\varphi$. If the normalized gradient exceeds $1/\varphi$, the mass diffusion effects oppose the heat diffusion effects. If $\varepsilon_D > (\gamma/\gamma-1)(n_2^0/n_1^0)$ and the normalized gradient is between 0 and $1/\varphi$, the COP of the wet system will be greater than the COP of the dry system with the same dry properties.

B. Example analysis for selected inert gas-vapor mixtures

As an indicator of the potential of inert gas-condensing vapor mixtures to improve thermoacoustic refrigeration, we have calculated the ideal COPs relative to Carnot from Eq. (38) for a thermoacoustic cooler operating between 280 and 310 K as a function of the normalized temperature gradient Γ . Physical properties of the pure gas and vapor at standard state and as functions of temperature may be found in numerous reference books.^{10,11} Transport properties, such as viscosity, thermal conductivity, or diffusion coefficient, of pure gases and binary mixtures of gases are calculated based on gas dynamic theory.¹² Thermophysical properties such as the specific heat and the ratio of specific heats of the mixture

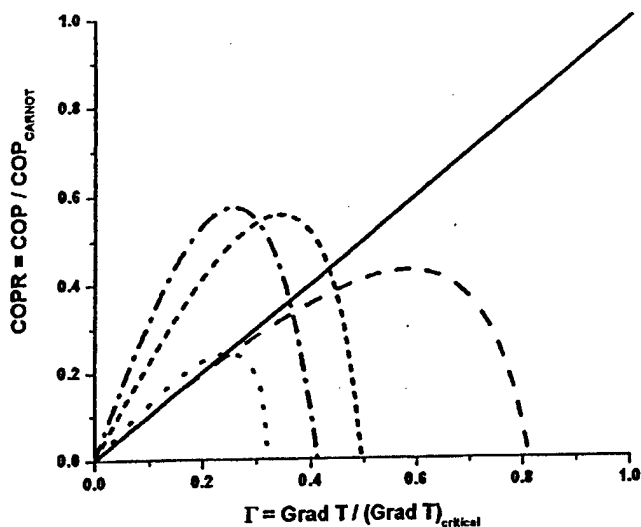


FIG. 2. Coefficient of performance relative to the Carnot coefficient of performance versus normalized temperature gradient for pure helium —, helium and water vapor —, helium and ammonia ···, helium and butane ---, helium and R134a —.

are calculated with mole fraction weighting.¹³ The mole fractions of gas and vapor in the mixture are calculated from the Clausius–Claperyon equation as a function of ambient local temperature.¹⁴ When calculating the mole fractions it is assumed that the mean pressure in the model refrigerator is a constant; thus, an air and water vapor mixture would have equal mole fractions for a mean pressure of 2 atmospheres at 373 K. The numerator of the coefficient of performance relative to Carnot, Eq. (38), is the heat pumped from the cold side of the stack. Thus, the thermophysical quantities of the mixture in the numerator are calculated at an ambient temperature of 280 K. The denominator of Eq. (38) is the work required to pump the heat and is evaluated at the average temperature across the stack (295 K).

Figure 2 indicates that the coefficient of performance of the helium-condensing vapor mixture is higher than that of helium for low normalized temperature gradients. The pure helium system can achieve higher COPs relative to Carnot at higher critical gradients, but as will be demonstrated below, for much lower cooling powers than the helium–ammonia, helium–butane, or helium–R134a mixtures.

Swift² suggests that the potential for different gas mixtures to transport energy can be investigated by assuming $|P_{AC}| \approx \rho c |u_{AC}|$ and that the highest acoustic Mach number ($M = |u_{AC}|/c$) achievable in an acoustic system is constant at approximately 0.1. Further, we set the ratio δ_T/R for each system equal. This corresponds to optimizing the stack spacing for each mixture. Under these assumptions Eq. (33) becomes

$$|\bar{Q}_c| = \frac{\rho c^3 M^2}{2} \left(\frac{\delta_T}{R} \right) [(1 - \Gamma) + \varepsilon_D (1 - \phi \Gamma)]. \quad (39)$$

In Fig. 3 we plot the normalized cooling power

$$|\bar{Q}|_{\text{normalized}} = \frac{\rho c^3 [(1 - \Gamma) + \varepsilon_D (1 - \phi \Gamma)]}{(\rho c^3)_{\text{helium}}}. \quad (40)$$

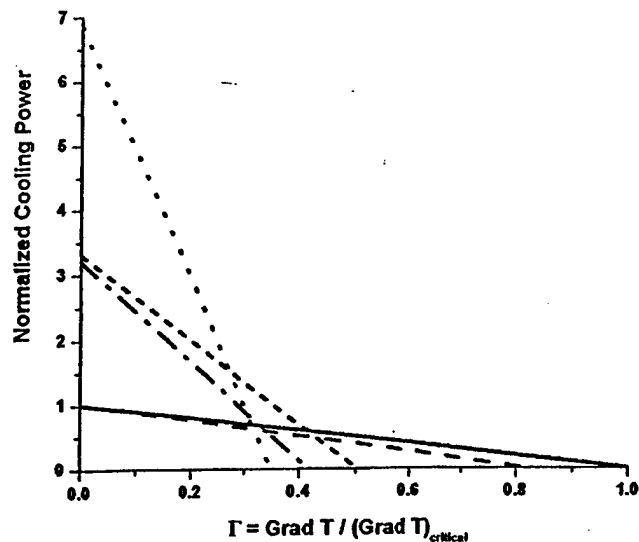


FIG. 3. Normalized cooling power versus normalized temperature gradient for pure helium —, helium and water vapor —, helium and ammonia ···, helium and butane ---, helium and R134a —.

The relative cooling power for the pure helium system is then given by $(1 - \Gamma)$. The thermophysical properties for this calculation are evaluated at 10 atmospheres and 280 K. Large gains in heat flux from the cold heat exchanger are predicted at relatively high COPs. These results are encouraging, but a more realistic calculation should include the additional stack length and attendant increased losses. Initial estimates of the new loss terms in Eq. (25) which have not been included in this analysis indicate that they are at most on the order of the heat conduction losses in inert gas thermoacoustics, but this must also be confirmed by numerical calculations.

VII. CONCLUSIONS

The transport equations for wet thermoacoustics have been developed. The heat energy transported and the coefficient of performance are both increased for wet stacks operated between a temperature gradient of zero and the critical temperature gradient for mass transport. The cooling by vapor transport is analogous to a conventional vapor cycle refrigerator. High entropy vapor is transported from the cold side of the stack to the ambient where it condenses. This system combines thermoacoustic refrigeration with vapor cycle refrigeration in a simple acoustically driven device.

Several experimental and calculational questions must be answered before it can be determined if inert gas-condensing vapor thermoacoustics can be exploited to improve thermoacoustic refrigerators.

- (1) A full numerical calculation must be performed to see if the improvement in cooling power shown above can be achieved in a realistic refrigerator. In this paper we have derived the necessary relations for calculations in DeltaE.⁸
- (2) The behavior of the condensed liquid layer in the stacks must be investigated experimentally for a variety of stack materials and vapor substances. We have performed our calculations with the simplest assumption:

that the liquid layer is thin everywhere and that natural flow occurs in the steady state to return the transported and condensed vapor.

- (3) The behavior of the heat and mass transfer at the heat exchangers must be investigated. Our analysis of enthalpy flow is only valid within the stacks.
- (4) The assumption that the temperature-driven diffusion effect (k_T terms) are negligible should be investigated in more detail. We have relied on the analysis of Ref. 6 in our neglect of k_T , but k_T may be larger in a given candidate system.

There are, of course, other questions and considerations besides those listed above. Nonetheless, this is a promising and interesting field of investigation.

ACKNOWLEDGMENTS

This work is supported by the Office of Naval Research. The authors thank H. E. Bass and Greg Swift for general discussions and the reviewers for their insightful comments and suggestions.

¹R. Raspet, W. Slaton, C. Hickey, and R. Hiller, "Theory of inert gas—condensing vapor thermoacoustics: The propagation equation," *J. Acoust. Soc. Am.* **112**, 1414–1422 (2002).

²G. Swift, "Thermoacoustic engines," *J. Acoust. Soc. Am.* **84**, 1145–1180 (1988).

³W. Arnott, H. Bass, and R. Raspet, "General formulation of thermoacoustics for stacks having arbitrarily shaped pore cross sections," *J. Acoust. Soc. Am.* **90**, 3228–3237 (1991).

⁴G. Swift, "Thermoacoustics: A Unifying Perspective for some Engines and Refrigerators," LA-UR-99-895 (1999).

⁵R. Raspet, C. Hickey, and J. Sabatier, "The effect of evaporation—condensation on sound propagation in cylindrical tubes using the low reduced frequency approximation," *J. Acoust. Soc. Am.* **105**, 65–73 (1999).

⁶C. Hickey, R. Raspet, and W. Slaton, "Effects of thermal diffusion in evaporating and condensing gas–vapor mixtures in tubes," *J. Acoust. Soc. Am.* **107**, 1126–1130 (2000).

⁷W. Slaton, R. Raspet, and C. Hickey, "The effect of the physical properties of the tube wall on the attenuation of sound in evaporating and condensing gas–vapor mixtures," *J. Acoust. Soc. Am.* **108**, 2120–2124 (2000).

⁸B. Ward and G. Swift, *Design Environment for Low-amplitude Thermoacoustic Engines* (Los Alamos National Library, Los Alamos, NM, 1994).

⁹L. D. Landau and E. M. Lifshitz, *Fluid Mechanics*, 2nd ed. (Butterworth-Heinemann, Oxford, 1997).

¹⁰D. R. Lide, *Handbook of Chemistry and Physics* (CRC Press, New York, 1997).

¹¹Carl L. Yaws, *Chemical Properties Handbook* (McGraw-Hill, New York, 1999).

¹²J. V. Hirschfelder, C. Curtiss, and R. B. Bird, *Molecular Theory of Gases and Liquids* (Wiley, New York, 1964).

¹³J. R. Belcher, W. V. Slaton, R. Raspet, H. E. Bass, and J. Lightfoot, "Working gases in thermoacoustic engines," *J. Acoust. Soc. Am.* **105**, 2677–2684 (1999).

¹⁴F. Reif, *Fundamentals of Statistical and Thermal Physics* (McGraw-Hill, New York, 1965).

J. ERNEST KENNEY
EUGENE MAR
RICHARD E. FICHTER
THOMAS J. MOORE
ERIC S. SPECTOR
FELIX J. D'AMBROSIO
JOSEPH DEBENEDICTIS *
BENJAMIN E. URCIA *
WONKI PARK *
JUSTIN J. CASSELL

GEORGE CHUNG CHIN CHEN :

* BAR OTHER THAN VA
: REGISTERED PATENT AGENT

LAW OFFICES
BACON & THOMAS
A Professional Limited Liability Company
PATENT, TRADEMARK AND COPYRIGHT CAUSES
625 SLATERS LANE-FOURTH FLOOR
ALEXANDRIA, VIRGINIA 22314-1176

TELEPHONE
(703) 683-0500
FACSIMILE
(703) 683-1080
(703) 683-0884
E-MAIL
mail@baconthomas.com

February 19, 2004

COPY

Mr. Walter G. Chambliss, Ph.D.
National Center for Natural Products Research
School of Pharmacy
THE UNIVERSITY OF MISSISSIPPI
P.O. Box 907
125 Old Chemistry
University, MS 38677

Re: U.S. Patent Application No. 10/277,817
U.S. Patent Provisional Application No. 60/334,945
Thermoacoustic Refrigeration Device and Method
Inventor: Richard RASPET et al.
Our Ref: BEU/RASP3001
Sponsor's Grant No. N00014-96-1-0074

Dear Mr. Chambliss:

We are pleased to enclose the official United States Letters Patent No. 6,688,112 which matured from the above application on February 10, 2004. The expiration date of the patent is October 23, 2022.

Products using the invention covered by the patent should be marked appropriately with the patent number on the product or the packaging. The absence of such marking may limit one's right to recover from an innocent infringer who has not received notice of the existence of the patent.

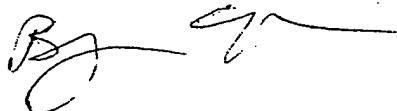
Periodic renewal fees will need to be paid to keep this patent in force. The fees are payable at 3½, 7½ and 11½ years from the grant date of the patent to maintain the patent in force beyond 4, 8 and 12 years, respectively. We will send you a timely reminder for each renewal fee in advance of each due date for payment. Please be sure to keep us advised of any change of your address to enable us to send you timely maintenance fee reminders. Also, please advise us immediately if there is any change of fee status; i.e., small entity or large entity. Maintenance fees must be paid on the basis of the patent owner's current fee status at the time the maintenance fee is paid.

Mr. Walter G. Chambliss, Ph.D.
National Center for Natural Products Research
School of Pharmacy
THE UNIVERSITY OF MISSISSIPPI
February 19, 2004
Page 2

The patent has not been examined in detail to determine if any errors appear therein. It is suggested that you promptly review the patent to determine if any serious errors appear thereon and, if this is the case, that you advise us immediately so that we may take appropriate action. If you wish us to completely proofread the patent against the application file, please advise us accordingly.

Please acknowledge receipt of the enclosed Letters Patent by returning the enclosed copy of this letter to our office.

Very truly yours,
BACON & THOMAS, PLLC

A handwritten signature in black ink, appearing to read 'Bj' followed by a long horizontal stroke.

BENJAMIN E. URCIA

BEU/jsh
Enclosures

The United States of America



The Director of the United States Patent and Trademark Office

Has received an application for a patent for a new and useful invention. The title and description of the invention are enclosed. The requirements of law have been complied with, and it has been determined that a patent on the invention shall be granted under the law.

Therefore, this

United States Patent

Grants to the person(s) having title to this patent the right to exclude others from making, using, offering for sale, or selling the invention throughout the United States of America or importing the invention into the United States of America for the term set forth below, subject to the payment of maintenance fees as provided by law.

If this application was filed prior to June 8, 1995, the term of this patent is the longer of seventeen years from the date of grant of this patent or twenty years from the earliest effective U.S. filing date of the application, subject to any statutory extension.

If this application was filed on or after June 8, 1995, the term of this patent is twenty years from the U.S. filing date, subject to any statutory extension. If the application contains a specific reference to an earlier filed application or applications under 35 U.S.C. 120, 121 or 365(c), the term of the patent is twenty years from the date on which the earliest application was filed, subject to any statutory extensions.

Jon W. I. Dudas

Acting Director of the United States Patent and Trademark Office

NOTICE

If the application for this patent was filed on or after December 12, 1980, maintenance fees are due three years and six months, seven years and six months, and eleven years and six months after the date of this grant, or within a grace period of six months thereafter upon payment of a surcharge as provided by law. The amount, number or timing of the maintenance fees required may be changed by law or regulation. Unless payment of the applicable maintenance fee is received in the United States Patent and Trademark Office on or before the date the fee is due or within a grace period of six months thereafter, the patent will expire as of the end of such grace period.



US006688112B2

(12) **United States Patent**
Raspet et al.

(10) Patent No.: **US 6,688,112 B2**
(45) Date of Patent: **Feb. 10, 2004**

(54) **THERMOACOUSTIC REFRIGERATION
DEVICE AND METHOD**

(75) Inventors: **Richard Raspet, Oxford, MS (US);
William V. Slaton, Eindhoven (NL);
Craig J. Hickey, Oxford, MS (US);
Robert A. Hiller, Oxford, MS (US);
Henry E. Bass, Salt Lake City, UT
(US)**

(73) Assignee: **University of Mississippi, University,
MS (US)**

(*) Notice: Subject to any disclaimer, the term of this
patent is extended or adjusted under 35
U.S.C. 154(b) by 0 days.

(21) Appl. No.: **10/277,817**

(22) Filed: **Oct. 23, 2002**

(65) **Prior Publication Data**

US 2003/0101734 A1 Jun. 5, 2003

Related U.S. Application Data

(60) Provisional application No. 60/334,945, filed on Dec. 4,
2001.

(51) Int. Cl.⁷ **F25B 9/00**

(52) U.S. Cl. **62/6**

(58) Field of Search **62/6, 118, 119,
62/467, 515**

(56) **References Cited**

U.S. PATENT DOCUMENTS

4,114,380 A 9/1978 Ceperley
4,355,517 A 10/1982 Ceperley
4,398,398 A 8/1983 Wheatley et al.
4,489,553 A 12/1984 Wheatley et al.

4,584,840 A	4/1986	Baumann	
4,722,201 A	2/1988	Hofler et al.	
4,858,441 A	8/1989	Wheatley et al.	
4,953,366 A	9/1990	Swift et al.	
5,051,066 A	9/1991	Lucas	
5,165,243 A	11/1992	Bennett	
5,174,130 A	12/1992	Lucas	
5,263,341 A	11/1993	Lucas	
5,303,555 A	4/1994	Chrysler et al.	
5,349,813 A	9/1994	Eisinger	
5,489,202 A	2/1996	Eisinger	
5,515,684 A	5/1996	Lucas et al.	62/6
5,647,216 A	7/1997	Garrett	
5,673,561 A	10/1997	Moss	
5,901,556 A	5/1999	Hofler	
5,953,920 A	9/1999	Swift et al.	
6,032,464 A	3/2000	Swift et al.	
6,145,320 A	11/2000	Kim	
6,164,073 A	12/2000	Swift et al.	
6,233,946 B1	5/2001	Mastuda	
6,248,126 B1	6/2001	Lesser et al.	
6,307,287 B1	10/2001	Garrett et al.	
6,367,263 B1	4/2002	Scott	
2002/0043065 A1	4/2002	Ban et al.	60/320

Primary Examiner—Timothy L. Maust

Assistant Examiner—Malik N. Drake

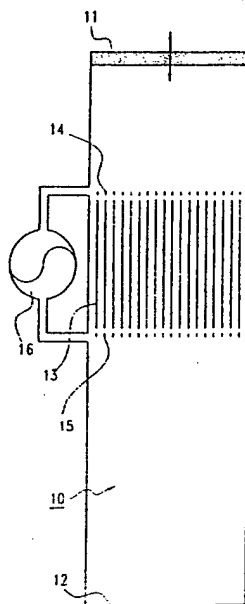
(74) *Attorney, Agent, or Firm*—Bacon & Thomas, PLLC

(57)

ABSTRACT

A thermoacoustic refrigeration device employs a gas-vapor mixture as the working fluid. As a result, the refrigeration device operates according to a modified thermoacoustic refrigeration cycle that adds a condensation-vaporization cycle to the thermoacoustic cycle. The resulting modified refrigeration cycle increases the efficiency of heat transport by harnessing the translational motion of the vapor, as well as the usual acoustic oscillations, to transport the heat energy from one end of a thermal stack to the other.

10 Claims, 2 Drawing Sheets



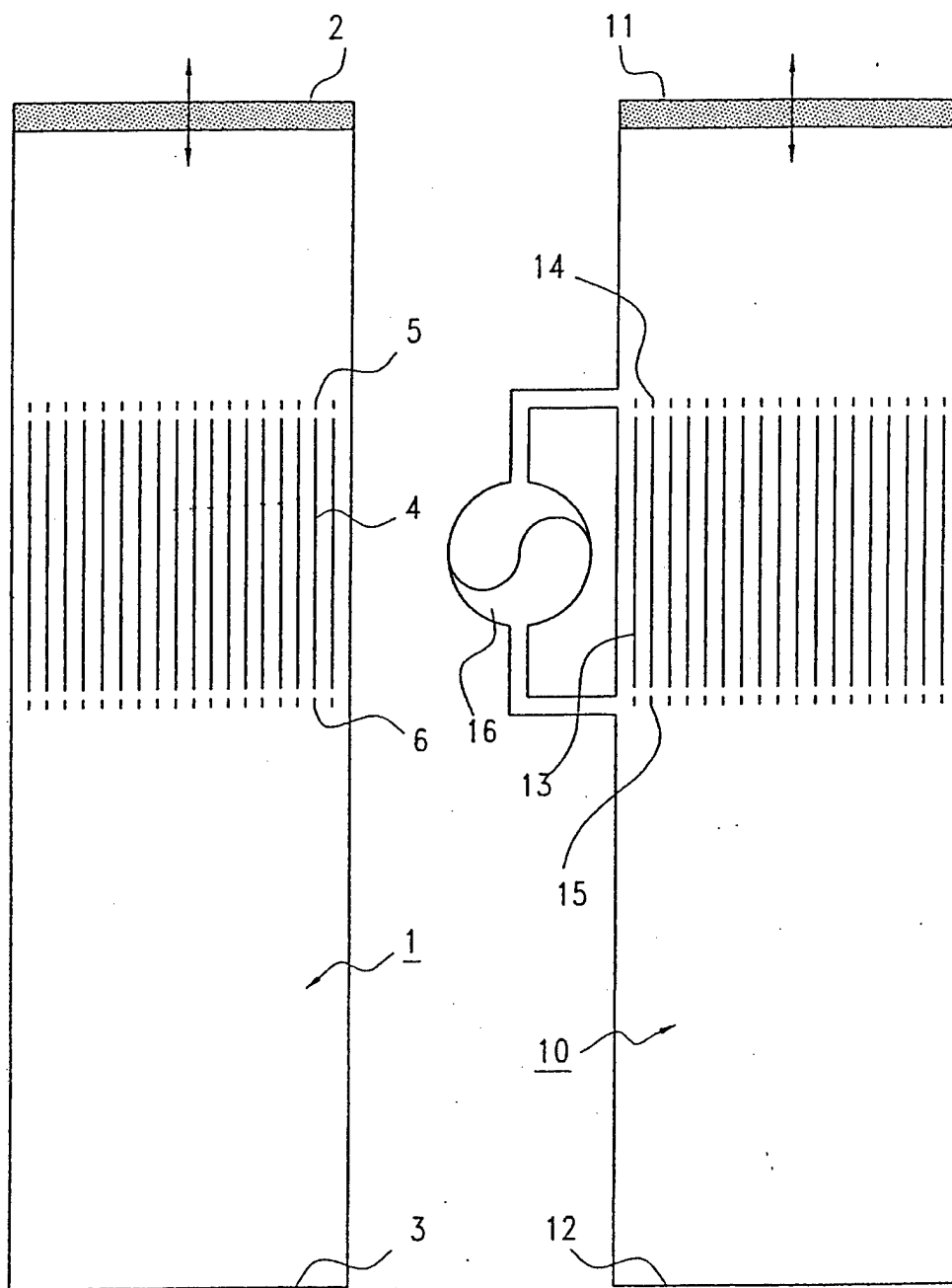


FIG. 1(a)

FIG. 1(b)

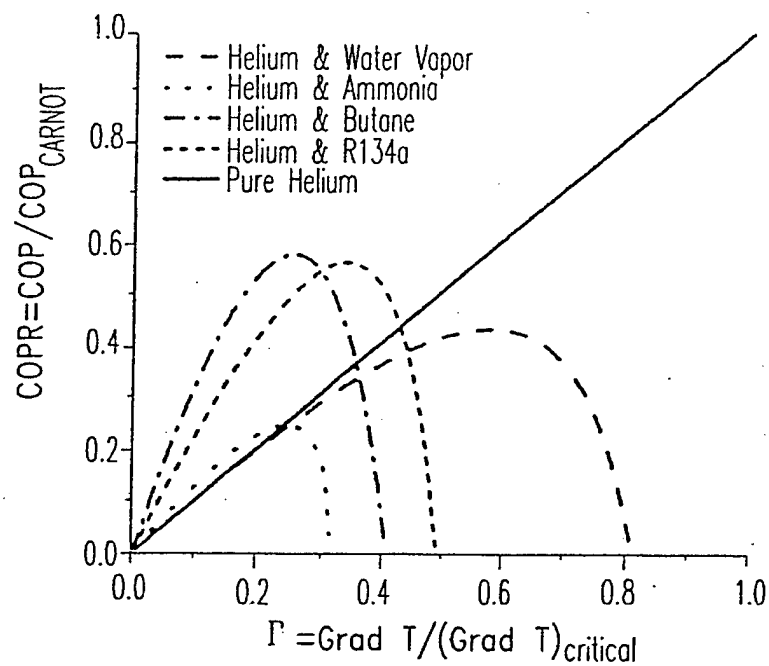


FIG.2(a)

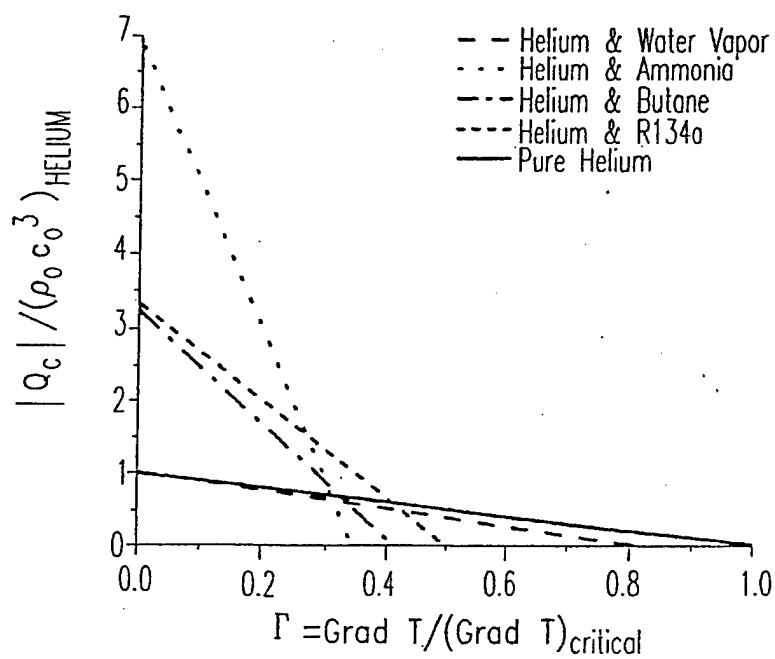


FIG.2(b)

THERMOACOUSTIC REFRIGERATION DEVICE AND METHOD

This application claims the benefit of provisional application No. 60/334,945, filed Dec. 4, 2001.

BACKGROUND OF THE INVENTION

1. Field of the Invention

This invention relates to improvements in thermoacoustic refrigeration, and in particular to a thermoacoustic refrigeration device which employs a gas-vapor mixture as the working fluid.

The invention also relates to a refrigeration method, and in particular to a thermoacoustic refrigeration method that modifies the conventional thermoacoustic refrigeration cycle by adding condensation and vaporization to the thermoacoustic cycle.

In conventional thermoacoustic refrigeration, heat energy is transported primarily or solely by waves acoustically induced in an inert gas. The waves may be standing waves or traveling waves that oscillate or travel from one side of the thermal stack to the other, but in either case are arranged to exploit the temperature differential between areas of compression and areas of rarefaction relative to a thermal stack or regenerator, the thermal stack transferring heat energy from the cold areas to the hot areas to achieve refrigeration. The purpose of the vaporization-condensation cycle of the invention is to increase the efficiency of heat transport by harnessing the translational motion of the vapor, as well as the usual acoustic oscillations, to transport the heat energy from one end of the thermal stack to the other, i.e., by using acoustic mass transfer as well as acoustic heat transfer to transport heat energy up the heat-absorbing stack.

2. Description of Related Art

The basic principles of thermoacoustic refrigeration have been known for more than a decade. In its most basic form, thermoacoustic refrigeration is a process that utilizes acoustic energy to pump or transport heat through a thermal stack between a cold heat exchanger at one end and a hot heat exchanger at the other end, the acoustic energy being in the form of standing or traveling acoustic waves generated by a loudspeaker or similar moving part to cause the mechanical compression and expansion of a working fluid needed for the cooling cycle.

In all such devices, heat is transported solely by acoustic waves in an inert gas. Since the acoustic wave generator is the only moving part in a thermoacoustic refrigeration device, thermoacoustic refrigeration devices have the potential for greater reliability, smaller size, and lower cost than conventional refrigeration devices. Despite these potential advantages, however, thermoacoustic refrigeration has one substantial disadvantage that has heretofore prevented more widespread application of the technology, namely relatively low cooling power in comparison with conventional vapor cycle refrigeration devices. Essentially, the problem is that the oscillations in temperature resulting from application of an acoustic wave to the inert gas used as a working fluid are relatively small and thus have a limited ability to transfer heat.

The basic standing wave version of the conventional thermoacoustic device, illustrated in FIG. 1, is simply a hollow resonance tube 1 filled with an ordinary inert gas and having a speaker or acoustic driver 2 at one end, a hard termination 3 at the other end, and a dry stack or regenerator 4 sandwiched between hot and cold heat exchangers 5,6. The dry stack or regenerator is composed of a solid material and finely divided into sections or passages with which the working fluid exchanges heat with the solid material. In the case of a standing wave, a temperature differential is estab-

lished between areas of compression, in which heat is transferred from the working fluid to the thermal stack, and rarefaction, in which heat is transferred from the thermal stack to the working fluid.

Details of the refrigeration device shown in FIG. 1 may be found in T. Hofler, "Thermoacoustic refrigeration design and performance," Ph.D. dissertation, Physics Department, University of California at San Diego, 1986, while additional information and background on standing or traveling wave refrigeration devices may be found in U.S. Pat. Nos. 4,114,380 (Ceperley); 43,555,517 (Ceperley); 4,398,398 (Wheatley et al.); 4,489,553 (Wheatley et al.); 4,722,201 (Hofler et al.); 4,858,441 (Wheatley et al.); 4,953,366 (Swift et al.); 5,165,243 (Bennett); 5,647,216 (Garrett); 5,673,561 (Moss); 5,901,556 (Hofler); 6,032,464 (Swift et al.); 6,164,073 (Swift et al.); and 6,233,946 (Matsuda).

The present invention, in contrast, augments the purely acoustic heat transfer of previously proposed thermoacoustic refrigeration devices by adding an evaporation-condensation cycle similar to that of conventional vapor-cycle based refrigeration devices, but without the mechanical complexity of the conventional refrigeration device. This is achieved by mixing vapor with an appropriate gas working fluid, and by permitting the working fluid to locally evaporate and condense on the hot and cold ends or sides of the thermal stack, thereby transferring heat energy by acoustic mass transfer as well as by acoustic heat transfer.

With the proper selection of the gas-vapor mixtures used as working fluids in the thermoacoustic refrigeration devices of the invention, criteria for which are described below, predicted heat pumping power and coefficient of performance relative to the Carnot cycle can be increased for an inert gas-vapor working fluid compared to a similar purely inert gas working fluid.

SUMMARY OF THE INVENTION

It is accordingly an objective of the invention to provide a thermoacoustic refrigeration device that provides improved performance without a substantial increase in complexity.

It is also an objective of the invention to provide a thermoacoustic refrigeration method that increases the heat transfer capability of the thermoacoustic refrigeration device by modifying the conventional thermoacoustic refrigeration cycle to include evaporation and condensation, thereby enlisting translation of vapors as a mechanism for heat transfer in addition to the conventional acoustic heat transfer.

It is a still further objective of the invention to provide criteria for selecting a gas-vapor mixture that can be used in a thermoacoustic refrigeration device in order to increase performance by making use of translating vapor to carry heat energy, and condensation of the vapor to transfer the heat energy to the refrigeration stack.

According to a preferred embodiment of the invention, the thermoacoustic refrigeration device of the invention may include, as in a conventional thermoacoustic refrigeration device, a resonance tube filled with a working fluid, an acoustic driver at one end, a hard termination at the other end, a thermal stack situated within the tube and made up of a finely divided structure composed of a solid material, and cold and hot heat exchangers at opposite ends of the stack. Unlike the inert gas of the conventional device, however, the working fluid employed by the refrigeration device of the preferred embodiment is a gas-vapor mixture, the stack is composed of a solid material that is wettable by condensed vapor, and means are provided to return condensed vapor from the cold side of the stack to the hot side. The return means may be a pump or, for simplicity, a wick.

Alternatively, the stack may be arranged to permit return solely or primarily by gravity.

The method of the preferred embodiment of the invention modifies conventional thermoacoustic cooling, which simply involves generating acoustic waves in the working fluid, by modifying the thermoacoustic refrigeration cycle to include at least the following steps:

- a. In response to an applied acoustic wave, a parcel of gas in the working fluid is caused to undergo translation along the stack and consequent acoustic compression, thereby decreasing the parcel's volume and increasing its temperature;
- b. The decreased volume and increased temperature increases the partial pressure of the vapor within the parcel;
- c. The parcel then slows, stops, and reverses its translational motion, while at the same time exchanging heat and vapor with the stack as a result of the parcel's increased temperature relative to the stack;
- d. At the time of reversal, the increased partial pressure relative to the vapor pressure at the stack wall causes vapor to condense from the parcel to the stack plate;
- e. The gas parcel then undergoes acoustic rarefaction and is translated back past the ambient position, increasing its volume and decreasing its temperature;
- f. The acoustic rarefaction in turn causes a decrease in partial pressure of vapor within the parcel;
- g. The parcel again slows, stops and reverses its translational motion while exchanging heat and vapor with the stack, this time absorbing heat from the stack;
- h. Since the partial pressure of the vapor in the parcel is lower than the vapor pressure at the stack wall, the vapor will evaporate to the parcel from the liquid layer coating the stack.

Because of the modifications to the conventional thermoacoustic refrigeration cycle, heat is transported from one end of the stack to the other, both as a result of the temperature differentials resulting from compression and rarefaction of the gas, and as a result of vapor moving up the stack and exchanging heat at each end.

The performance of the refrigeration device of the preferred embodiment depends on the characteristics of the gas-vapor mixture. According to another aspect of the invention, the gas-vapor mixture is chosen to:

- a.) maximize the amount of heat carried by mass relative to the amount of heat carried by thermal effects, represented by ϵ_D defined by the relationship:

$$\epsilon_D = \frac{1}{c_p} \frac{\rho_2^\circ}{\rho_o} \frac{n_o}{n_1^\circ} \frac{\gamma}{\gamma - 1} (s_{mix} - s_{liquid}),$$

where ρ_2° is the mass density of the vapor in the mixture, ρ_o is the mass density of the mixture, n_o is the number density of the mixture, n_1° is the number density of the inert gas, s_{mix} is the entropy per unit mass of the mixture, s_{liquid} the entropy per unit mass of the condensed liquid, and c_p is the heat capacity at constant pressure per unit mass of the mixture and,

- b.) minimize the heat transfer coefficient W defined by the relationship:

$$\varphi = \frac{\gamma - 1}{\gamma} \frac{l}{R_o T_o},$$

where γ is the ratio of the specific heats of the gas and of the mixture; l is the latent heat of vaporization of the mixture

per mole, T_o is the ambient temperature, and R_o is the universal gas constant. This parameter controls the critical gradient and therefore the stack length necessary to produce a given temperature difference.

Although a particular standing wave device is illustrated herein, those skilled in the art will appreciate that the device and the method of the invention may also be applied to traveling wave refrigeration techniques, and that the simple tube, stack, and heat exchange structure of the illustrated embodiment may be freely varied by those skilled in the art in accordance with the principles described in any of the above references, without departing from the scope of the invention, so long as the modified device employs a gas-vapor mixture as the working fluid.

BRIEF DESCRIPTION OF THE DRAWINGS

FIG. 1a is a schematic diagram of a conventional standing wave-type thermoacoustic refrigeration device.

FIG. 1b is a schematic diagram of a thermoacoustic refrigeration device constructed in accordance with the principles of a preferred embodiment of the invention.

FIG. 2a is a graph of the ideal coefficient of performance relative to Carnot plotted against the normalized temperature gradient.

FIG. 2b is a graph of the normalized cooling power for the inert gas-vapor mixtures whose coefficient of performance is plotted in FIG. 2a.

DETAILED DESCRIPTION OF THE PREFERRED EMBODIMENTS

As illustrated in FIG. 1b, which is a conceptual drawing of a refrigeration device constructed according to the principles of a preferred embodiment of the invention, the thermoacoustic refrigeration device of the preferred embodiment may include a resonance tube 10 filled with a working fluid, an acoustic driver 11 at one end, a hard termination 12 at the other end, a thermal stack 13 situated within the tube and made up of a finely divided structure composed of a solid material, and respective cold and hot heat exchangers 14, 15 at opposite ends of the stack. The heat exchangers may include conduits (not shown) through which are supplied hot and cold liquids, or any other heat conducting structure, for the purpose of transporting heat away from the thermal stack, in the manner of a conventional heat exchanger. The working fluid employed by the refrigeration device of the preferred embodiment is a gas-vapor mixture whose composition meets the criteria described below, while the stack is composed of a solid material that is wettable by condensed vapor such that a thin sheet of liquid will cover the stack. Finally, means are provided to return condensed vapor from the cold side of the stack to the hot side. The return means may be a pump 16, as illustrated or, for simplicity, a wick. Alternatively, the stack may be arranged to permit return solely or primarily by gravity.

According to the preferred embodiment of the invention, a modified thermoacoustic refrigeration cycle, including vaporization and condensation steps, is provided as follows:

- a. In response to an acoustic wave applied by acoustic driver 11, a parcel of gas in the working fluid is caused to undergo translation along the stack and consequent acoustic compression, thereby decreasing the parcel's volume and increasing its temperature;
- b. The decreased volume and increased temperature increases the partial pressure of the vapor within the parcel;
- c. The parcel then slows, stops, and reverses its translational motion, while at the same time exchanging heat and vapor with the stack 13 as a result of the parcel's increased temperature relative to the stack;

d. At the time of reversal, the increased partial pressure relative to the vapor pressure at the stack wall causes vapor to condense from the parcel to the adjacent stack plate;

e. The gas parcel then undergoes acoustic rarefaction and is translated back past the ambient position, increasing its volume and decreasing its temperature;

f. The acoustic rarefaction in turn causes a decrease in partial pressure of vapor within the parcel;

g. The parcel again slows, stops and reverses its translational motion while exchanging heat and vapor with the stack, this time absorbing heat from the stack;

h. Since the partial pressure of the vapor in the parcel is lower than the vapor pressure at the stack wall, the vapor will evaporate to the parcel from the liquid layer coating the stack.

This thermodynamic cycle describes how an inert gas-vapor working fluid will transport heat and vapor from one end of the stack to the other. The vapor is chosen so that the stack remains wet over the temperature range of interest. With the properly chosen inert gas and condensing vapor, heat energy is carried up the stack by acoustic mass transfer as well as by acoustic heat transfer. The vapor moving up the stack condenses on the walls of the stack and will be returned either by gravity or by an external wicking arrangement or pump 16.

The equations describing acoustic propagation in an inert gas-vapor mixture in a thermoacoustic stack are the acoustic wave equation and the heat pumping equation, both of which are well-known and not further described here. From these equations, figures of merit such as the coefficient of performance and the normalized cooling power may be derived. These figures of merit are used as criteria for selection of the gas-vapor mixture.

The coefficient of performance (COP) is a measure of the efficiency of a refrigerator and is equal to the amount of heat pumped from a cold reservoir divided by the net work input. An upper bound for this efficiency may be calculated by making well-known simplifications to the full acoustic propagation equations. These simplifications include neglecting viscous losses, assuming boundary layer behavior of the acoustic propagation equations and assuming an acoustic standing wave is present; a further simplification may be made by assuming a linear temperature gradient within the stack. The COP relative to the Carnot efficiency for an inert gas-vapor mixture with the above simplifications is then,

$$COPR = \Gamma \frac{\delta_T(1 - \Gamma) + \epsilon_D \delta_D(1 - \phi\Gamma)}{\delta_T(1 - \Gamma) + \frac{\gamma}{\gamma - 1} \frac{n_2^0}{n_1^0} \delta_D(1 - \phi\Gamma)}$$

where Γ is the actual temperature gradient across the stack normalized by the dry critical temperature gradient, δ_T and δ_D are the thermal and diffusion penetration depths within the mixture, γ is the ratio of specific heats for the mixture, n_1^0 and n_2^0 are the number densities of the inert gas and vapor respectively. The heat transfer coefficient ϕ is defined by the relationship:

$$\phi = \frac{\gamma - 1}{\gamma} \frac{l}{R_0 T_0}$$

where Γ is the ratio of the specific heats of the gas and of the mixture; l is the latent heat of vaporization of the mixture per mole, T_0 is the ambient temperature, and R_0 is the universal gas constant. An expression that describes the relative amount of heat transported by thermal or mass diffusion effects is,

$$\epsilon_D = \frac{1}{c_p} \frac{\rho_2^0}{\rho_0} \frac{n_2^0}{n_1^0} \frac{\gamma}{\gamma - 1} (s_{mix} - s_{liquid}),$$

where ρ_2^0 is the mass density of the vapor in the mixture, ρ_0 is the mass density of the mixture, n_2^0 is the number density of the mixture, n_1^0 is the number density of the inert gas, s_{mix} is the entropy per unit mass of the mixture s_{liquid} the entropy per unit mass of the condensed liquid, and c_p is the heat capacity at constant pressure per unit mass of the mixture.

The expression for the idealized COPR may now be considered in more detail. If there is no vapor within the gas mixture the ϵ_D and n_2^0 terms go to zero and the expression reduces to the accepted idealized efficiency for a dry thermoacoustic refrigerator. It is also clear from the expression for the ideal COPR for an inert gas-vapor mixture that the efficiency will be increased relative to a comparable dry mixture for values of the normalized temperature gradient between zero and $1/\phi$ and if ϵ_D is greater than

$$\frac{\gamma}{\gamma - 1} \frac{n_2^0}{n_1^0}$$

This expression for the ideal coefficient of performance relative to Carnot for 5 different working fluids as a function of the normalized temperature gradient is depicted in FIG. 2a. The thermal properties of the working fluids, such as density, number density, and specific heat, were calculated using well-known formula from gas property handbooks, further the mean pressure is assumed to be a constant at 10 bar for all working fluids. Since the numerator of the idealized efficiency represents the heat pumped from a cold reservoir the working fluid properties in the numerator are evaluated at a temperature of 280 K (7° C.), while the denominator of the idealized efficiency represents the work required to pump this heat from a hot thermal reservoir at 310 K (37° C.) and so the working fluid properties in the denominator are evaluated at an average temperature of 295 K (22° C.).

FIG. 2a indicates that the idealized efficiency is increased for helium-condensing vapor working fluids compared to a pure helium working fluid at low values of the normalized temperature gradient. For the helium-butane and helium-R134a working fluids at low values of Γ the idealized efficiency may be increased by a factor of 3. FIG. 2a also demonstrates the dependence of the COPR on the value of ϕ for the working fluids under consideration. The COPR of the inert gas-vapor working fluid is greater than the dry COPR as long as the normalized temperature gradient lies between zero and $1/\phi$.

A further figure of merit for an inert gas-vapor thermoacoustic refrigerator is an expression for the normalized cooling power given by,

$$\bar{Q}_c |_{Normalized} = \frac{\rho_0 c^3 [(1 - \Gamma) + \epsilon_D (1 - \phi\Gamma)]}{(\rho_0 c^3)_{Helium}}$$

where c is the speed of sound in the working fluid and other variables are the same as defined before. Standard assumptions were used to derive this formula such as assuming a constant acoustic Mach number and assuming the ratio of the thermal penetration depth in the working fluid to the characteristic open dimension within the stack is the same for the wet and dry working fluids.

The normalized cooling power for various working fluids is depicted in FIG. 2b as a function of the normalized

temperature gradient. The working fluids considered in this calculation are the same as those shown in FIG. 2a. The thermal properties of the working fluids are calculated using standard formula from gas property handbooks at a mean pressure of 10 bar and an ambient temperature of 280K (7° C.). The normalized cooling power for the helium-butane and helium-R134a working fluids at low values of Γ is approximately a factor of 3 greater than the pure helium working fluid. FIGS. 2a and 2b when taken together demonstrate that for properly chosen inert gas-vapor working fluids the idealized efficiency and normalized cooling power will be increased compared to a dry working fluid as long as the normalized temperature gradient lies between zero and $1/\phi$.

Having thus described a preferred embodiment of the invention in sufficient detail to enable those skilled in the art to make and use the invention, it will nevertheless be appreciated that numerous variations and modifications of the illustrated embodiment may be made without departing from the spirit of the invention, and it is intended that the invention not be limited by the above description or accompanying drawings, but that it be defined solely in accordance with the appended claims.

We claim:

1. A thermoacoustic refrigeration device, comprising:
 - a housing arranged to contain a working fluid;
 - an acoustic driver arranged to induce acoustic waves in said working fluid; and
 - a thermal stack situated within the housing and arranged to transfer heat energy from the working fluid to a hot heat exchanger, and to supply heat energy from a cold heat exchanger to the working fluid,
 wherein the working fluid is a gas-vapor mixture, and wherein the stack is wettable by condensed vapor such that vapor condenses on the stack during a refrigeration cycle in order to expedite said transfer of each energy from the working fluid to the hot heat exchanger.
2. A thermoacoustic refrigeration device as claimed in claim 1, wherein said stack is a finely divided structure composed of a solid material and having a length that is less than a wavelength of said waves.
3. A thermoacoustic refrigeration device as claimed in claim 1, wherein said housing includes a hard termination at an end opposite an end where the acoustic driver is situated, and wherein said acoustic waves are standing waves.
4. A thermoacoustic refrigeration device as claimed in claim 1, wherein said working fluid is selected to:
 - a. maximize the amount of heat carried by mass relative to the amount of heat carried by thermal effects, represented by ϵ_D defined by the relationship:

$$\epsilon_D = \frac{1}{c_p} \frac{\rho_2^o}{\rho_o} \frac{n_o}{n_1^o} \frac{\gamma}{\gamma-1} (s_{mix} - s_{liquid}),$$

where ρ_2^o is the mass density of the vapor in the mixture, ρ_o is the mass density of the mixture, n_o is the number density of the mixture, n_1^o is the number density of the inert gas, s_{mix} is the entropy per unit mass of the mixture, s_{liquid} the entropy per unit mass of the condensed liquid, and c_p is the heat capacity at constant pressure per unit mass of the mixture and,

- b. minimize the heat transfer coefficient ϕ defined by the relationship:

$$\phi = \frac{\gamma-1}{\gamma} \frac{l}{R_o T_o},$$

where γ is the ratio of the specific heats of the gas and of the mixture; l is the latent heat of vaporization of the mixture per mole, T_o is the ambient temperature, and R_o is the universal gas constant. This parameter controls the critical gradient and therefore the stack length necessary to produce a given temperature difference.

5. A thermoacoustic refrigeration device as claimed in claim 1, further comprising return means for transporting condensed vapor from one end of said stack to the other.

6. A thermoacoustic refrigeration device as claimed in claim 5, wherein said return means is an external wick.

7. A thermoacoustic refrigeration device as claimed in claim 5, wherein said return means is an external pump.

8. A thermoacoustic refrigeration device as claimed in claim 1, wherein said condensed vapor is arranged to return to an opposite side of the stack by force of gravity.

9. A thermoacoustic refrigeration method, comprising the steps of:

acoustically driving a working fluid to cause waves in the working fluid to transport heat energy from one side of a thermal stack to the other side;

evaporating a vapor in the working fluid to increase heat transfer to the working fluid at one end of the stack; and

condensing the vapor to increase heat transfer from the working fluid at a second end of the stack.

10. A thermoacoustic refrigeration method, comprising the following refrigeration cycle:

a. an acoustic wave applied by an acoustic driver causes a parcel of gas in a working fluid to undergo translation along a thermal stack and consequent acoustic compression, thereby decreasing the parcel's volume and increasing its temperature;

b. the decreased volume and increased temperature increases the partial pressure of the vapor within the parcel;

c. the parcel then slows, stops, and reverses its translational motion, while at the same time exchanging heat and vapor with the stack as a result of the parcel's increased temperature relative to the stack;

d. at the time of reversal, the increased partial pressure relative to the vapor pressure at the stack wall causes vapor to condense from the parcel to the adjacent stack plate;

e. the gas parcel then undergoes acoustic rarefaction and is translated back past the ambient position, increasing its volume and decreasing its temperature;

f. the acoustic rarefaction in turn causes a decrease in partial pressure of vapor within the parcel;

g. the parcel again slows, stops and reverses its translational motion while exchanging heat and vapor with the stack, this time absorbing heat from the stack; and

h. since the partial pressure of the vapor in the parcel is lower than the vapor pressure at the stack wall, the vapor will evaporate to the parcel from the liquid layer coating the stack.

* * * * *

**An Impedance Tube Investigation of Porous Materials
in the Presence of a Multi-phase Working Fluid**

**A Thesis
Presented for the
Master of Science
Degree
The University of Mississippi**

Dan Brown

August 2003

Abstract

An impedance tube is used to measure the acoustical impedance of a porous sample (thermoacoustic stack) with a working fluid in multiple phases. The acoustic medium is a mixture of an inert gas, helium, and a condensable fluid, either n-butane or acetone. The results are compared to predictions of first order acoustical theory. Two-microphone impedance measurements, impedance translation, and problems of fluid handling are discussed.

Table of Contents

Chapter	Page
I. Introduction.....	1
II. Theory – Wet Thermoacoustics.....	2
III. Theory - Measurement.....	17
IV. Experimental Setup.....	19
a. General Description.....	21
b. Corrosive Vapors.....	22
c. Transducer separation.....	23
d. Transducer Selection.....	24
e. Data Sets.....	27
V. Data & Analysis.....	31
VI. Discussion.....	45
Appendix A.....	49

Bibliography

Vita

List of Figures

Figure Page

(1): A Lagrangian model for a dry thermoacoustic refrigerator.	3
(2): Comparison of normalized coefficient of performance and normalized cooling power for wet and dry thermoacoustic refrigerators.....	6
(3): A Lagrangian model for a wet thermoacoustic refrigerator.....	7
(4): The influence of mass diffusion on the wavenumber in the stack and the impedance of our system.....	14
(5): Flow chart for acquisition of data from the experimental system.....	15
(6): Flow chart for theoretical prediction of impedance at stack face using the impedance translation theorem (ITT).....	16
(7): Schematic of System.....	19
(8): Photo of system.....	20
(9): Sample holder and transducers.....	21
(10): Damaged driver.....	23
(11): Endevco Model 8510B-1 piezoresistive pressure transducer	25
(12): Endevco 8510B-1 response to DC pressure.....	26
(13): Coherence when proper signal-to-noise ratio is not obtained.....	27
(14): FFT of data set with insufficient signal-to-noise ratio.....	28
(15): Example of proper coherence.....	29
(16): FFT of data set with sufficient signal-to-noise ratio.....	30
(17): Celcor stack.....	31
(18): Measured and calculated impedance at the face of the stack.....	37
(19): Comparing our code to deltaE.....	39
(20): Effect of Porous Walls	43
(21): Wet data	45
(A1): Transducers mounted in radial symmetry for calibration.....	52

List of Symbols

A	cross sectional area
c_p	isobaric heat capacity
c	speed of sound
d_w	depth (wall pores)
D_{12}	mass diffusion coefficient
f	frequency
F	dissipation function
H_{12}	transfer function
k	wave number
l	separation (first transducer and stack face)
n_1, n_2	number density gas, number density vapor
$N_{Pr} = \frac{\mu c_p}{\kappa}$	Prandtl number
$N_{Sc} = \frac{\mu}{\rho_0 D_{12}}$	Schmidt number
P	pressure
R	characteristic radius (ratio; circumference and area)
\bar{R}_0	universal gas constant
s	separation (transducers)
S_{12}, S_{11}	cross spectrum, auto spectrum
T	temperature
U	volumetric velocity
z	position perpendicular to sound propagation

Z	impedance
α	attenuation factor
Γ	normalized temperature gradient
γ	ratio; isobaric and isochoric specific heats
κ	thermal conductivity
$\lambda_{\mu} = R\sqrt{\frac{\rho\omega}{\mu}}$	shear wave number
$\lambda_T = R\sqrt{\frac{\rho\omega c_p}{\kappa}}$	thermal wave number
$\lambda_D = R\sqrt{\frac{\omega}{D_{12}}}$	diffusion wave number
μ	dynamic viscosity
$\Omega, \Omega_w, \Omega_T$	traditional porosity, wall porosity, adjusted total porosity
ω	angular frequency
ϕ	latent heat parameter
ρ	density

I. Introduction

Thermoacoustic refrigerators will never achieve widespread use unless their efficiency can be increased. The inefficiency of these machines is not limited by current engineering, but is inherent to this method of heat pumping. Recent theoretical developments [Raspet (2002), Slaton (2002)] look to increase both the efficiency and heat pumped in the thermoacoustic cycle by adding a condensable vapor to the inert working gas. This additional vapor undergoes phase changes between liquid and gas during an acoustic cycle. Exploitation of the latent heat accompanying the phase changes may allow increases in both efficiency and power density for temperature gradients that provide significant heat transfer conditions.

This theory requires the surface of the stack be coated with a thin fluid layer. We propose a method for wetting the stack. Will the presence of a saturated condensable vapor form a thin layer over all the surfaces of a stack? If so, does the proposed theory correctly describe acoustic propagation in an inert gas/vapor mixture? How does the presence of vapor such as acetone, isopropanol, or n-butane affect the elements of an acoustic system?

To answer these questions, we built a two-microphone impedance tube capable of measuring stacks in the presence of condensable vapors. We directly measured the impedance at the face of the stack and compared this to the predicted impedance at the same location. A model using the theory proposed by Slaton, et. al., generated the predicted impedance.

We begin by outlining the basic theory of thermoacoustics with a vapor present and the equations relevant to our impedance tube measurements. An explanation of the two-microphone method of measuring acoustic impedance follows, as well as the description of the system we have built. We conclude with the data collected and discuss what we learned and ideas for future work.

II. Theory – Wet Thermoacoustics

In this section, we establish a qualitative understanding of the importance and mechanism of thermoacoustics in the presence of a condensable working fluid. After this is covered, we want to study the equations governing acoustic propagation in this type of working fluid. These equations illustrate that the effects of a condensable working fluid will create a detectable change in the measured impedance of a stack. Finally, we discuss the code used to generate the theoretical data to which the measured data is compared.

The details of wet thermoacoustics can be daunting; a simplified explanation will illuminate the important concepts. In the Lagrangian picture of thermoacoustic refrigerators [Swift (1988)], Fig. (1), we have a parcel of gas near some surface whose position and pressure oscillate. At each extreme of its displacement the parcel experiences either a maximum or minimum acoustic pressure. The compression and rarefaction cause a temperature difference between the gas parcel and surface. Heat will be absorbed from the surface by the rarefied parcel and deposited to the surface by the compressed parcel. This develops a temperature difference along the surface near the oscillating parcel. This is shown in Figure (1) as heat is pumped from left to right.

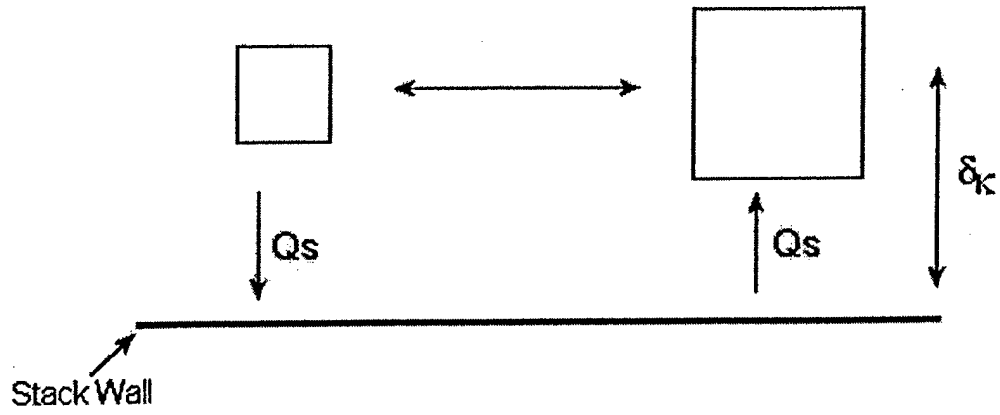
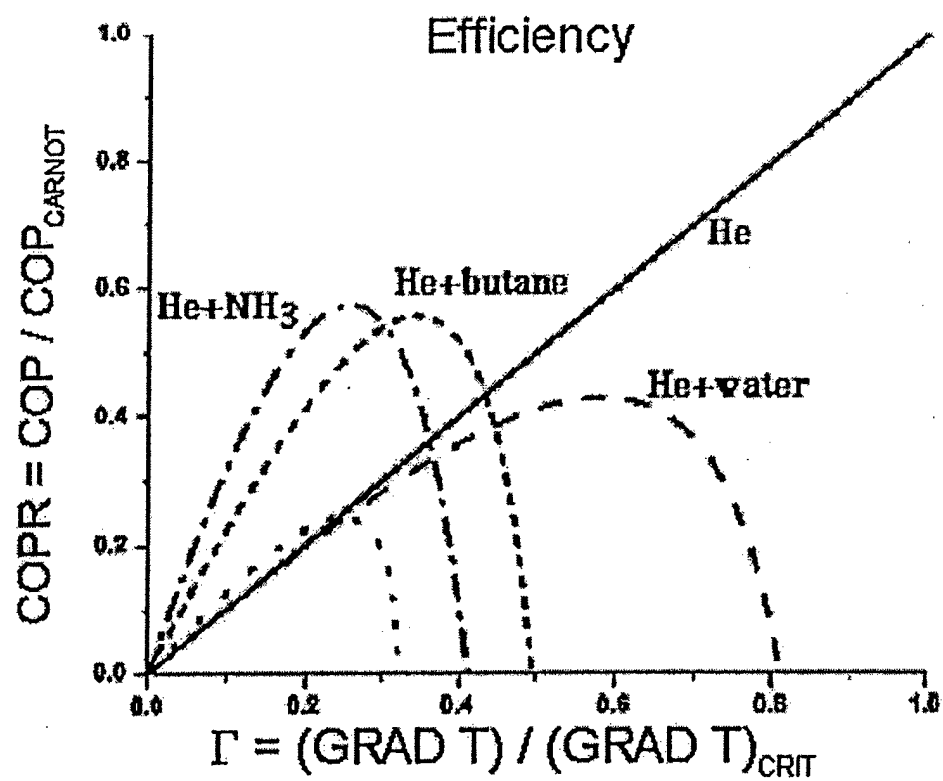


Figure (1): A Lagrangian model for a dry thermoacoustic refrigerator. Compression and rarefaction of a gas parcel in the acoustic cycle allow for heat pumping due to changes in gas temperature.

Although the practical design of a thermoacoustic refrigerator is simple, applications are hampered by their inherent inefficiencies. The addition of a condensable vapor to these machines may increase their efficiency as well as power density. For temperature gradients near the critical temperature gradient, thermoacoustic refrigerators are extremely efficient (Figure 2), but these operating conditions are not useful because of the small power density associated with efficient heat pumping. For significant heat pumping, as required by realistic machines, the efficiency is lower, and the temperature gradient may be less than 50% of the critical temperature gradient. Looking at the efficiency and power density of a helium refrigerator at $\Gamma = 0.5$, we see an equal or better efficiency can be attained using a helium/n-butane mixture over $0.25 \leq \Gamma \leq 0.40$, and the power density is superior to that of helium over the entire range.

A compromise between efficiency and cooling power must be reached in the design of thermoacoustic refrigerators. The addition of condensable working fluids creates regions over certain temperature gradients where increases in both efficiency and cooling power are possible.



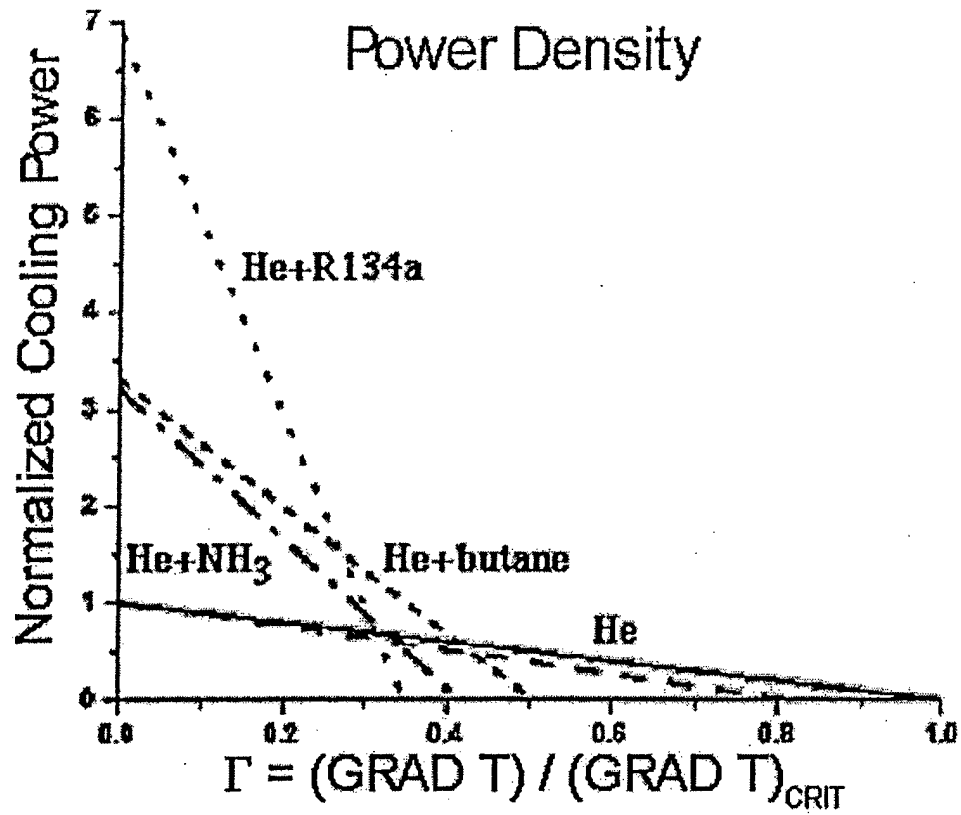


Figure (2): Comparison of normalized coefficient of performance and normalized cooling power for wet and dry thermoacoustic refrigerators. For a given temperature gradient, it is possible to increase both cooling power and efficiency over that of a dry system [Slaton (2002)].

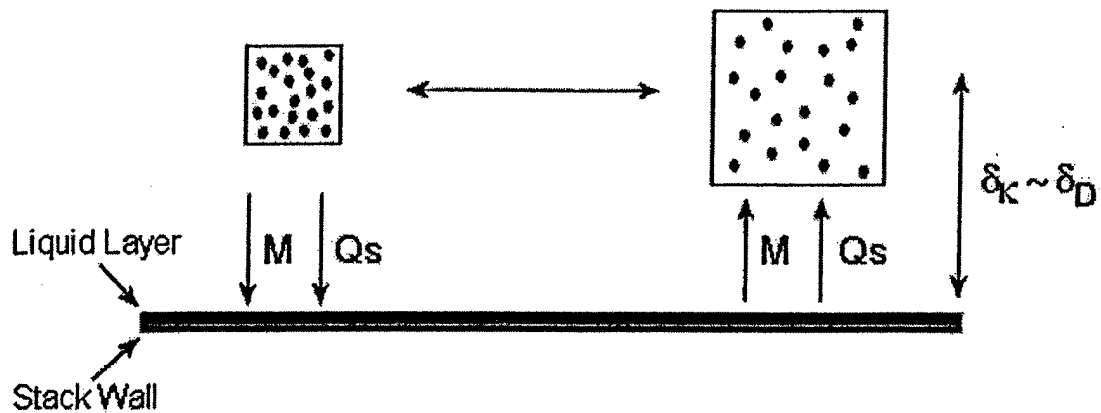


Figure (3): A Lagrangian model for a wet thermoacoustic refrigerator. Mass diffusion is present along with sensible heat pumping. Evaporation and condensation at the liquid layer increases the heat pumped with each acoustic cycle.

In the previous example of dry thermoacoustics, the only working fluid present in the system is an inert gas or a mixture of inert gasses. In a wet thermoacoustic refrigerator, the working fluid consists of a mixture of inert gas and condensable vapor. The vapor is added to the inert working gas until the system is saturated. This occurs when the rate of liquid evaporation equals the rate of vapor condensation, or when the vapor's partial pressure equals the liquid's vapor pressure. It is assumed that once saturation is reached, all surfaces have a thin layer of liquid present on them. The presence of both the liquid and gas phase in equilibrium is the key to wet thermoacoustics.

During the acoustic cycle, the equilibrium is disturbed. The vapor's partial pressure will depart from the liquid's vapor pressure, resulting in evaporation or

condensation. In a Lagrangian picture similar to that for the dry case (Figure 3), a concentration gradient develops between the rarefied and compressed parcels and the surrounding vapor. The result is mass diffusion. As the gas parcel is rarefied, the partial pressure of the vapor in that parcel is reduced below the partial pressure of the vapor above the adjoining liquid layer. A concentration gradient develops and vapor will pass into the parcel. The vapor that passes into the parcel must be replaced in order to maintain equilibrium with the liquid layer. As a result, some of the liquid evaporates. The surface now loses the latent heat of vaporization in addition to the sensible heat lost due to adiabatic expansion of the gas parcel. Likewise, a compressed parcel develops a concentration gradient because the partial pressure of the parcel's vapor is greater than that of the surrounding vapor. Vapor diffuses out of the parcel. Since the vapor at the surface is in equilibrium with the liquid, the diffused vapor must condense.

Condensation causes the surface to absorb the latent heat. Hence, we get additional heat pumping for an acoustic cycle. Firstly, we have the adiabatic heat pumping due to the standard model of thermoacoustics, but we also add the heat pumping caused by mass diffusion.

Now that we have a conceptual outline of wet thermoacoustics, we will look at the mathematics of acoustic propagation in saturated vapors. We are looking to see how the presence of vapor and accompanying mass diffusion will affect the impedance measured in our system. Looking at the equations that govern the acoustics of dry and wet gases, we see many similarities. The form of the wave equation is the same for both wet and dry pores [Raspert (2002)].

$$\frac{d^2 P}{dz^2} + 2\alpha \frac{dP}{dz} + k^2 P = 0 \quad (1)$$

Where for dry pores the attenuation factor, not to be confused with the imaginary part of k which is the attenuation, and wave number are given by

$$\alpha = \frac{1}{2} \frac{1}{T_0} \frac{dT_0}{dz} \left(\frac{F(\lambda_T)/F(\lambda_\mu) - 1}{1 - N_{Pr}} \right) \quad (2)$$

$$k^2 = \frac{\omega^2}{c^2} \frac{\gamma}{F(\lambda_\mu)} \left[1 - \frac{\gamma - 1}{\gamma} F(\lambda_T) \right] \quad (3)$$

And for wet pores,

$$\alpha = \frac{1}{2} \frac{1}{T_0} \frac{dT_0}{dz} \left(\frac{F(\lambda_T)/F(\lambda_\mu) - 1}{1 - N_{Pr}} + \phi \frac{\gamma}{\gamma - 1} \frac{n_2^0}{n_1^0} \frac{F(\lambda_D)/F(\lambda_\mu) - 1}{1 - N_{Sc}} \right) \quad (4)$$

$$k^2 = \frac{\omega^2}{c^2} \frac{\gamma}{F(\lambda_\mu)} \left[1 - \frac{\gamma - 1}{\gamma} F(\lambda_T) + \frac{n_2^0}{n_1^0} (1 - F(\lambda_D)) \right] \quad (5)$$

where,

$$\phi = \frac{\gamma - 1}{\gamma} \frac{l}{R_0 T_0} \quad (6)$$

is the latent heat parameter. For the square pores being investigated we have [Arnott (1991)]

$$F(\lambda) = \frac{64}{\pi^4} \sum_{m,n}^{\text{odd}} \frac{1}{m^2 n^2 Y_{mn}(\lambda)} \quad (7)$$

where,

$$Y_{mn}(\lambda) = 1 + \frac{i\pi^2(m^2 + n^2)}{4\lambda^2} \quad (8)$$

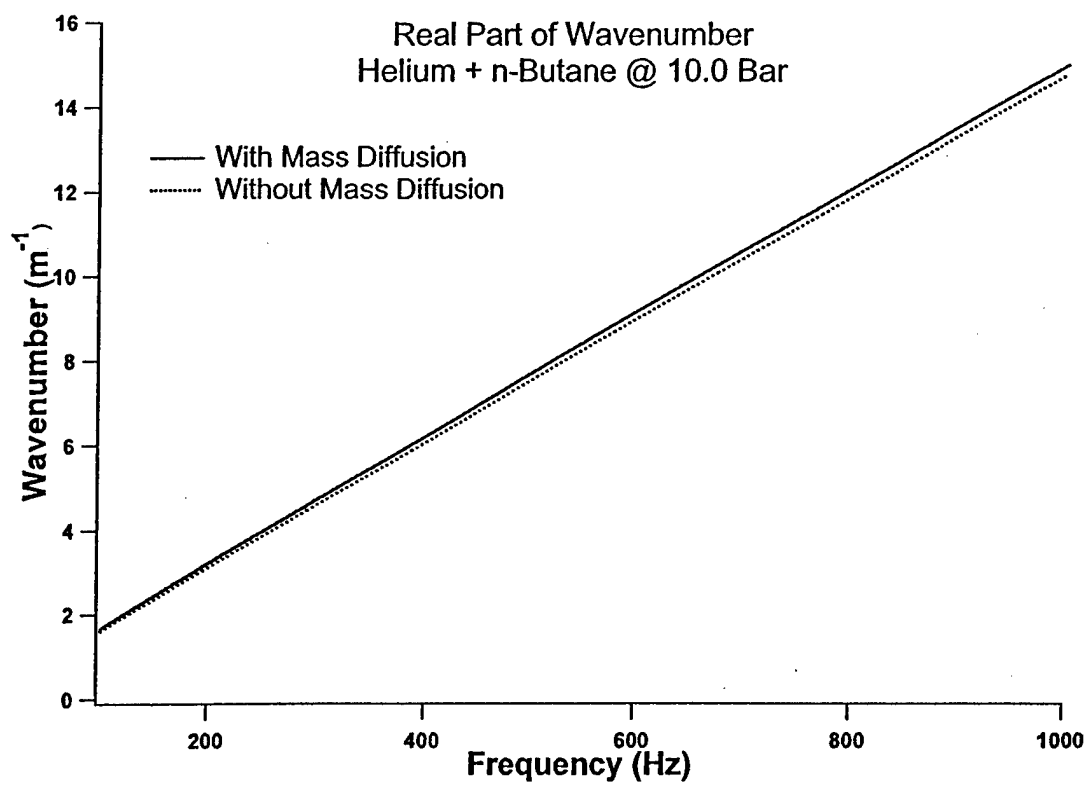
Reducing equation (1) to a pair of first order differential equations illuminates the way in which the pressure and volume velocity evolve in the system [Raspet (2002)].

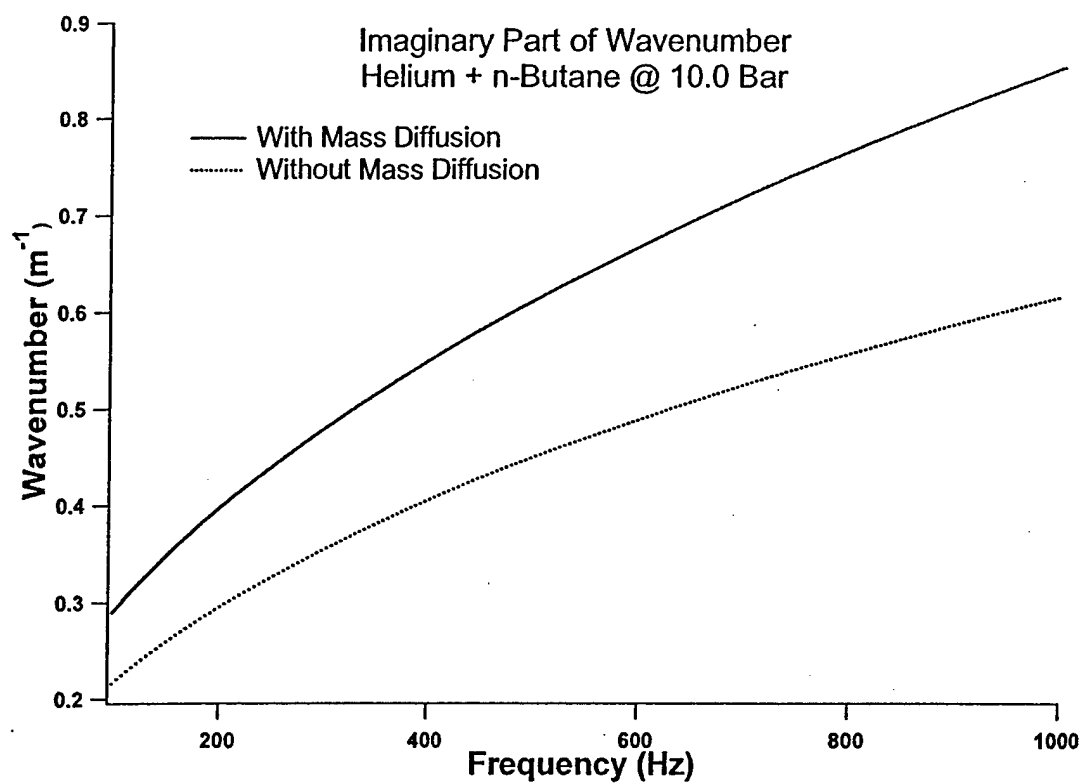
$$\frac{dP_{AC}}{dz} = \frac{i\omega\rho}{A_{mix}} \frac{U_{vol}}{F(\lambda_{\mu})} \quad (9)$$

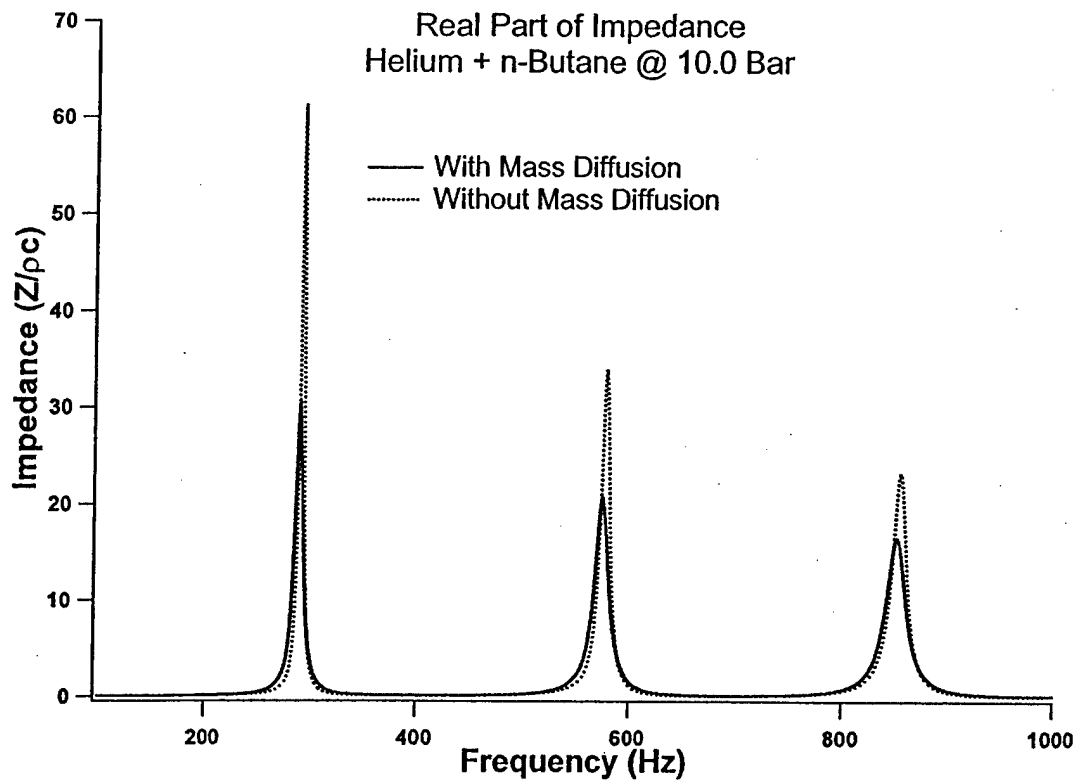
$$\frac{dU_{vol}}{dz} = \frac{A_{mix}}{i\omega\rho} F(\lambda_{\mu}) k^2 P_{AC} - 2\alpha U_{vol} \quad (10)$$

The imaginary part of k is the loss term due to both heat and mass transport, and α represents a thermoacoustic gain or attenuation factor. This set of equations is sufficient to model the acoustic behavior for a stack if the geometry of the system is known.

For this study, the resonator and stack are at constant temperature and the pressure amplitudes used are not sufficient to create a temperature gradient; consequently, $\alpha = 0$. Therefore, the effect of the vapor will only be detectable in changes to the complex wave number.







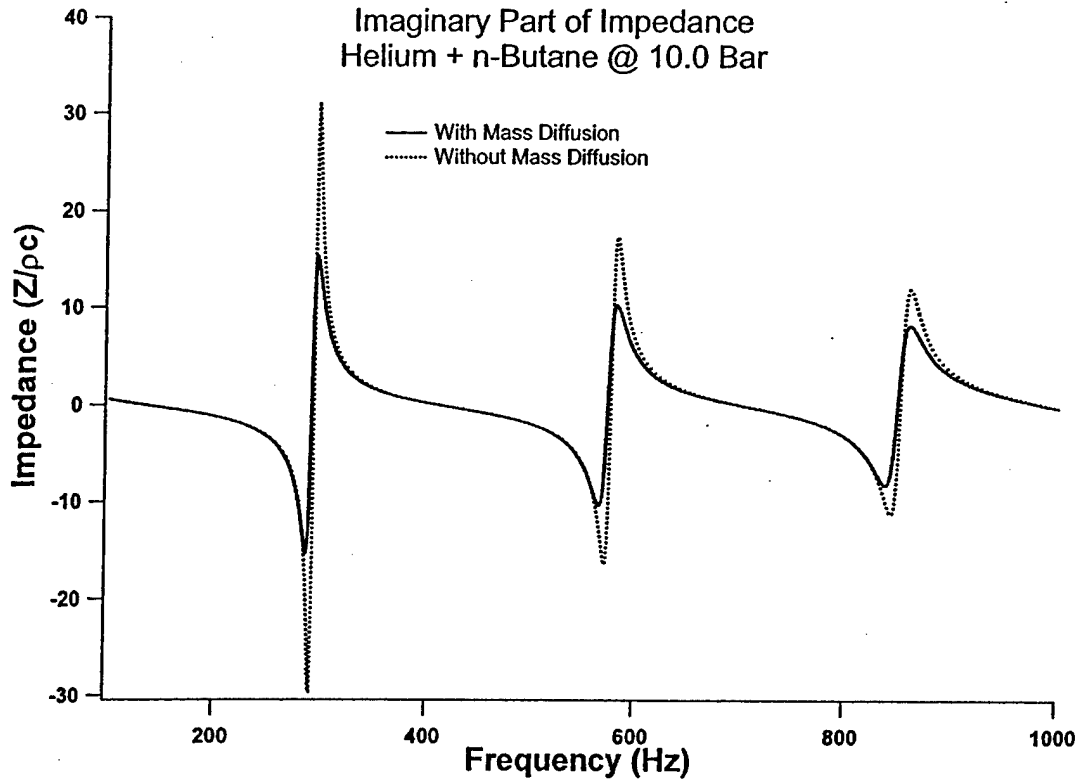


Figure (4): The influence of mass diffusion on the wavenumber in the stack and the impedance in a model of our system. The impedance shown is a theoretical prediction of the impedance we expect to model. The lines denoted “with mass diffusion” use equation (5) to calculate the wavenumber inside the stack. The lines denoted “without mass diffusion” set mass diffusion coefficient, D_{12} , to zero in the calculation of the gas properties. The effect of setting $D_{12} = 0$ is to calculate the wavenumber based on the gas properties of the helium + n-butane mixture without including the effects of mass transport. That is, we model a theoretical gas that has the same thermophysical properties as helium + n-butane but does not change phase during the acoustic cycle to obtain a “without mass diffusion” curve.

In Figure (4), we see a considerable change in the imaginary part of the wavenumber corresponding to an increase loss during the acoustic cycle. The real part

of the wavenumber does not change much, so we expect the resonance frequency to remain almost constant. The impedance graphs in Figure (4) indicate that mass diffusion significantly changes the amplitude of the measured impedance at the face of the stack. As suspected, the resonance frequency will not change dramatically. In order to identify this shift, our system must be able to resolve changes of 1 Hz.

The theory to which we compared our dry measurement was coded using work published by Arnott [Arnott (1991)]. We used the known value of the impedance of a hard end with thermal dissipation [Pierce (1991)] and the intrinsic impedances of the tube and stack to predict the impedance at the face of the stack using the impedance translation theorem [Pierce (1991)]. See Appendix B for these equations. This was compared to the impedance measured at the face of the stack (Figures 5 & 6).



Figure (5): Flow chart for acquisition of data from the experimental system.

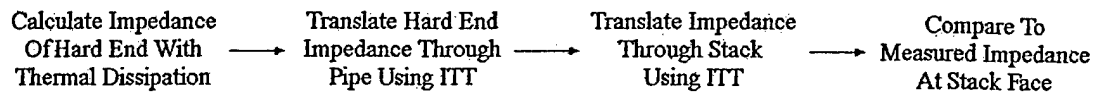


Figure (6): Flow chart for theoretical prediction of impedance at stack face using the impedance translation theorem (ITT).

The wet theory code was produced in the same manner. Of primary importance in the calculation of the wet impedance are the gas properties, which were obtained from gas dynamic theory [Hirschfelder (1964)]. Dr. William Slaton provided all theoretical calculations for the cases of wet stacks.

	Acetone	2-Propanol	n-Butane
Temperature (K)	3.000E+02	3.000E+02	3.000E+02
Density mixture (kg/m ³)	2.321E+00	1.764E+00	6.684E+00
cp mixture (J/kg K)	3.937E+03	4.877E+03	2.281E+03
Thermal Conductivity mixture (W/m K)	1.379E-01	1.539E-01	5.958E-02
sound speed mixture (m/s)	8.222E+02	9.596E+02	4.433E+02
Viscosity mixture (μPa s)	1.975E+01	2.009E+01	1.364E+01
mole fraction gas	9.680E-01	9.936E-01	7.689E-01
mole fraction vapor	3.204E-02	6.352E-03	2.311E-01
mole density gas	3.920E+02	4.024E+02	3.114E+02
mole density vapor	1.297E+01	2.572E+00	9.357E+01
Ratio of specific heats for mixture	1.554E+00	1.608E+00	1.301E+00
D12 (m ² /s)	4.538E-06	4.447E-06	3.515E-06
Prandtl Number	5.639E-01	6.366E-01	5.221E-01
Schmidt Number	1.875E+00	2.561E+00	5.804E-01
Phi – Latent heat parameter	4.581E+00	6.687E+00	1.930E+00
Thermal Diffusion Ratio	-2.888E-02	-6.485E-03	-1.273E-01

Table (1): Properties of Helium + vapor at 10 bar.

III. Theory - Measurement

In 1980, Chung and Blaser [Chung & Blaser (1980)] described a technique of measuring impedance by using broadband noise and two transducers mounted in an impedance tube. Through a comparison of the two measured pressures, the acoustic impedance is determined at any other position in the system.

Comparing the two signals, we take the ratio of the cross-spectrum $S_{12}(f)$ to the auto-spectrum $S_{11}(f)$. This ratio is also known as the transfer function $H_{12}(f)$. It is from the transfer function the impedance is calculated.

$$H_{12}(f) = \frac{S_{12}(f)}{S_{11}(f)} \quad (11)$$

$$\frac{Z}{\rho c} = i \frac{\sin[k(l-s)] - H_{12} \sin(kl)}{\cos[k(l-s)] - H_{12} \cos(kl)} \quad (12)$$

Where s is the separation of the transducers, k is the wavenumber, and l is the distance from the first transducer to the location where the impedance is measured. In this work this is taken at the face of the stack towards the driver. We use the real wavenumber

$$k = \frac{\omega}{c} \text{ neglecting the small attenuation, } \alpha = 0.0021 \text{ Np/m, between the microphone}$$

and the sample.

The two-transducer technique has several advantages over other methods of measuring acoustic impedance. Modern digital signal analyzers are capable of directly measuring the transfer function, thereby greatly reducing the need for complex signal processing routines to be coded. Additionally, the broadband nature of this measurement allows for rapid data acquisition over the frequency range of interest. However, measurement of the transfer function can be corrupted by error and nonlinearity in the pressure measurement. Detail of the measurement system and calibration procedure can be found in Appendix A.

IV. Experimental Setup

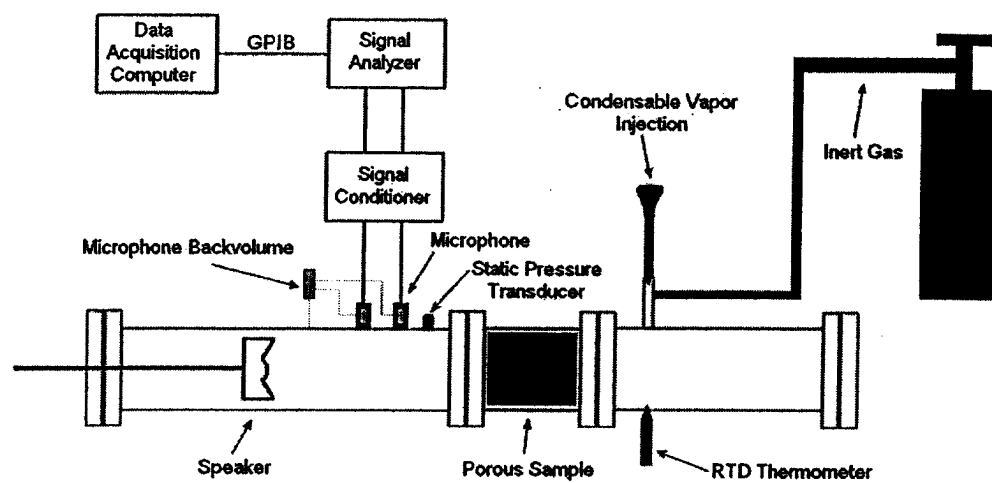


Figure (7): Schematic of System

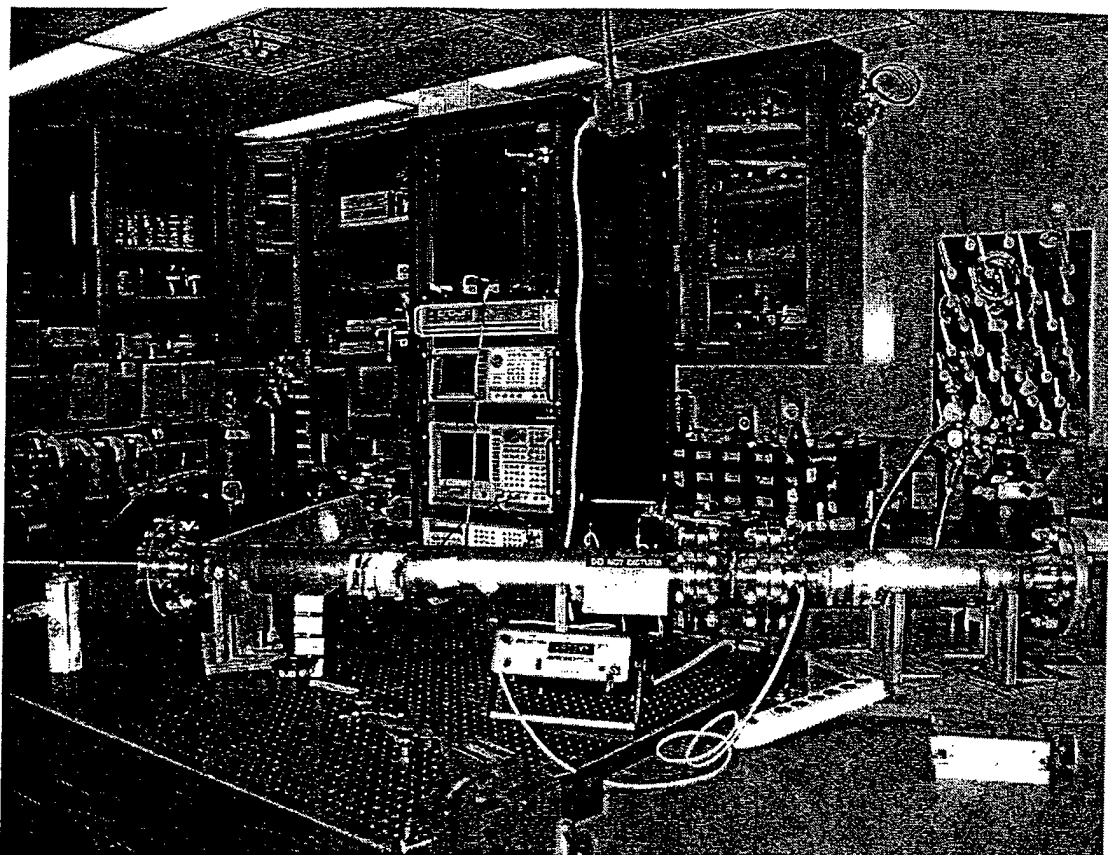


Figure (8): Photo of system

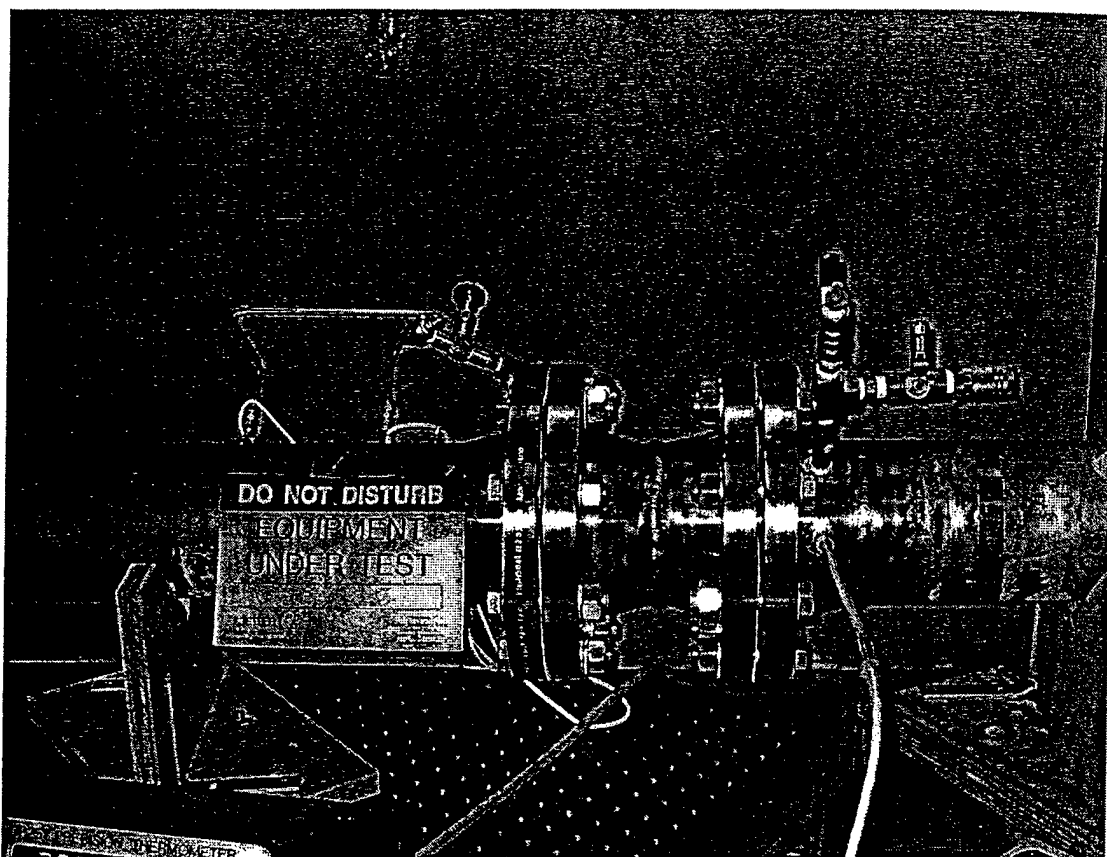


Figure (9): Sample holder and transducers

a. General Description

Figure (7) is a schematic of the impedance tube used in this work. The inner diameter of the tube is 0.1016 m. The total length is about 2.5 m. In figure (8), the mounting rod for the speaker can be seen protruding from the leftmost flange. The speaker used is a 0.1016 m driver clearanced to fit in the tube and powered by an external amplifier. Mounted on the right end of the tube is a blind flange used as the rigid termination. The tube and all flanges are made of stainless steel. The sample is housed in the short section shown in Figure (9). Just to the left of this section, the two

transducers are visible. Fine gauge stainless tubing is connected to the vent port of the transducers in order to maintain the reference side of the transducers at the static pressure of the tube. Once the tube is at operating pressure, a valve isolates the reference side of the transducer from the sound field. This allows the transducers to see a varying pressure only on the face exposed to the resonator. To the right of the sample holder, we have mounted a high precision thermometer as well as the fittings necessary to fill the tube with gas and vapor.

b. Corrosive Vapors

As previously stated, wet thermoacoustics uses a mixture of inert gas and vapor as the working fluid. This vapor must be present in quantities sufficient to coat all surfaces within the resonator with a thin layer of liquid. Typical candidates for the condensable component are hydrocarbons, alcohols, freon, and water.

One of the concerns when starting this project was the durability of the materials to various liquids and vapors. Acetone and n-butane are effective at dissolving bonding agents as well as some seals. This presents a problem with PTFE seals, silicone lubricants, and bonding agents. The glues used in the assembly of our drivers were particularly susceptible to exposure to acetone and butane, Fig. (10). Working fairly quickly, in less than a few hours, allowed collection of useful data before the disintegration of the driver.



Figure (10): Damaged driver (bonding agents dissolved) that was exposed to n-butane.

This driver was usable for approximately 150 minutes in a helium/butane environment, an obviously unacceptable result for any system designed for continuous use.

c. Transducer separation

We found that multiple transducer separations are necessary for the range of wavelengths we would encounter. The maximum separation s is given by

$$s \leq \frac{c}{2f_{\max}}, \quad (12)$$

where f_{max} is the minimum frequency to be investigated. This simply limits the separation to ensure that you have at most a half wavelength between microphones since the reduction algorithm assumes zero or one pressure node between transducers. A minimum separation is not as clearly defined. Narrowly separated transducers do not resolve differences in phase and amplitude well, especially when dealing with long wavelengths. We must strike a balance for the separation to be used. For any given mixture, we want maximum separation for amplitude and phase resolution, but we cannot exceed the limits placed by Eq. 12.

The mixtures we investigated have speeds of sound that vary by a factor of three, and we investigate them over a frequency range that spans an order of magnitude. With wavelengths ranging from 0.3 m to 10.0 m, multiple transducer separations were necessary. We settled on three separations: 0.0381m, 0.1143 m, and 0.1524 m. This range permits flexibility for gas/vapor selection.

d. Transducer Selection

Two factors were considered in the transducer selection: sensitivity and size. Initial measurements were made that showed pressure amplitudes on the order of 1.0 Pa. With acoustic signals 5 orders of magnitude smaller than anticipated maximum static pressures, differential transducers are necessary. Both sides of a differential transducer's membrane are exposed to the static pressure, allowing for a very high sensitivity since the membrane only reacts to acoustic pressures.

The size of the transducer determines how it will be mounted in the tube wall. In this system, the tube wall is 0.25" thick, and the pipe has an outer diameter of 4.5".

The curvature and thickness of the pipe dictated that a narrow transducer be used if extraordinary means of mounting are to be avoided. An Endevco model 8510-B1 satisfies the above parameters. It has a differential pressure range of 1 psi and a full-scale output of ~ 200 mV with 10 V excitation potential. In addition to satisfying the above characteristics, they are relatively inexpensive, so that damage due to over pressurization is not financially prohibitive.

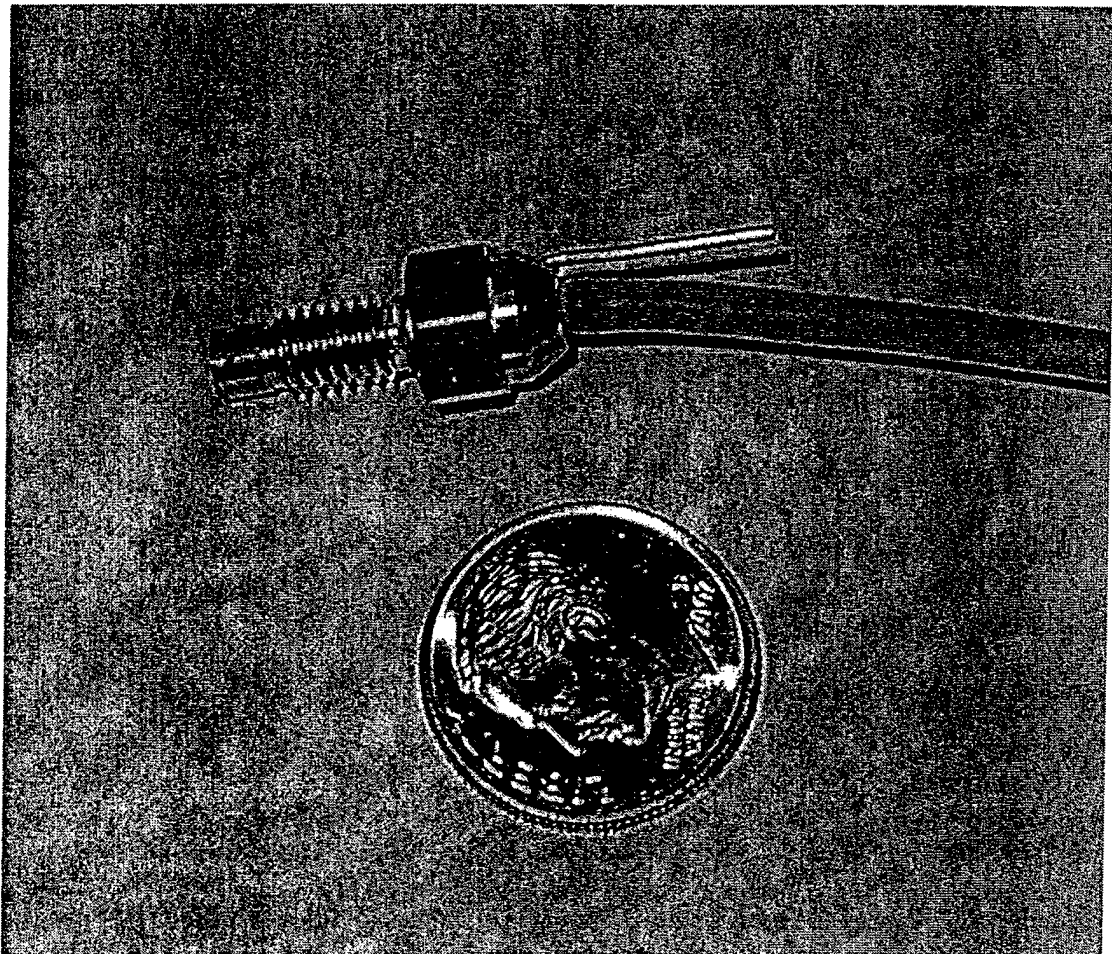


Figure (11): Endevco Model 8510B-1 piezoresistive pressure transducer

We examined several of the pressure transducers response to DC pressure in order to verify the linearity of its response. Figure (12) is typical of the several transducers we tested.

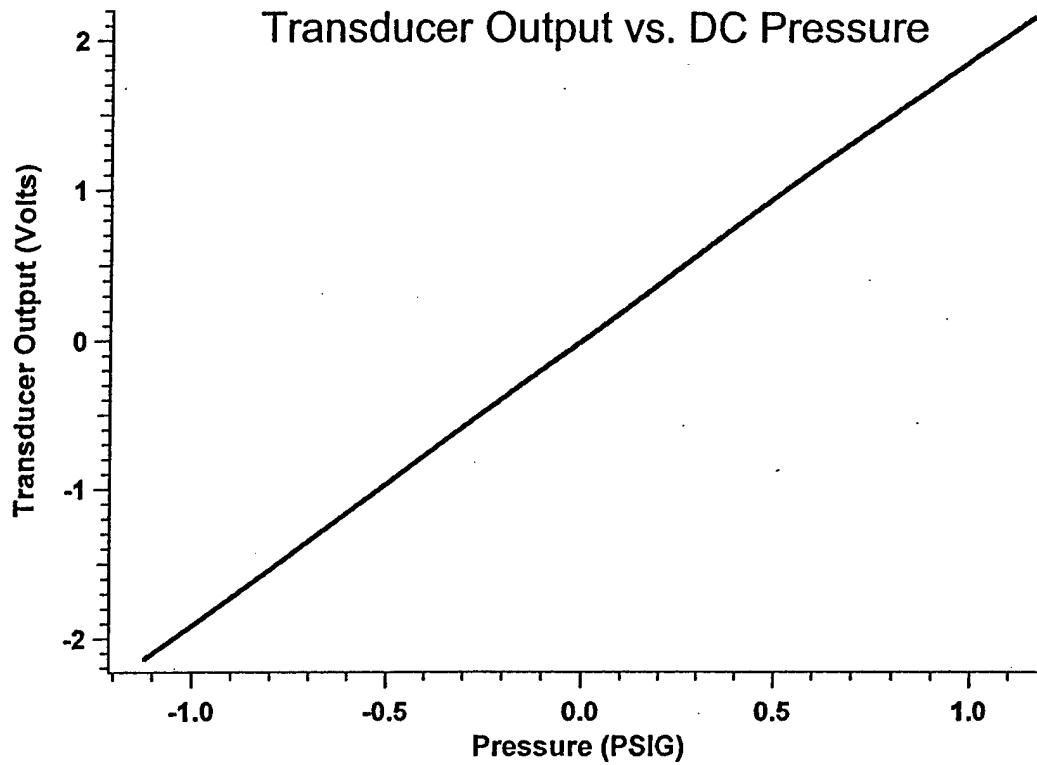


Figure (12): Examination of the Endevco 8510B-1 response to DC pressure

e. **Data Sets**

Data extracted from the spectrum analyzer consists of the FFT of each transducer's signal, the real and imaginary parts of the transfer function between transducers, and the coherence of the signal. The coherence is helpful in determining if the signal-to-noise ratio is adequate. Figure (11) shows coherence indicative of a poor signal-to-noise ratio.

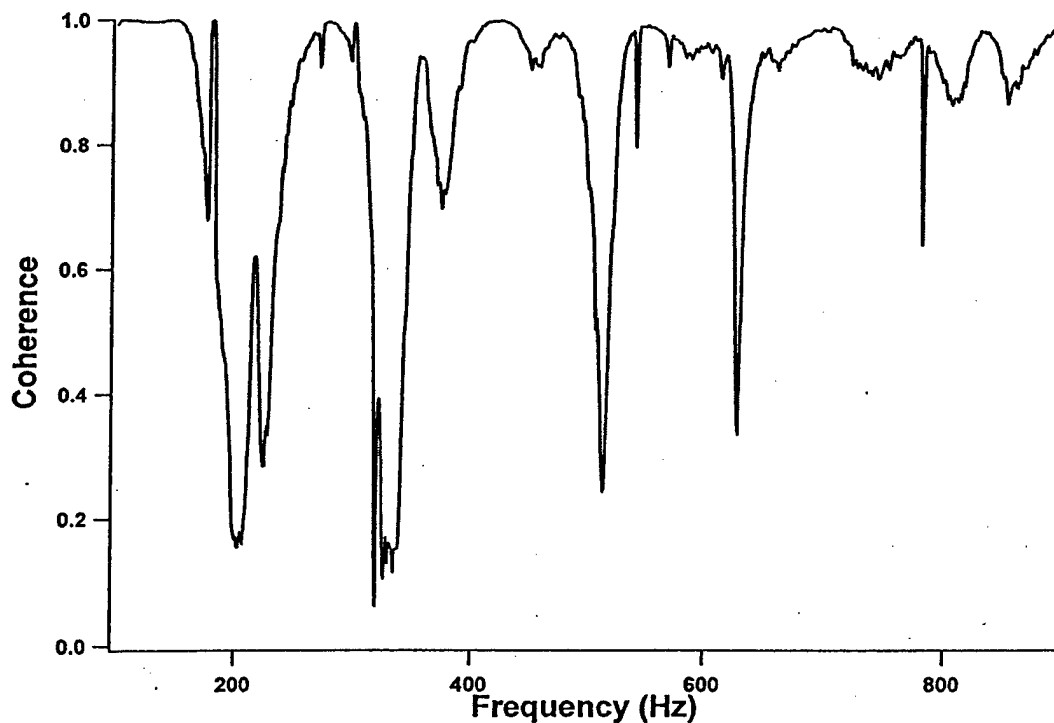


Figure (13): Coherence when proper signal-to-noise ratio is not obtained. This particular plot is of helium at 0.10 bar of pressure at room temperature.

The FFT of the two channels for this case is shown in Figure (14).

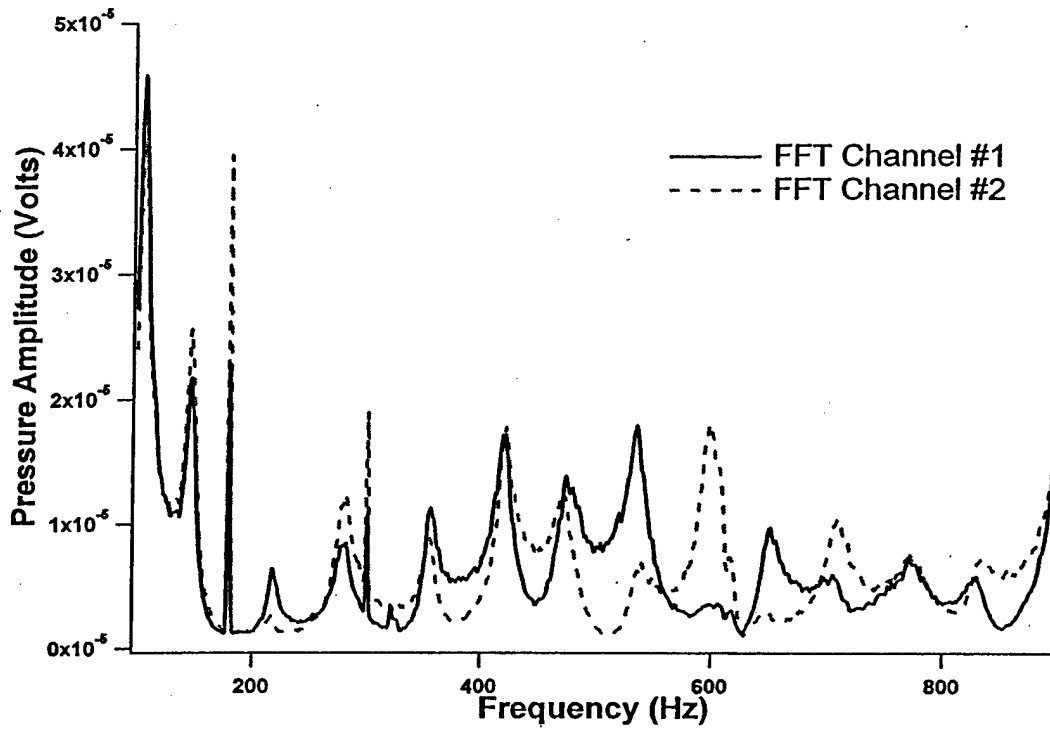


Figure (14): FFT of data set with insufficient signal-to-noise ratio.

Data shown in Figures (15), (16) demonstrates sufficient signal-to-noise ratios; consequently, the coherence is close to 1.

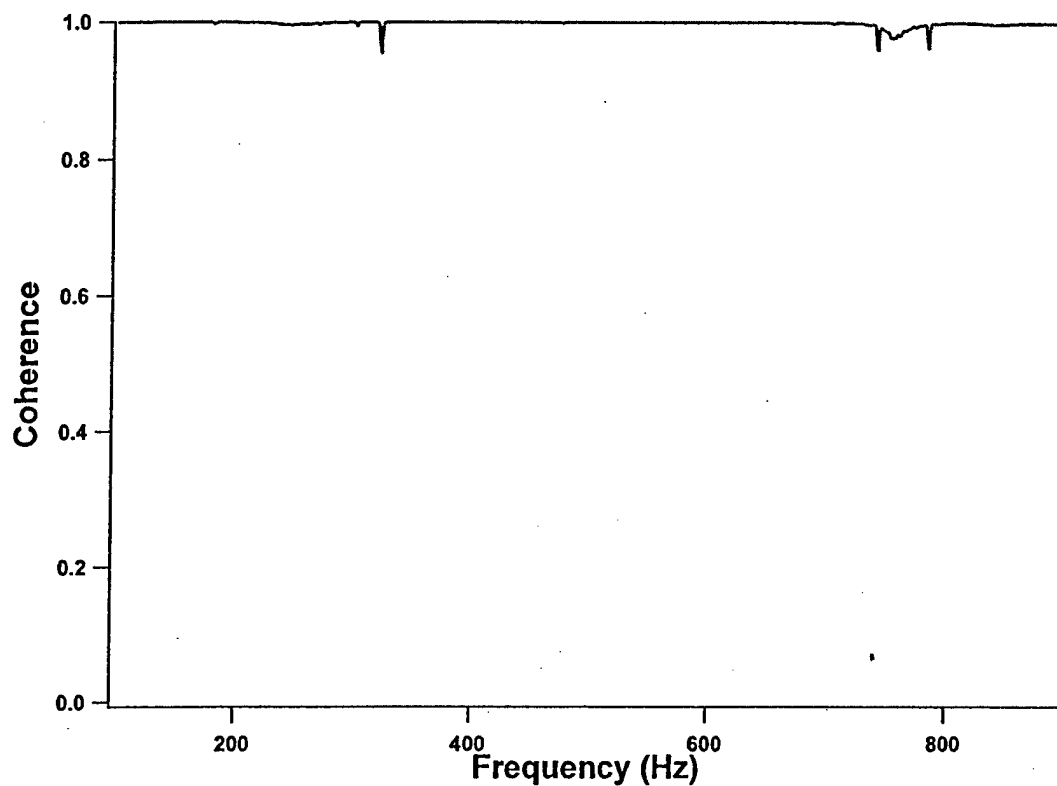


Figure (15): Example of proper coherence. Data set is helium at 10.13 bar with a 600 PPF^2 stack at ~ 295 K.

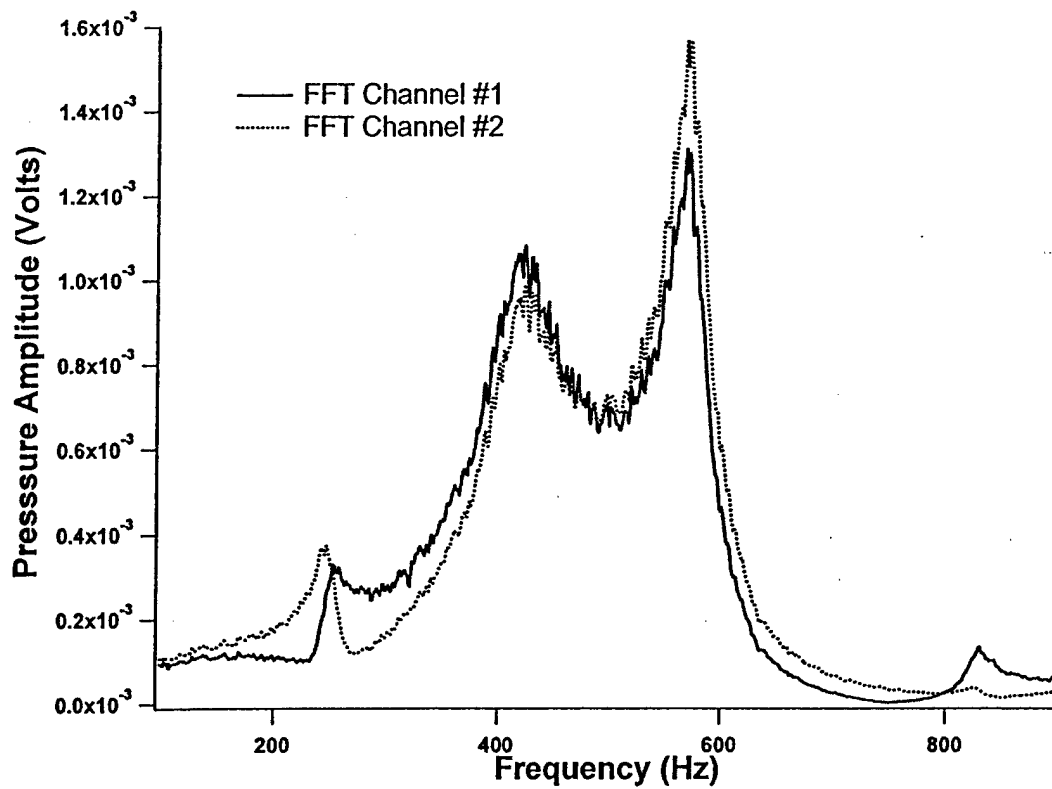


Figure (16): FFT of data set with sufficient signal-to-noise ratio.

V. Data & Analysis

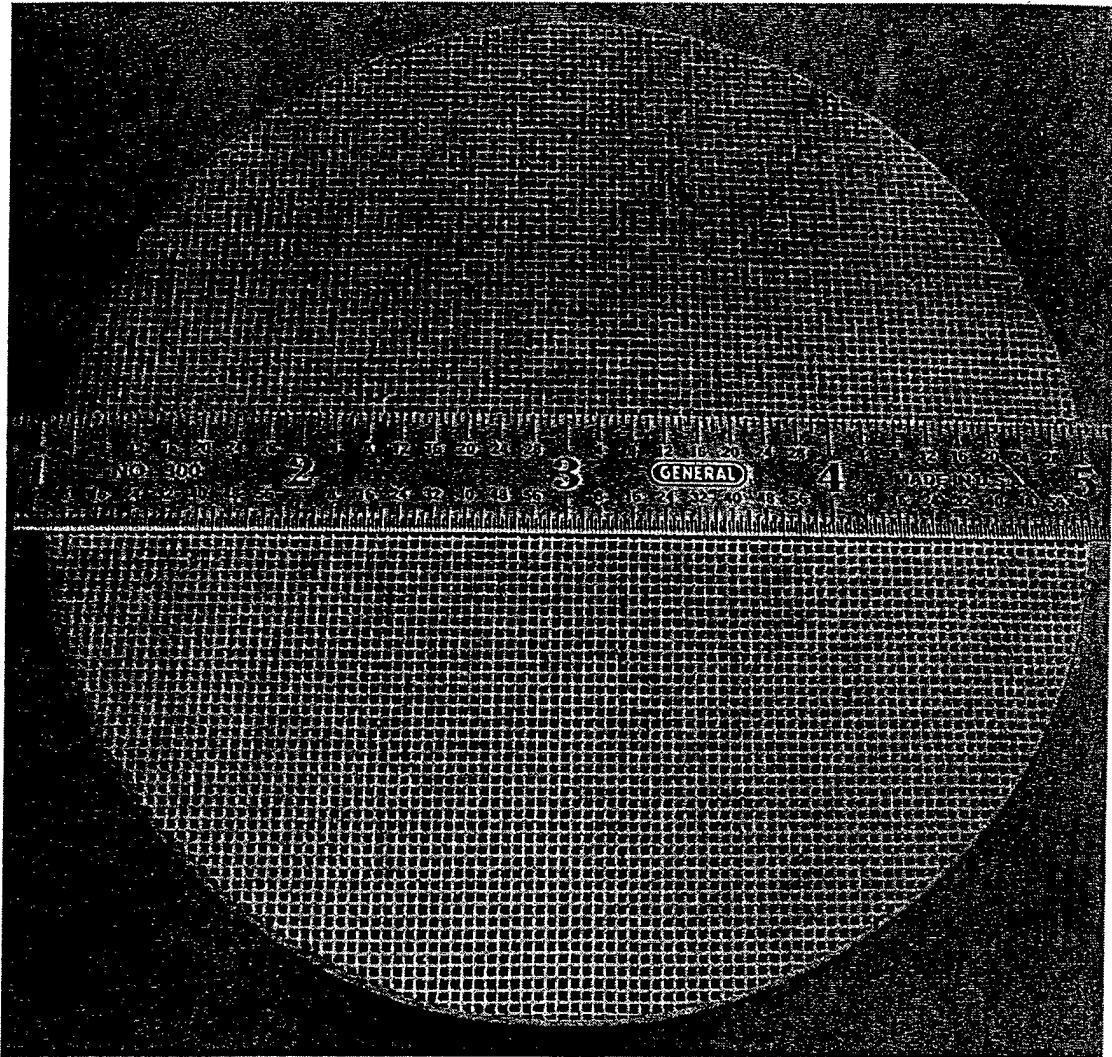
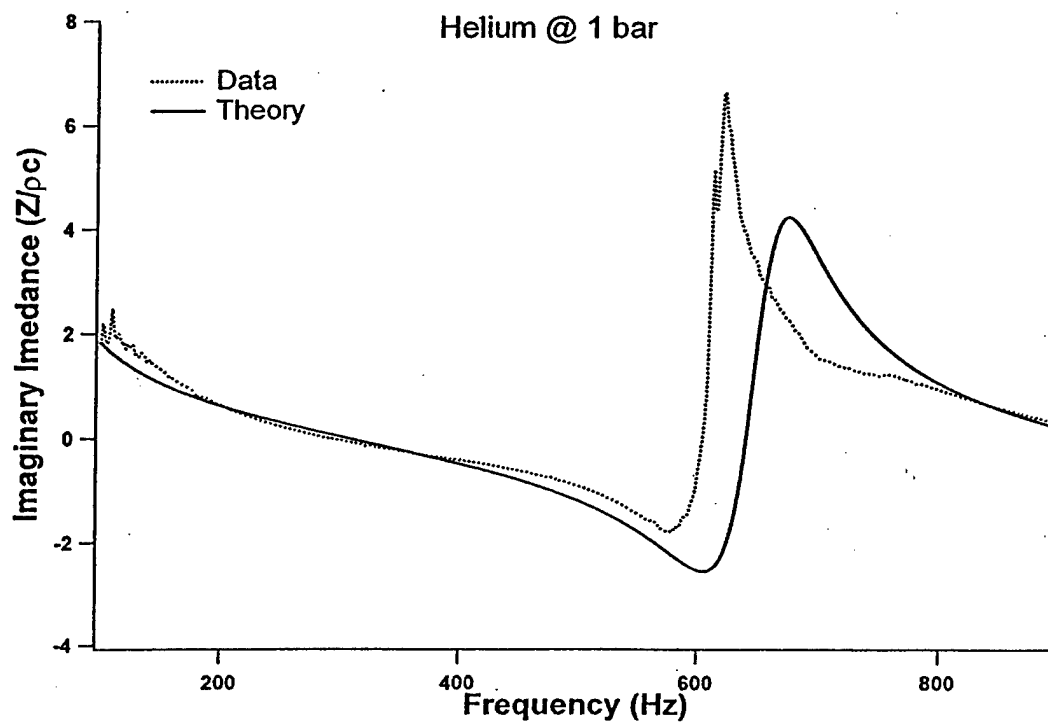
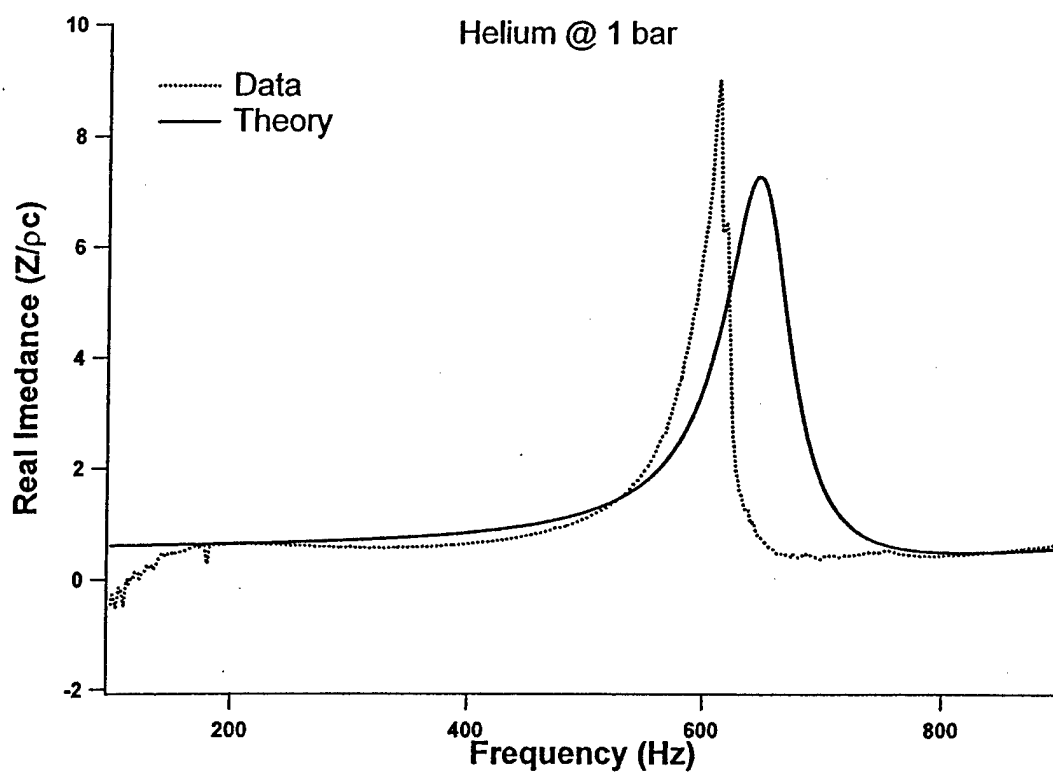
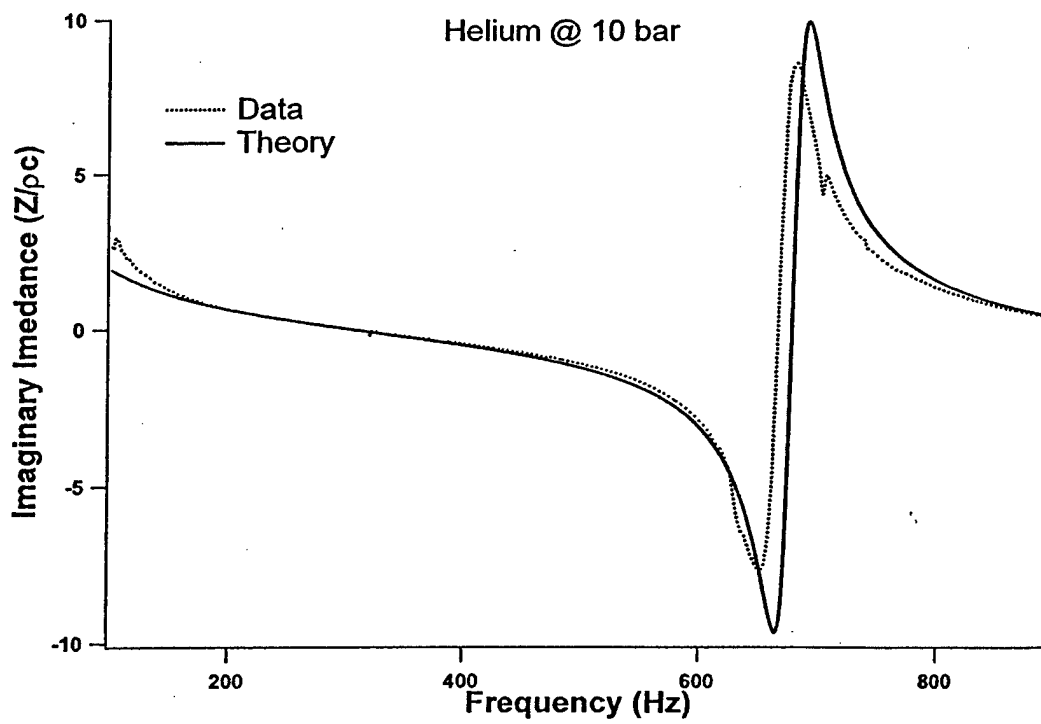
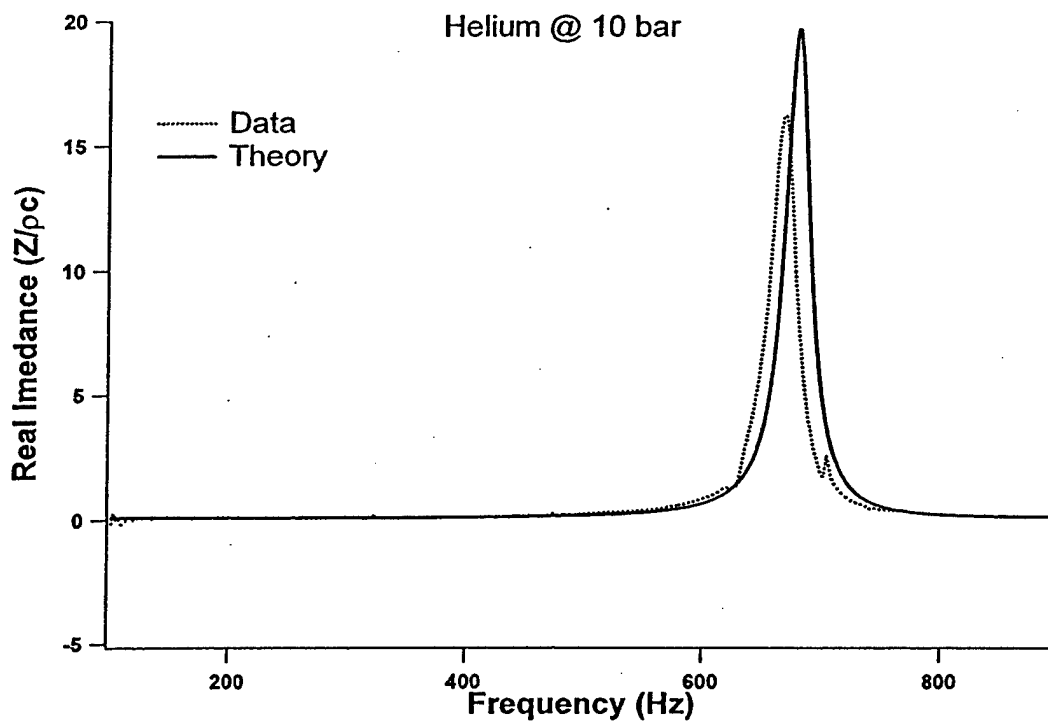
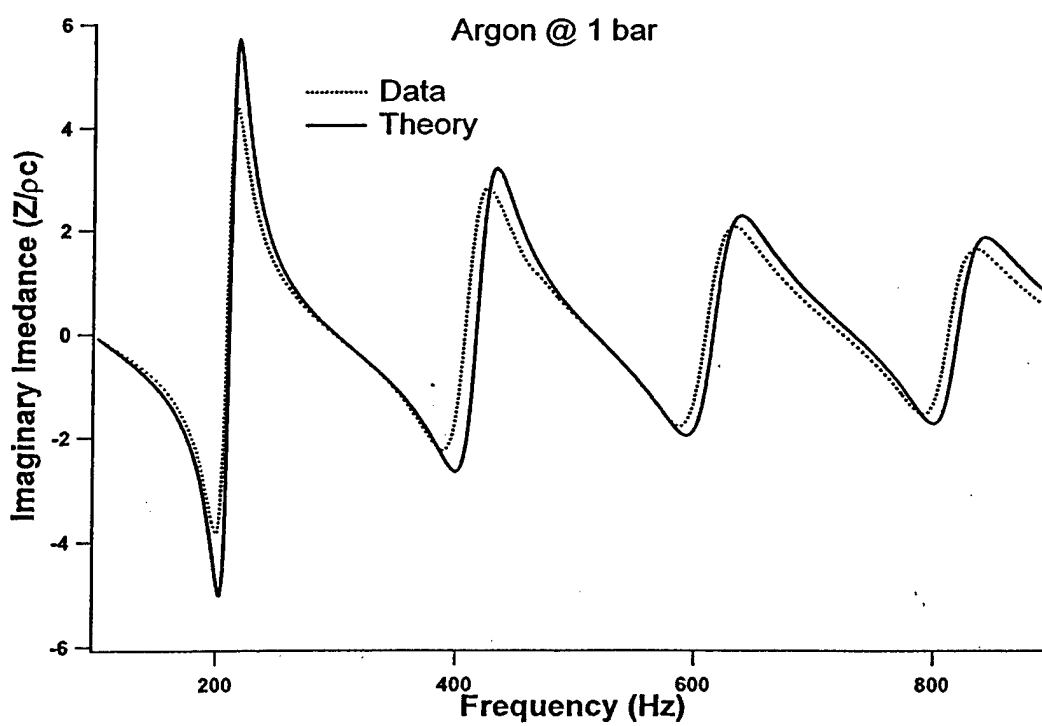
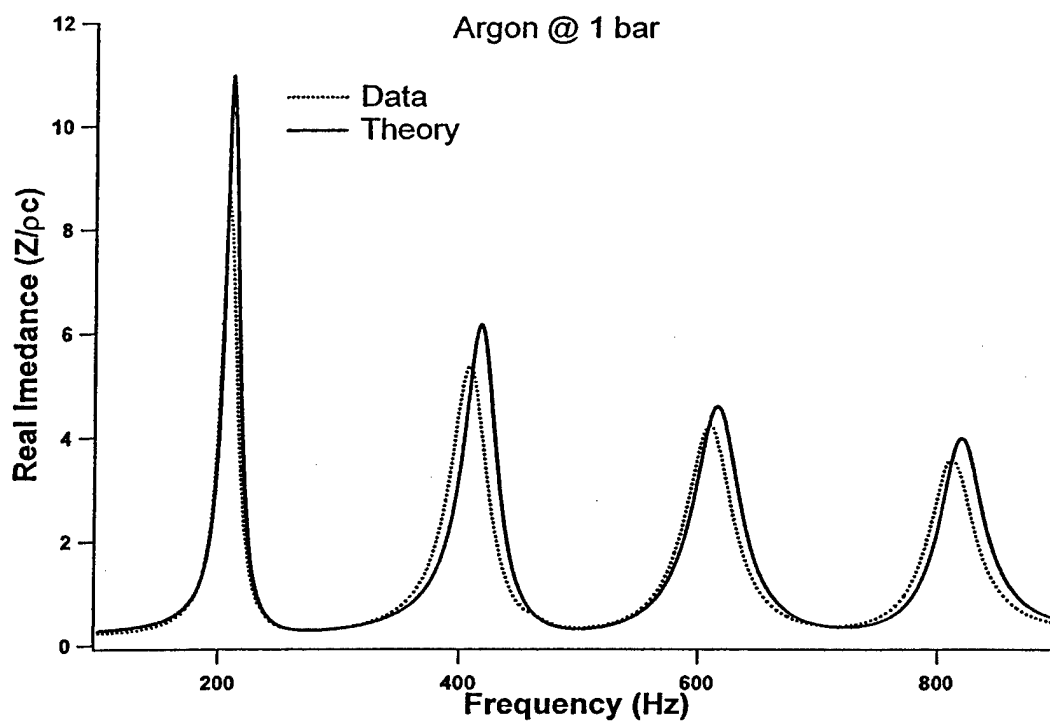


Fig. (17): Celcor stack. This is the same material as the stack we investigated. This stack has 600 pores per square inch and is made of ceramic.

We measured the specific acoustic impedance of Celcor stacks in both inert gas and inert gas/vapor mixtures - see Figure (17). The stack investigated has 600 pores per square inch, and a porosity of 78%. All data sets were taken at temperatures in the range of 294 K – 297 K. For the data using only inert gas, we investigated helium and argon at 1 bar and 10 bars. All of the following plots are of the specific acoustic impedance at the face of the stack.







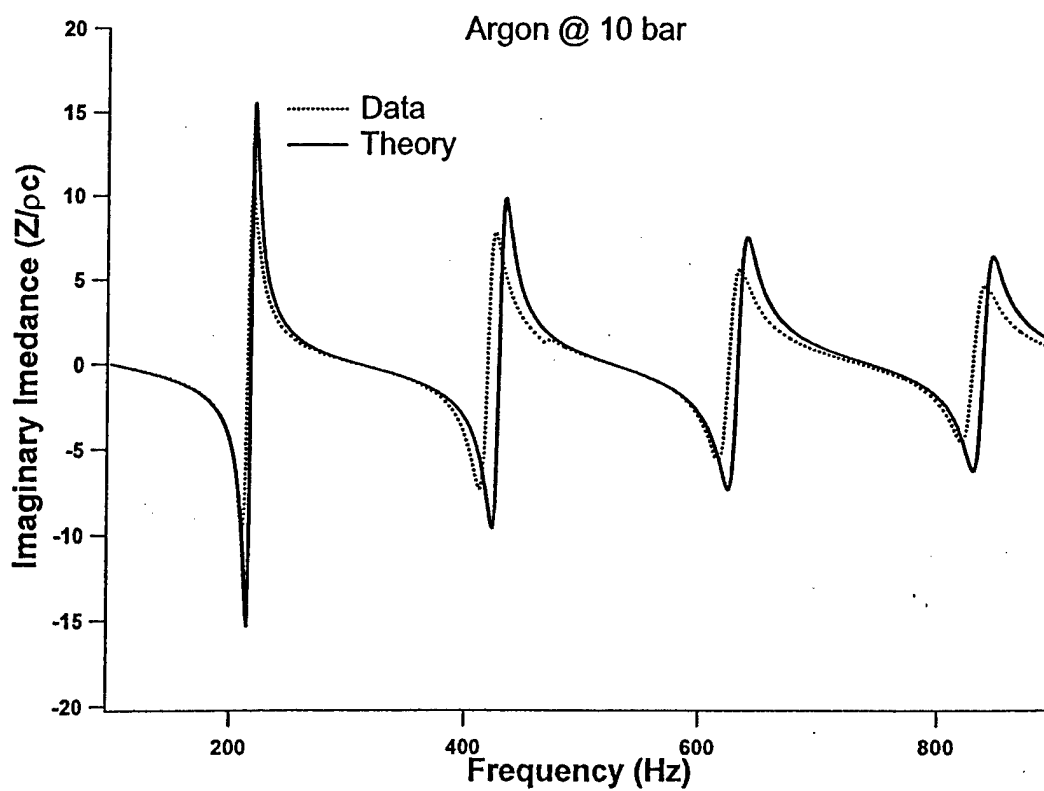
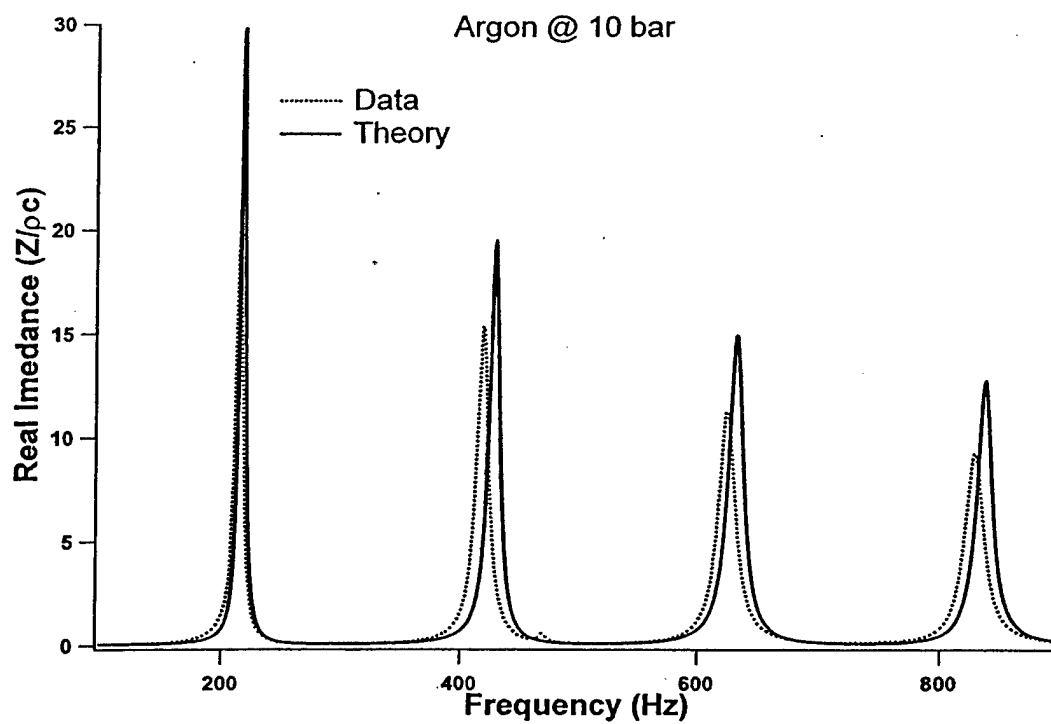


Figure (18): The above graphs compare the measured and calculated impedance at the face of the stack for helium and argon at 1.01 bar and 10.13 bar.

In all of these sets, we see that the data and theory have the same form; however, there is a discrepancy in both frequency and amplitude. Remembering the condensable vapor causes small shifts in the resonance frequency, this discrepancy is unacceptable. We must either eliminate the cause of this dissimilarity or characterize it. Examination of the frequency difference in the argon @ 10 bar graph shows characterization is difficult. The shift is not uniform or linear. At the first resonance peak, a difference of approximately 5 Hz exists between data and theory, while subsequent peaks show shifts of 10 Hz. Similar problems present themselves in attempts to characterize the amplitude discrepancies.

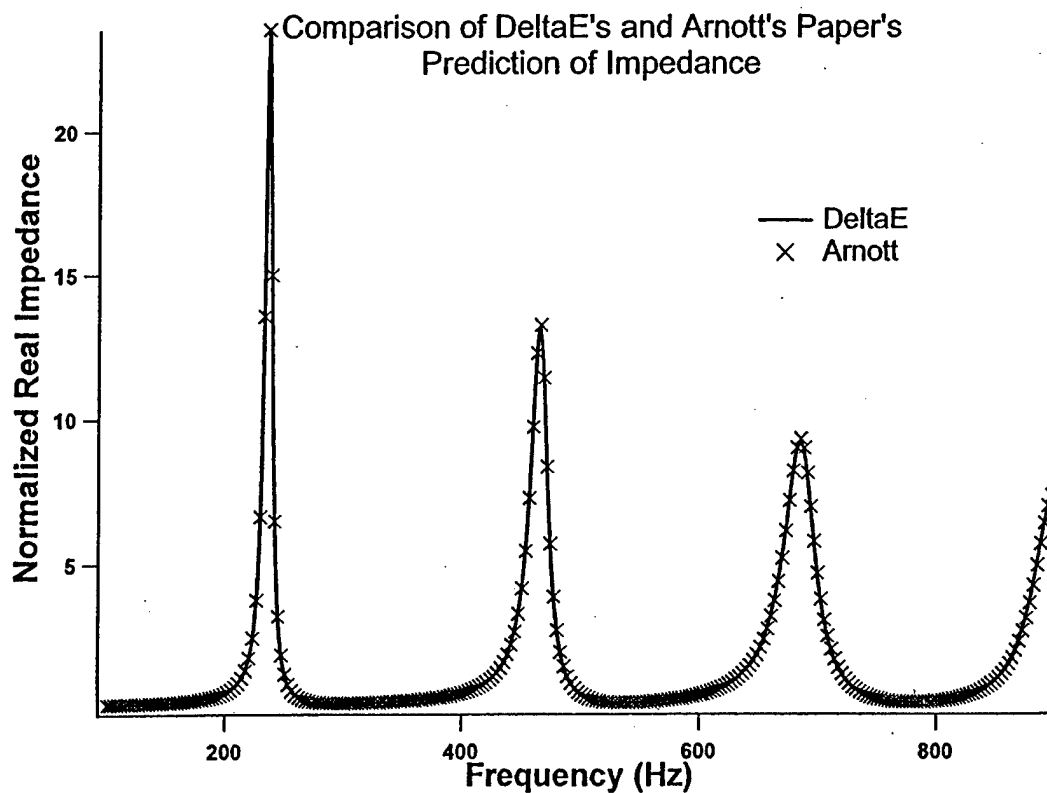
The source of the differences went undiscovered. Three possibilities exist: the data taken does not represent the impedance at the face of the stack; the theory used does not predict the intrinsic impedance of the stack correctly; or our assumptions regarding the resonator are not correct.

First, we examined the experimental measurement of the impedance at the face of the stack. All the appropriate dimensions were remeasured, and the amplifier/transducer system was recalibrated. The recalibration did not produce significant changes in the intrinsic transfer function, nor did the remeasurement reveal any errors.

As an alternative to using the intrinsic transfer function calibration (Appendix A), it is possible to employ sensor switching to eliminate gain and phase errors

introduced by the amplifier/transducer system. We measured the impedance using this technique and compared it to data taken using the calibration technique. The agreements between these two data sets led us to believe that the experimental measurements accurately represent the impedance at the face of the stack.

Next, we addressed the theory and its application. The theory published by Arnott was coded in C++. The output of this code was compared to an identical model prepared in deltaETM. Good agreement existed between these two simulations as shown in Fig. (19).



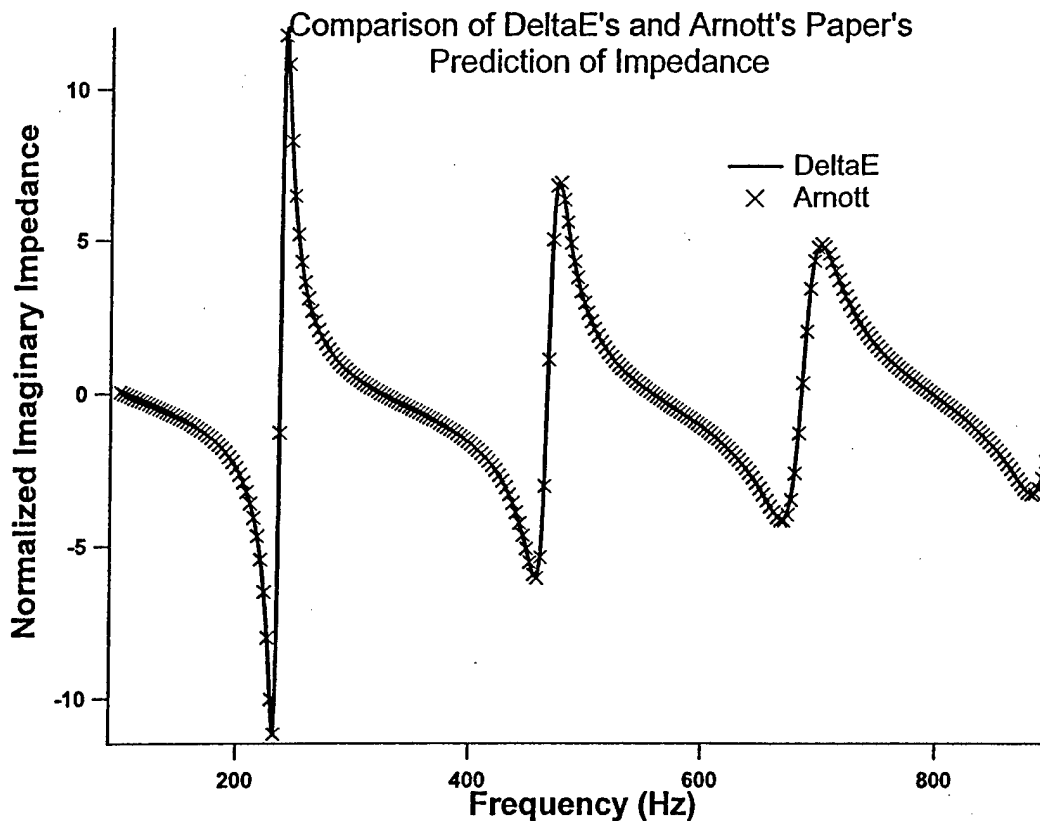


Figure (19): Comparing our code to deltaE to confirm it correctly predicts the impedance for the programmed geometry.

Now we turned to our assumptions in modeling sections of the impedance tube other than the stack. The model coded is that of a hard end followed by a duct, then a stack. We integrate the pressure and volume velocity equations from the termination through to the face of the stack and this gives a measure of the impedance. We do take into consideration the thermal dissipation at the hard end and the attenuation at the tube wall. We do not take into account any compliance that may come about due to the gas inlet tubes, the transducer reference pressure plumbing, or the gaskets between the flanges. These are all things that could be the cause of the problems we are facing.

While it may be possible to model these additional compliances, determination of their true influence may be difficult to ascertain.

Another source of error may be in the modeling of the stack material itself. The walls of the ceramic stack we are using are porous and this may affect the complex wavenumber within the stack. Arnott found wall porosities as high as 49% are needed to model Celcor properly [Arnott (1991)]. We conducted an experiment to determine both the wall porosity and the porosity due to the main pores. We immersed the stack in water, removed it, and used compressed air to blow the water out of the main pores. The mass of the stack changed by 86 g once the walls were wet. Assuming all 86 g are contained in the walls, the walls have 86 cc of pores. We reinserted the wet stack and measured how much water it displaced. With the walls wet, the volume of displaced water should equal the volume of the walls if they were solid. Knowing the total volume of the stack, we calculated a main pore porosity of 78% and a wall porosity of 39%. From Arnott, we have the dispersion relation for the wavenumber for porous walls

$$k_{porous} = \pm k_{nonporous} \xi \quad (13)$$

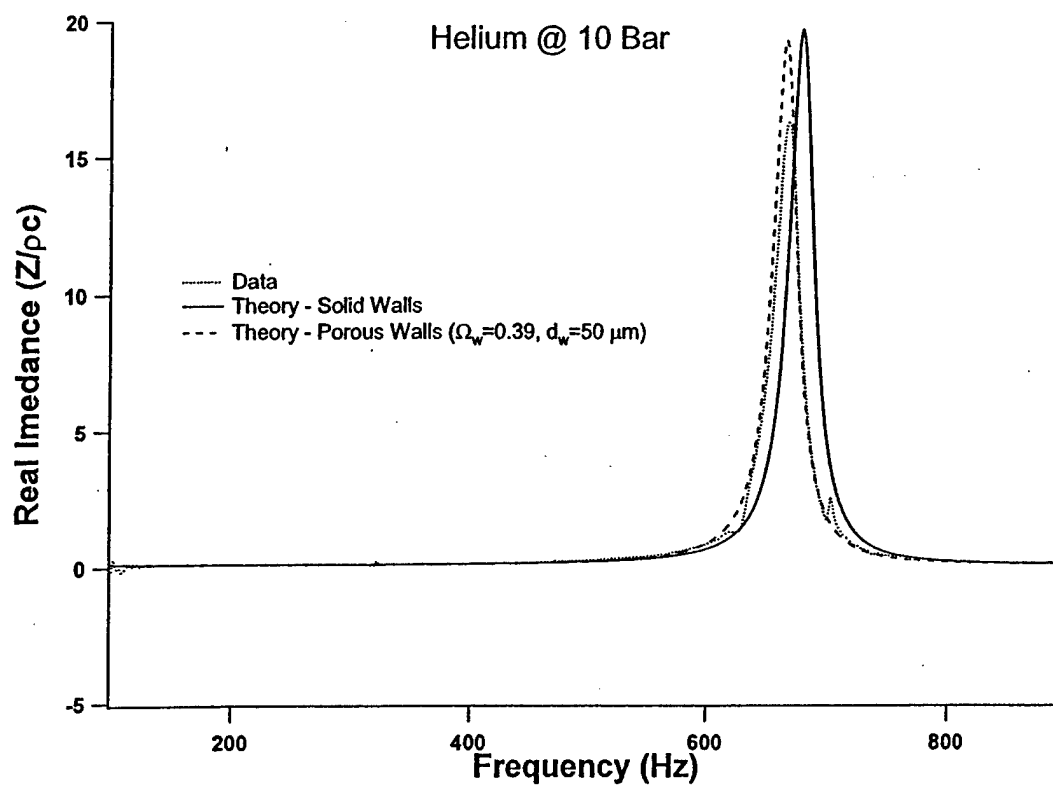
where,

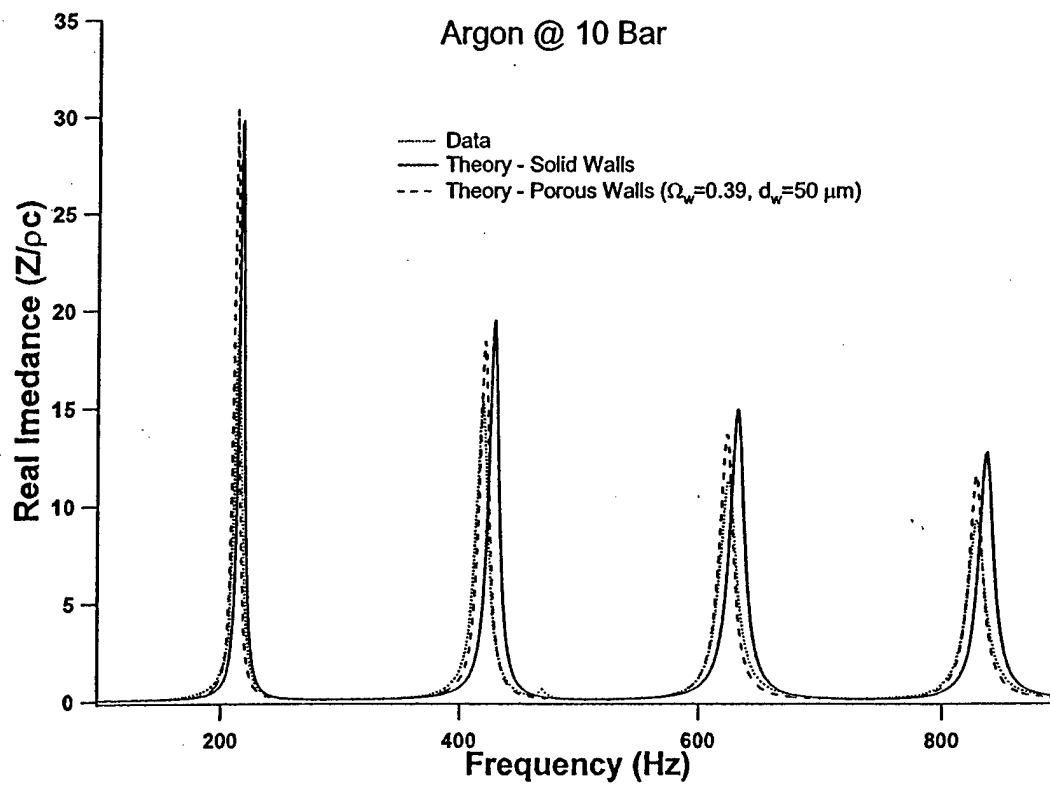
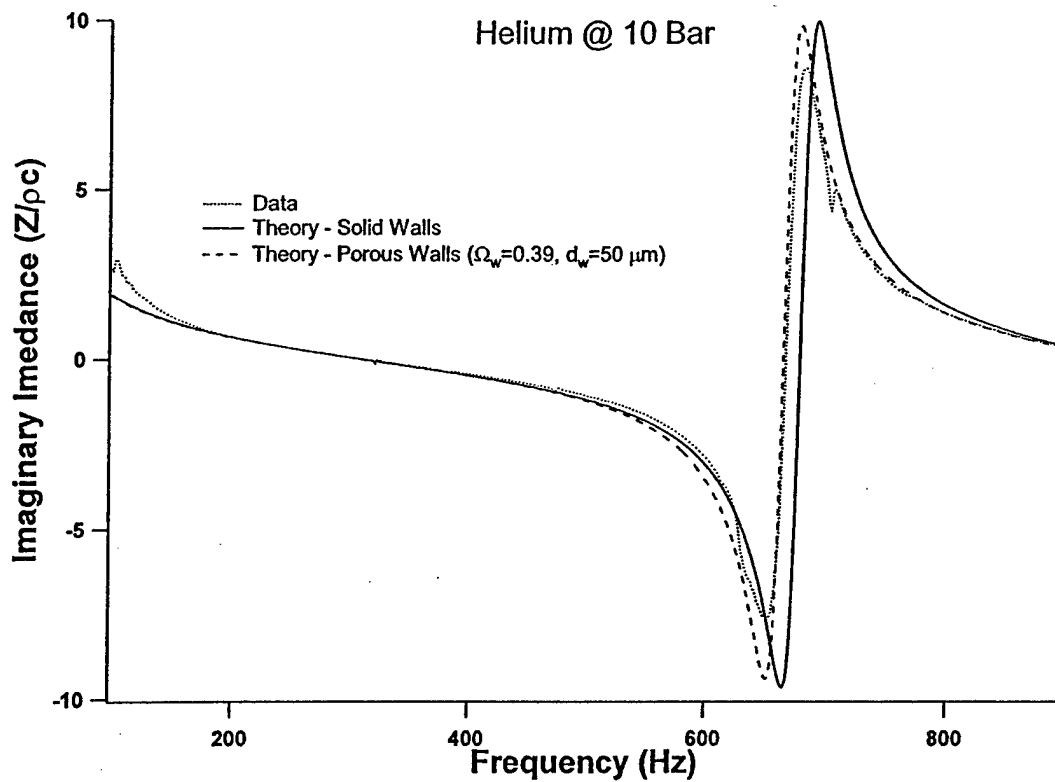
$$\xi \approx 1 + \frac{\gamma}{\gamma - (\gamma - 1)F(\lambda_T)} \frac{\Omega_T - \Omega}{2\Omega} \quad (14)$$

and

$$\Omega_T = \Omega \left(1 + 2 \frac{\Omega_w d_w}{R} \right) \quad (15)$$

for the total porosity. d_w is the average depth of the wall pores and, assuming it is 50 μm , good agreement exists between data and theory.





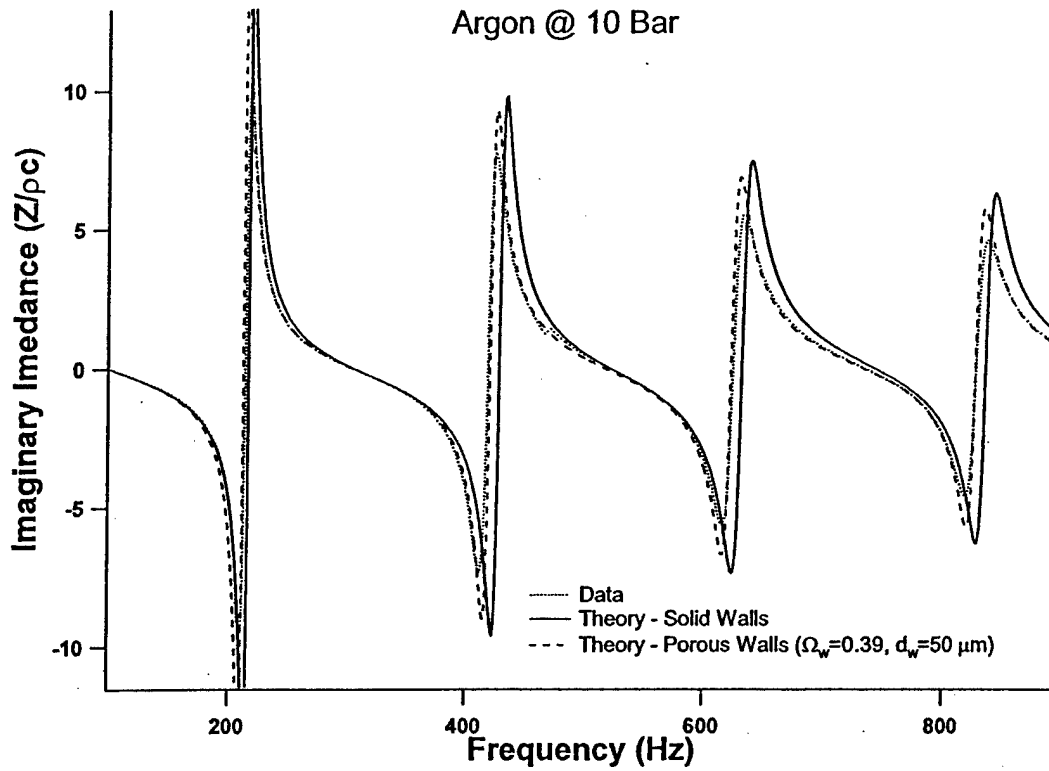


Figure (20): Examining the influence of changing the complex wavenumber in the stack to account for the porous walls of a ceramic stack.

We should mention that the value used for d_w , one third of wall thickness, was chosen to give good agreement between data and theory. Verification of this number is beyond the scope of this work.

Though perplexed by the shifts in data, we still investigated the inert gas/vapor mixture. What follows is one set of that data:

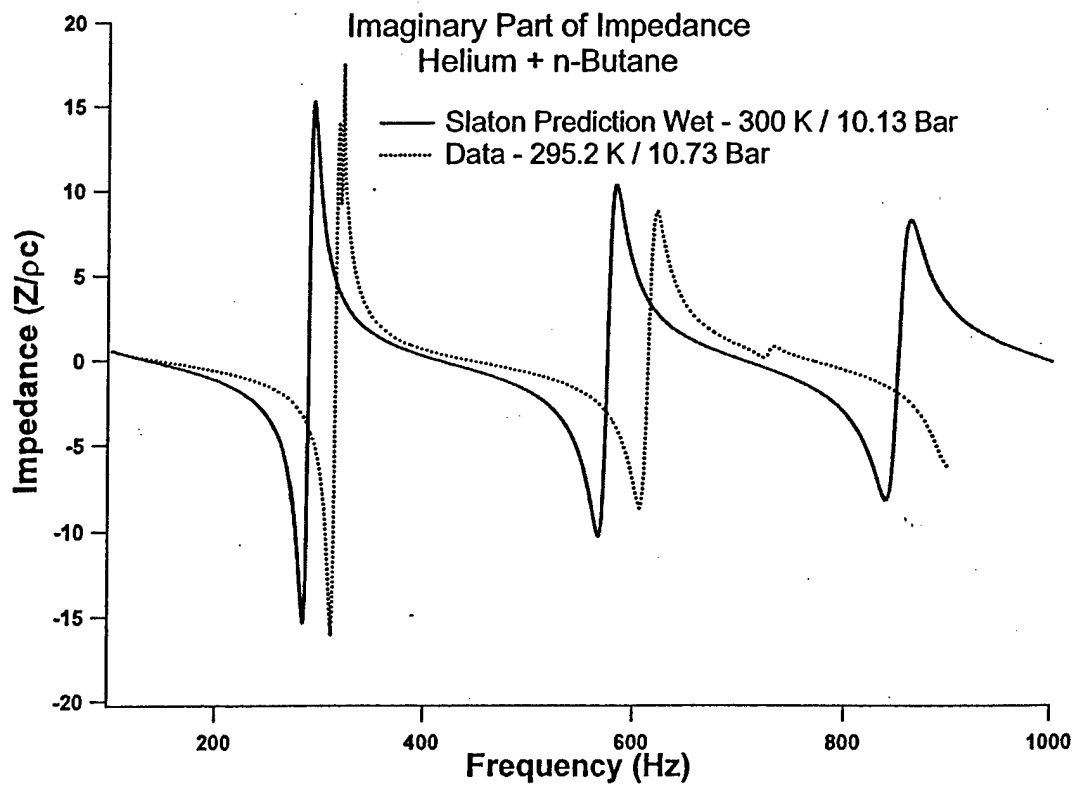
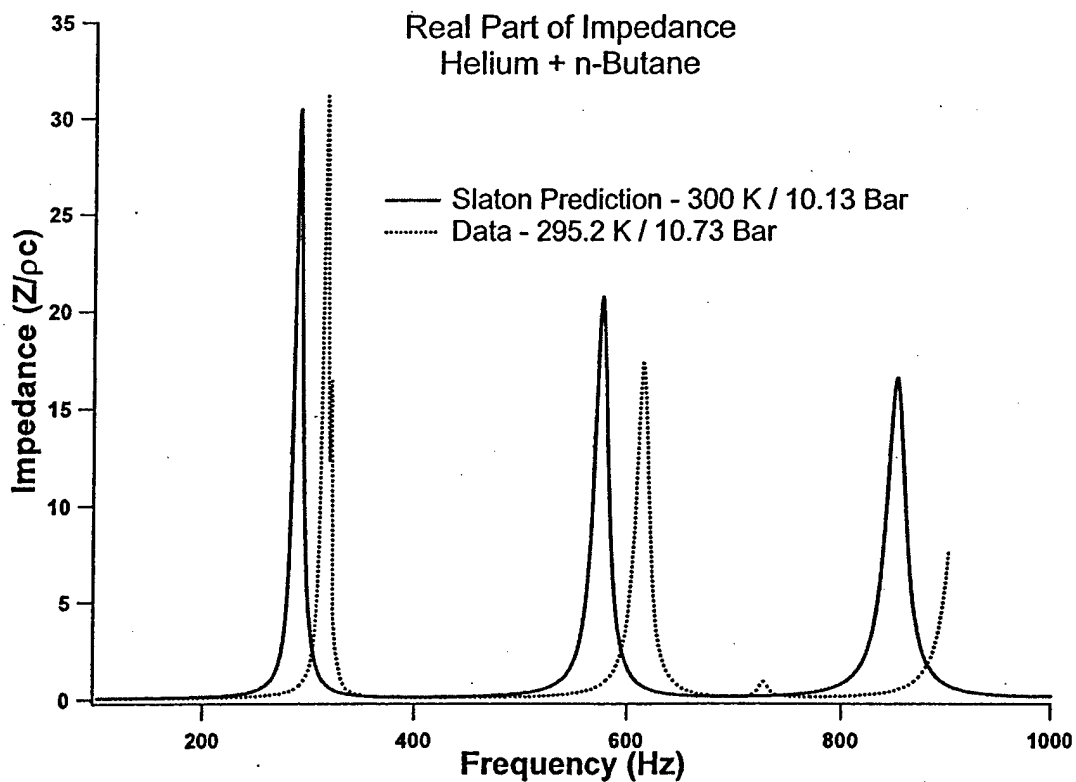


Figure (21): The above data compares the theoretical predictions by Slaton to the measured data. At the time of writing, the only simulation available for comparison was that of 300 K at 10.13 bar. The temperature difference accounts for a 1% change in speed of sound. The pressure difference will cause a change in the molar concentration of the vapor and hence all the gas properties. The effects of this pressure difference are not apparent due to the complex nature of the equations.

The data shown in Figure (21) show good agreement in amplitude, and this is promising. However, the errors in frequency are quite large. In addition to this, the errors seem to be proportional to the frequency, unlike the shift in the dry data. How the presence of a fluid layer would affect the porous walls of the stack is unclear, thus this was not investigated.

VI. Discussion

The original goals of this project were to determine if a stack exposed to a saturated vapor develops a thin layer of fluid over all its surfaces, to confirm the validity of the predicted complex wavenumber in the presence of a saturated vapor, and to characterize the effects vapors would have on the elements of an acoustic system.

The agreement in amplitude in our wet data is hopeful, but the offsets in frequency must be resolved before we can certify the wetting of the stack and the changes to the wavenumber. In order to accomplish this, several changes are recommended for future work.

The system should be redesigned to eliminate as many potential sources of compliance as possible. A single tube that is terminated with a hard end would be best.

Using a single tube instead of multiple sections reduces the possibility of misalignment as well as removes the gasket materials. The differential microphones should be abandoned as well. This would eliminate the plumbing necessary to create the reference side pressure they require. Of course, this presents the problem of finding a transducer that is sensitive to pressure fluctuations on the order of a 1 Pa, but is not damaged by pressures as high as 10^6 Pa. Additionally, the location of gas and vapor filling should be moved to the speaker side of the transducers so as not to influence the measurement.

Elimination of the wall porosity of the stack would be useful as well, either by applications of varnish [Bernard (1996)], or by selecting a material that does not have porous walls, such as stainless steel. This would allow verification, through dry measurements, that the system correctly measures predicted impedance. However, the porous walls may be useful as an indicator of wetness in future measurements. As the walls become coated with fluid the pores begin to fill. This changes the value of d_w in Eq. (15), and the effects of the wall porosity on the complex wavenumber. Eventually the pore will be filled, $d_w = 0$, and the wall porosity no longer influences the measured impedance. As vapor is added to the system, and d_w grows smaller, this shift in impedance should be detectable.

Handling the corrosive vapors presented some problems. Acetone and n-Butane had pronounced effects on our system, the destruction of the speakers being the most frequent problem. Finding a method of exciting sound waves that is not susceptible to

the vapors being investigated will be important if multiple data runs are to be conducted with each filling of the system.

Future work in this area is promising. With the proposed changes above, I am confident that definitive answers can be given to the presented questions.

Bibliography

- R. Raspet, W. Slaton, C. Hickey, and R. Hiller, "Theory of inert gas-condensing vapor thermoacoustics: Propagation equation," *J. Acoust. Soc. Am.* **112**, 1414-1422 (2002).
- W. Slaton, R. Raspet, C. Hickey, and R. Hiller, "Theory of inert gas-condensing vapor thermoacoustics: Transport equations," *J. Acoust. Soc. Am.* **112**, 1423-1430 (2002).
- G. Swift, "Thermoacoustic Engines," *J. Acoust. Soc. Am.* **84**, 1145-1180 (1988).
- W. P. Arnott, H. E. Bass, and R. Raspet, "General formulation of thermoacoustics for stacks having arbitrarily shaped pore cross sections," *J. Acoust. Soc. Am.* **90**, 3236-3237 (1991)
- A. D. Pierce, *Acoustics* (Acoust. Soc. Am.), Woodbury, New York, (1991)
- J. V. Hirschfelder, C. Curtiss, and R. B. Bird, *Molecular Theory of Gases and Liquids* (Wiley, New York, 1964)
- J. Y. Chung and D. A. Blaser, "Transfer Function Method of Measuring In-duct Acoustic Properties, I. Theory," *J. Acoust. Soc. Am.* **68**, 907-913 (1980).
- J. Y. Chung and D. A. Blaser, "Transfer Function Method of Measuring In-duct Acoustic Properties, II. Experiment," *J. Acoust. Soc. Am.* **68**, 914-921 (1980).
- W. P. Arnott, J. M. Sabatier, and R. Raspet, "Sound propagation in capillary-tube-type porous media with small pores in the capillary walls," *J. Acoust. Soc. Am.* **90**, 3299-3306 (1991)
- M. Bernard, D. Velea, J. M. Sabatier, "Permanent removal of the wall porosity in monolithic catalyst support ceramics," *J. Acoust. Soc. Am.* **99**, 2430-2432 (1996)

Appendix A

The purpose of measuring the transfer function between two transducers is to gain information about the signals present. Unfortunately, the measurement system (transducer and amplifier) itself affects the transfer function. In addition to the transfer function due to the signal, H_{12}^{Signal} , the measured transfer function $H_{12}^{Measured}$ includes the intrinsic transfer function of the data acquisition system $H_{12}^{Intrinsic}$.

$$H_{12}^{Measured} = H_{12}^{Signal} * H_{12}^{Intrinsic} \quad (A1)$$

Fortunately, accounting for the nonlinear properties of the data acquisition channels is straightforward. To do this both channels must be exposed to an identical sound field. This reduces equation (A1) to

$$H_{12}^{Measured} = 1 * H_{12}^{Intrinsic} \quad (A2)$$

To achieve an identical sound field, the transducers were mounted in radial symmetry into a flange (See Picture). This flange is mounted onto a pipe and exposed to broadband noise. Assuming we have plane waves, the signal at each transducer is identical. Therefore, any non-unity transfer function will be due to the measurement system alone, $H_{12}^{Intrinsic}$. To account for this in further measurements, $H_{12}^{Measured}$ is simply divided by $H_{12}^{Intrinsic}$.

It is worthwhile to note that $H_{12} \neq H_{21}$. In addition, we must be consistent in determining which of the two transducers will be labeled as #1 or "reference."

Equation (12) requires the reference transducer be placed farthest from the stack.

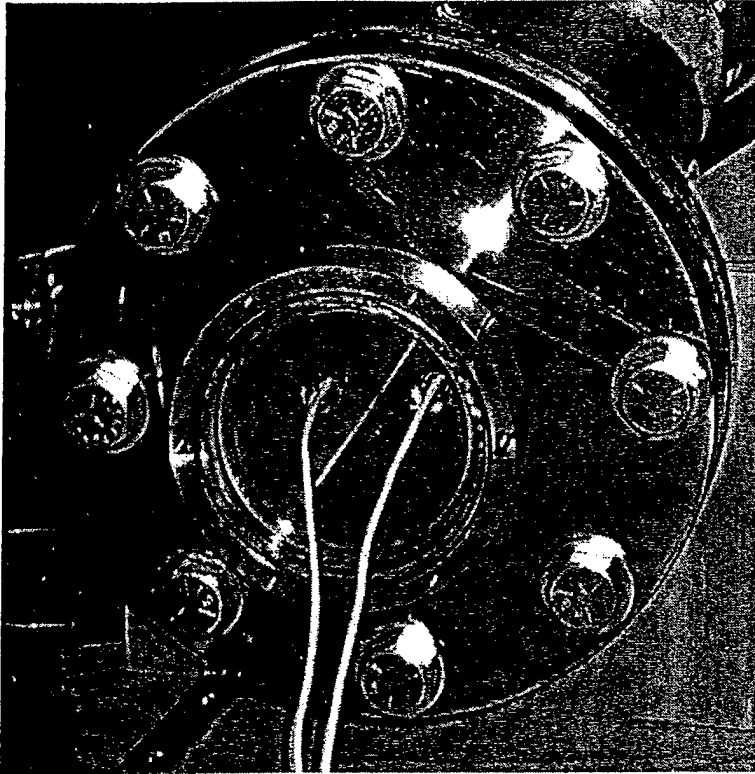


Figure (A1): Transducers mounted in radial symmetry for calibration.

The transfer functions for our system follow. The figures also show a cubic fit to the intrinsic transfer function, which was used to speed data reduction.

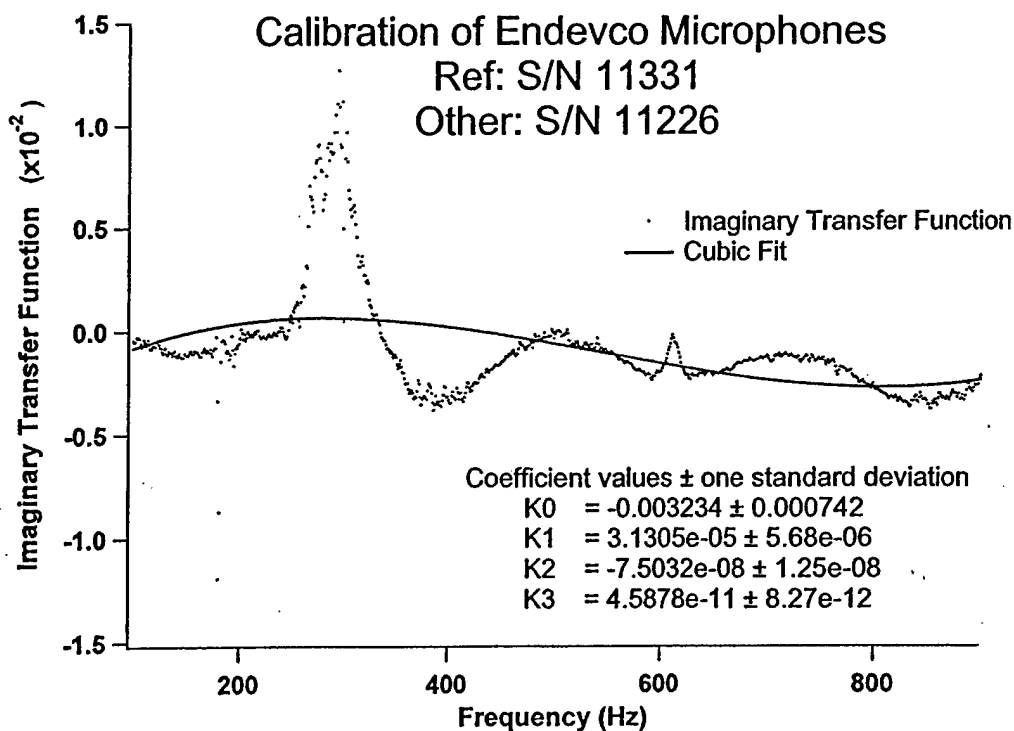
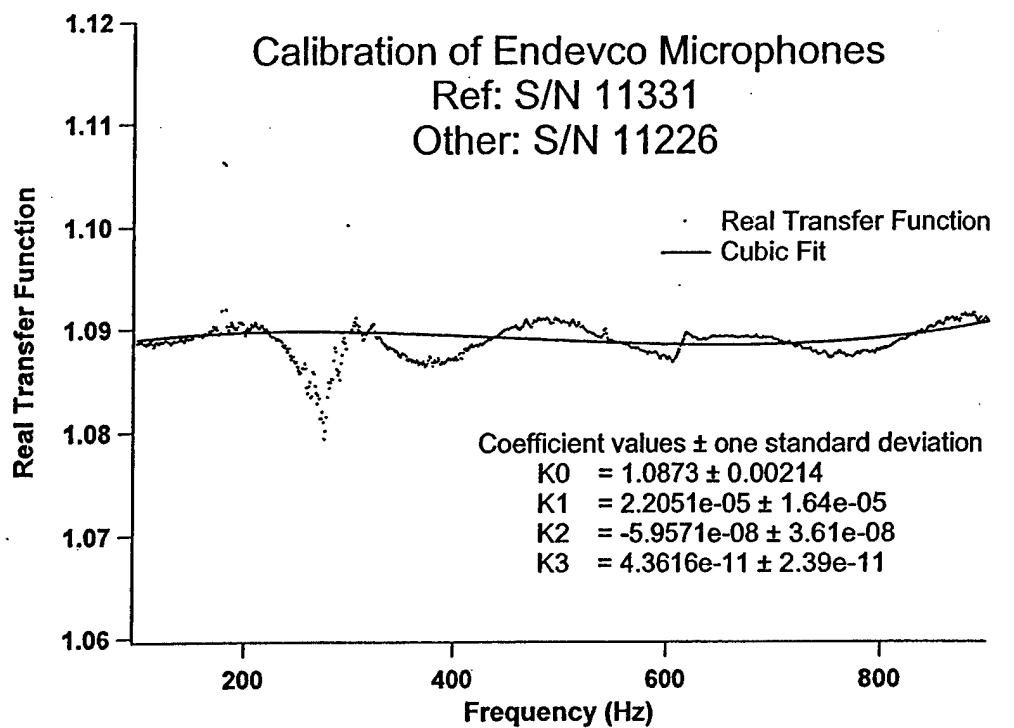


Figure (A1): Intrinsic transfer functions for the transducer – amplifier system.

Appendix B

The following equations are used in conjunction with the impedance translation theorem to model the impedance at the face of the stack with out the presence of a condensable vapor. We begin with the impedance of normal incidence plane wave reflection at a solid surface due to thermal conduction and viscosity at that surface [Pierce (1991)].

$$\frac{1}{Z} = \frac{e^{\frac{i\pi}{4}}}{\rho c} \eta_{\mu}(\omega) \left[\frac{\gamma - 1}{\sqrt{N_{Pr}}} \right] \quad (B1)$$

where,

$$\eta_{\mu}(\omega) = \sqrt{\frac{\omega \mu}{\rho c^2}} \quad (B2)$$

This is translated through the intrinsic impedance of our 0.1016 m diameter pipe. This was calculated using the boundary layer approximation [Arnott (1991)].

$$Z_{int} = \frac{\rho_0 \omega}{\Omega F(\lambda) k} \quad (B3)$$

where,

$$k^2 = \frac{\omega^2}{c^2} \frac{\gamma - (\gamma - 1)F(\lambda_T)}{F(\lambda)} \quad (B4)$$

and,

$$F(\lambda) = 1 - \frac{\sqrt{2}}{\lambda} (1 + i). \quad (B5)$$

Now this impedance can be translated through the intrinsic impedance of the porous sample; thus, predicting the impedance at the face of the stack. The intrinsic

impedance of the stack was calculated using Eqs. B3 and B4. For the dissipation function we have

$$F(\lambda) = \frac{64}{\pi^4} \sum_{m,n}^{odd} \frac{1}{m^2 n^2 Y_{mn}(\lambda)} \quad (B6)$$

where,

$$Y_{mn}(\lambda) = 1 + \frac{i\pi^2(m^2 + n^2)}{4\lambda^2}. \quad (B7)$$

VITA

Daniel Cleary Brown, Jr. was born in Memphis, Tennessee November 23, 1976. He attended Rhodes College, graduating with a Bachelor of Science in 1999. He has worked as a laboratory physicist under the direction of Dr. Robert Hiller and Dr. Richard Raspet at the National Center for Physical Acoustics at the University of Mississippi from 2001 to 2003.